Chronic Thromboembolic Pulmonary Vascular Disease:

Physiological Concepts and Genetic Predisposition

Colm Thomas McCabe

Thesis submitted to Imperial College for

Doctor of Medicine (M.D. Res)

March 2014

Pulmonary Vascular Disease Group

Papworth Hospital

Papworth Everard

Cambridge

CB23 3RE

Imperial College London

Papworth Hospital NHS

NHS Foundation Trust

Copyright Declaration

Declaration of Originality

This thesis represents all my own work except where specific contributions are mentioned in the acknowledgements. All other peoples' contributions are referenced appropriately.

Abstract

Chronic thromboembolic pulmonary hypertension (CTEPH) is an uncommon sequela of acute pulmonary embolism and, untreated, leads to right ventricular (RV) failure and death. Despite its growing recognition, methods for the detection of early RV insufficiency and prediction of clinical deterioration, important to optimum preservation of RV function, are currently suboptimal. Furthermore, underlying genetic predisposition to CTEPH, unexplained by defective fibrinolysis, remains largely unexplored.

The RV's physiological response to chronic thromboembolic obstruction is arguably best described by RV pressure volume loops which, historically, are best obtained using the conductance catheter. Although invasive, conductance has an indisputable advantage over current imaging modalities; catheters measure dynamic ventricular pressure and volume throughout the cardiac cycle. Using this technique, abnormal RV pressure volume loops are demonstrated in response to chronic thrombotic obstruction, independent of resting haemodynamic criteria diagnostic of CTEPH. Pressure volume differences and accrual of an exercise gas exchange deficit further suggest early 'subclinical' RV adaptation. The genetic architecture of CTEPH is also explored using high-throughput sequencing of unrelated patients. This shows that rare DNA variants in CTEPH that are predicted to harbour deleterious effects are not over-represented in fibrinolytic pathways. Finally, prognostication in CTEPH is evaluated using a clinical deterioration model which is shown to be predicted by patient-reported outcomes at diagnosis.

In conclusion, RV and pulmonary circulatory function in chronic thromboembolic pulmonary vascular disease are inadequately characterised by existing routine methods. Links between the observed physiological deficits, risk of clinical deterioration and abnormal genetic architecture warrant further evaluation in this rare disease.

Acknowledgements

I would like to thank my supervisors, Joanna Pepke-Zaba and Nick Morrell who gave me the opportunity to study for a MD degree in their Pulmonary Vascular Disease research group in Cambridge. In addition, Martin Wilkins acted as my Imperial College Supervisor and very generously donated funds towards University tuition fees. Whilst in Cambridge, my two years at Papworth have been richly stimulating and taught me much about the challenges of academic medicine and clinical aspects of pulmonary vascular disease. In particular I have benefitted from working closely with Joanna at Papworth with regular clinical commitments to the PH service. During this period, I have learnt much from them both about patient care and research methodology and with their input, was successful in achieving local funding in open competition from a Papworth Research 'Pump-Priming' Fund. This enabled me to undertake the genetic work described in Chapter 5 as well as funding several trips to international conferences to present aspects of this thesis. Finally, Martin Wilkins kindly contributed £1000 per annum to my tuition fees and acted as my Imperial College supervisor for Medicine.

I am indebted to my colleagues working in PH at Papworth who have provided invaluable support throughout my two years, especially Dolores Taboada, and Rob Mackenzie Ross who taught me right heart catheterisation and much about the management of PH when I arrived. The PH research nurses, Carmen Treacy, Kathy Page and Natalie Doughty were hugely accommodating helping to familiarise me with clinical research methods and each contributed in no small measure to my completion of these projects. In my final six months Charaka Haddinapola was my desk neighbour and a knowledgeable and intelligent colleague with whom to discuss problems and solutions.

Several other staff members at Papworth and Addenbrookes deserve particular mention. Paul White provided invaluable expertise and greatly contributed to my understanding of right ventricular physiology as well as providing much of the raw materials and pressure volume background needed

for the right ventricular study in Chapter 3. Similarly, Richard Axell provided critical support in both experimentation and analysis of this work. Stephen Hoole gave an overly generous amount of his time to both practical aspects and analysis of this work and along with Len Shapiro, allowed me first-hand experience of simultaneous cardiac catheterisation the RV and LV. As a chest physician in training, this has been especially rewarding.

I wish also to thank Stefan Graf who lent his time in fine-tuning the exome pipeline described in Chapter 5, as well as Lu Long and Jennifer Jolley who both assisted with the wet lab DNA preparation. Deepa Gopalan kindly examined cardiac magnetic resonance data to exacting standards and Nicholas Screaton assisted with the CT analysis of data described in Chapter 4. Gael Deboeck and Ian Harvey in Papworth's respiratory physiology department also lent much of their time and expertise assisting with this study. In Chapter 6, Maxine Bennett and Linda Sharples provided expert statistical analysis on the study of patient reported outcomes in PH and were an invaluable source of advice for other statistical issues. Lastly, I am grateful to my mother and fiancée, Emma, for their continued support throughout my two year research period whilst living away in Cambridge.

Index of Contents

Chapter 2. Materials and Methods

Chapter 3. Right Ventricular Dysfunction in Chronic Thromboembolic Obstruction of the Pulmonary Artery

Chapter 4. Inefficient exercise gas exchange identifies pulmonary hypertension in chronic thromboembolic obstruction following pulmonary embolism

List of Figures

List of Tables

List of abbreviations

Throughout the manuscript, abbreviations are defined on their first use. A list of some of the more common are included below.

CI	cardiac Index
CMR	cardiac Magnetic Resonance
CO	cardiac Output
CPET	cardiopulmonary exercise test
DSV	DNA sequence variation
mPAP	mean pulmonary artery pressure
PAH	pulmonary arterial hypertension
PH	pulmonary hypertension
PVR	pulmonary vascular resistance
RHC	right heart catheterisation
SNP	single nucleotide polymorphism

Chapter 1. Introduction

1.1 Definition and Classification of Pulmonary Hypertension

Pulmonary hypertension (PH) is a severe but rare disorder characterised by increased pulmonary vascular resistance (PVR) secondary to progressive obstruction within the pulmonary circulation. It is defined by a mean pulmonary arterial pressure (mPAP) >= 25 mmHg at rest assessed at right heart catheterisation (RHC). The most updated clinical classification is outlined in Table 1.1 and takes into account shared pathological and clinical features (Simonneau et al., 2009).

1 Pulmonary arterial hypertension (PAH)
- 1.1 Idiopathic PAH
- 1.2 Heritable
  - 1.2.1 BMPR2
  - 1.2.2 ALK1, endoglin (with or without hereditary hemorrhagic telangiectasia)
  - 1.2.3 Unknown
- 1.3 Drug- and toxin-induced
- 1.4 Associated with
  - 1.4.1 Connective tissue diseases
  - 1.4.2 HIV infection
  - 1.4.3 Portal hypertension
  - 1.4.4 Congenital heart diseases
  - 1.4.5 Schistosomiasis
  - 1.4.6 Chronic hemolytic anemia
- 1.5 Persistent pulmonary hypertension of the newborn

1' Pulmonary veno-occlusive disease (PVOD) and/or pulmonary capillary hemangiomatosis (PCH)

2 Pulmonary hypertension owing to left heart disease
- 2.1 Systolic dysfunction
- 2.2 Diastolic dysfunction
- 2.3 Valvular disease

3 Pulmonary hypertension owing to lung diseases and/or hypoxia
- 3.1 Chronic obstructive pulmonary disease
- 3.2 Interstitial lung disease
- 3.3 Other pulmonary diseases with mixed restrictive and obstructive pattern
- 3.4 Sleep-disordered breathing
- 3.5 Alveolar hypoventilation disorders
- 3.6 Chronic exposure to high altitude
- 3.7 Developmental abnormalities

4 Chronic thromboembolic pulmonary hypertension (CTEPH)

5 Pulmonary hypertension with unclear multifactorial mechanisms
- 5.1 Hematologic disorders: myeloproliferative disorders, splenectomy
- 5.2 Systemic disorders: sarcoidosis, pulmonary Langerhans cell histiocytosis: lymphangioleiomyomatosis, neurofibromatosis, vasculitis
- 5.3 Metabolic disorders: glycogen storage disease, Gaucher disease, thyroid disorders
- 5.4 Others: tumoral obstruction, fibrosing mediastinitis, chronic renal failure on dialysis

Table 1.1
Clinical Classification of PH (Dana Point 2008)

1.1.1 Group 1: Pulmonary Arterial Hypertension (PAH)

Pulmonary arterial hypertension (PAH) makes up Group 1 of the PH classification and is denoted by increased pulmonary artery pressure in the absence of left heart disease (McLaughlin and Rich, 2004). PAH is predominantly a disorder of distal pulmonary arterioles that demonstrate vessel wall remodelling, inflammation, local thrombosis and vasoconstriction. Pulmonary endothelial dysfunction produces an inequality between vasoconstricting and vasodilating mediators culminating in increased pulmonary arterial smooth muscle cell tone. This occurs in response to excess endothelin-1 levels and depleted nitric oxide and prostacyclin levels (Humbert et al., 2004). Vessel wall remodelling is stimulated by upregulation of growth factors which act as potent chemoattractants on smooth muscle cells and fibroblasts. In hereditary and idiopathic forms, PAH is strongly associated with germ line mutations in the gene coding for the bone morphogenetic protein receptor – 2 protein (BMPR2) which impair its suppressive effects on pulmonary artery smooth muscle cell growth. Inflammation is strongly implicated in the pathogenesis of PAH evidenced by elevated circulating levels of inflammatory cytokines (interleukin 1 and 6) (Humbert et al., 1995; Soon et al., 2010), which have been shown to predict survival and clinical deterioration (Quarck et al., 2009).

Clinical symptoms in all forms of PH may be non-specific with a typical diagnosis relying on a history of progressive exercise intolerance and confirmation of abnormal pulmonary haemodynamics. Untreated, PH causes chronic pressure overload of the right ventricle (RV) leading to RV hypertrophy and failure. Progressive disease is in part determined by maladaptive neurohormonal signalling, inflammatory responses and oxidative stress that accelerate the degree of RV dilatation and failure. Prognostic markers include right atrial pressure and cardiac index, acute vasodilator responsiveness, functional class, exercise capacity and biomarkers including serum pro-brain natriuretic peptide which correlates well with the degree of RV failure (Badesch et al., 2009). PAH-specific therapy consists of pulmonary arterial vasodilators which target endothelin, prostaglandin and nitric oxide pathways. Multiple randomised control trials have shown these therapies to improve haemodynamic indices and functional capacity with epoprostenol and macitentan currently the only agents with evidence for

improvement in long term survival (Channick et al., 2001; Galie et al., 2009a; Galie et al., 2005; Galie et al., 2008a; Pulido et al., 2013; Rubin et al., 2002; Sitbon et al., 2002). Surgical therapies include atrial septostomy and lung transplantation and are only considered in patients with advanced disease refractory to medical therapy (Keogh et al., 2009).

1.2 Chronic Thromboembolic Pulmonary Hypertension

1.2.1 Definition

Chronic thromboembolic pulmonary hypertension (CTEPH) occupies Group 4 of the Dana Point 2008 classification and is characterised by unresolved pulmonary thromboemboli associated with obliterative destruction and fibrous stenosis of the pulmonary arteries. It differs from PAH in that pulmonary artery obliteration is more proximal in CTEPH. A distal arteriopathy is also described thought to result from overperfusion of unobstructed lung segments (Hoeper et al., 2006). Similar to PAH, CTEPH is haemodynamically defined by a mPAP >= 25mmHg at rest with a pulmonary capillary wedge pressure (PCWP) ≤ 15 mmHg. Radiologically, CTEPH requires evidence of at least one (segmental) perfusion defect that persists following at least three months of therapeutic anticoagulation (Moser et al., 1990).

CTEPH is a rare but important complication of acute pulmonary embolism (PE). Traditionally, retrospective estimates have suggested it complicates just 0.1% of patients who survive acute PE and that a lengthy 'honeymoon' period exists between initial presentation and subsequent development of symptomatic disease (Fedullo et al., 1995). Subsequent prospective studies have suggested a potentially larger disease burden quoting the cumulative incidence of CTEPH at between 1 and 9.1% following PE that predominantly occurs within 2 years of presentation (Becattini et al., 2006; Dentali et al., 2009; Fedullo et al., 2001; Pengo et al., 2004; Surie et al., 2010). This wide estimated range in prevalence stems from differences in haemodynamic diagnostic cut-offs, patient risk profiles and the

inconsistent use of RHC to confirm the diagnosis. Charting the epidemiological behaviour of CTEPH remains challenging given that a significant number of patients suffer no prior episode of acute venous thrombosis (VTE) and present with sporadic disease (Auger et al., 2004).

1.2.2 Aetiopathogenesis

The aetiology and mechanisms of development of CTEPH remain unknown. However, a majority consensus has emerged predicated on a theory of disordered thrombus resolution following acute VTE/PE. A central theorem is that individuals respond differently to acute thrombotic insult. A recent European CTEPH Registry has revealed that previous PE may be detected in 74.8% of patients with CTEPH while previous deep vein thrombosis (DVT) is present in 56.1% (Pepke-Zaba et al., 2011). The shorfall in patients where no antecedent VTE can be identified is approximately 30% and in general, prothrombotic states are not observed in CTEPH. Although prior asymptomatic VTE is recognised (Dartevelle et al., 2004), marked differences in risk profiles exist between patients with CTEPH and those with isolated VTE indicating additional unknown factors may be important.

Plasmatic risk factors have been the subject of detailed investigation with traditional prothrombotic factors explaining less than 10% of reported CTEPH cases. In particular, deficiency in antithrombin, protein C or protein S, all known to predispose to recurrent VTE, share no association (Wolf et al., 2000). Similarly, mutation in Factor V R506Q (Factor V Leiden) shows no significant association. In contrast, high titres of antiphospholipid antibodies have been demonstrated in patients with CTEPH as well as increased Factor VIII and von Willebrand Factor antigen levels (VWF:Ag) (Bonderman et al., 2003; Bonderman et al., 2009; Wolf et al., 2000; Wong et al., 2010). The presence of a lupus anticoagulant, strongly associated with recurrent VTE, also accounts for a minority of cases (Auger et al., 1995).

Non-plasmatic risk factors have emerged from registry data and include previous splenectomy, congestive cardiac failure, family history of VTE, inflammatory bowel disease, infected pacemaker wires and chronic osteomyelitis (Pepke-Zaba et al., 2011). There are also strong epidemiological associations between the development of CTEPH and clinical features at the time of presentation with acute PE. These include a larger clot burden, evidence of right heart strain, younger age and biochemical evidence of myocardial enzyme leakage at presentation (Lankeit et al., 2008; Pengo et al., 2004). Chronic thyroid replacement therapy and a history of malignancy have also emerged as novel risk factors (OR 6.10, 3.76 respectively) along with chronic Staphylococcal sepsis (Bonderman et al., 2008).

Disordered clot resolution was first implicated in the pathogenesis of CTEPH from experimental evidence in dogs where pharmacological inhibition of fibrinolysis potentiated the development of chronic organised fibrous material in the pulmonary artery (Moser et al., 1991). This raised suspicion that patients with CTEPH may harbour a fibrinolytic genetic defect. Discovery of *in vitro* dysfibrinogenaemia demonstrated patients with CTEPH may have particular fibrin properties that confer an enhanced resistance to lysis (Firth et al., 2009; Morris et al., 2006). Rare genetic variants within the fibrinogen gene have also been associated with relative resistance to plasminogen-mediated fibrinolysis (Linenberger et al., 2000) with our own group demonstrating an over-represented fibrinogen A alpha-chain Thr312Ala polymorphism in CTEPH (Suntharalingam et al., 2008). However, the effect of such variants *in vivo* remains unknown and, significantly, no difference exists in tissue plasminogen activator (tPA) or plasminogen activator inhibitor – 1 (PAI – 1) levels between patients with CTEPH and controls (Olman et al., 1992). Human gene expression studies comparing CTEPH thrombi with native pulmonary arterial tissue samples have suggested abnormal regulation of pathways involved with proliferation and endothelial function (Lang et al., 1994). In addition, a recent underpowered genome wide association study has shown an association between HLA loci B*5201 and DPB1*0202 in patients with CTEPH (Kominami et al., 2009) although no downstream protein target has been identified.

Integral to the thromboembolic concept of CTEPH is how the venous system degrades and removes large vessel thrombi in the *non-diseased* state. This involves a complex process of adaptive thrombus remodelling, neovascularisation and recanalisation of the pulmonary arterial vessel wall, analogous to granulation tissue formation in the healing wound. Recruitment and margination of monocytes and neutrophils enhance thrombus clearance and deregulation of monocyte recruitment has been shown to be detrimental to this process (Ali et al., 2006; McGuinness et al., 2001). Both cell types recruit inflammatory mediators and upregulate growth factor expression including Vascular Endothelial Growth Factor (VEGF). This is known to enhance tissue factor-mRNA and protein levels on endothelial cells (Mechtcheriakova et al., 1999). Transforming growth factor-beta (TGF-β), fibroblastic growth factor (FGF), proteases (matrix metalloproteases/urokinase-type plasminogen activator) and chemoattractants including monocyte chemotactic protein-1 (MCP-1) are also upregulated during thrombus clearance and appear to accelerate the organisation and resolution of venous thrombi (Waltham et al., 2003). However, how these factors interplay to give rise to cellular remodelling, inflammation and neovascularisation culminating in delayed thrombus resolution is still subject to debate.

1.2.3 Treatment

The first line therapy for CTEPH is pulmonary thromboendarterectomy (PTE). This involves the surgical removal of both recent and chronically organised thrombotic material from the pulmonary artery endolumen as well as neointimal and tunica medial resection of the pulmonary arterial wall (Figure 1.1). In the only UK centre offering PTE surgery, operative mortality is under 5% with considerable importance placed on case selection and preoperative haemodynamic assessment (Freed et al., 2008).

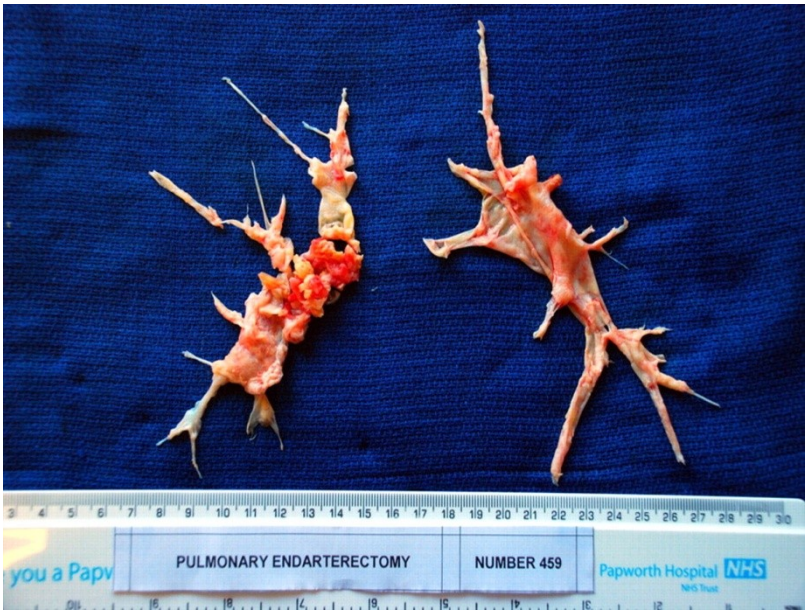

Figure 1.1

Pulmonary thromboendarterectomy specimen (reproduced with permission of Mr D Jenkins, Papworth Hospital)

In inoperable CTEPH, that is disease lying within surgically inaccessible sites usually distal to subsegmental level pulmonary arteries, patients may be treated with medical vasodilator therapies including prostaglandin analogues (Cabrol et al., 2007), endothelin receptor antagonists (Hoeper et al., 2005a) and phosphodiesterase V inhibitors (Reichenberger et al., 2007). In separate analyses, bosentan, prostacyclin analogues (epoprostenol, treprostinil) and sildenafil have all been demonstrated to improve exercise capacity and/or haemodynamic parameters in inoperable CTEPH although not all trials have been placebo controlled. More recently, Riociguat, a guanylate cyclase activator, has been shown to have a beneficial effect on exercise capacity (Ghofrani et al., 2013).

1.3 Functional assessment of the Right Ventricle

1.3.1 Physiology of Right Ventricle and the Pulmonary Circulation

Early understanding of the function of the RV regarded it as simply a conduit delivering blood from the cavae to the pulmonary circulation. However, in recent decades the importance of the RV as a contractile pump has emerged from studying the clinical effects of RV failure, PH and congenital heart disease (Dell'Italia, 2012). Often neglected in comparison to the left ventricle (LV), the RV is anatomically more complex than its neighbour and due to the fundamental differences between pulmonary and systemic circulations, parameters of contractile performance are not directly transferable between ventricles (Bellofiore and Chesler, 2013). This difference is typified by the low resistance and high compliance of the pulmonary circulation which maintains pulmonary arterial pressure at sub-systemic levels. In contrast, the higher afterload systemic circulation has different ventricular adaptive responses to disease (Haddad et al., 2008). This is clearly demonstrated by marked differences in response to unloading in the RV and LV, with the former capable of almost immediate and sustained reverse remodeling (Mauritz et al., 2012; Rensing et al., 1997).

In health, the RV has a crescentic short axis shape, bound by a thin free-wall and shared interventricular septum within a fixed pericardial sac. Its anatomy can be described by three components; 1) the inlet consisting of the tricuspid valve apparatus, 2) the trabeculated apical myocardium and 3) the infundibulum or RV outflow tract. Prominent internal muscular bands provide structural support and attachment to papillary muscles. Under normal loading conditions and electrical conduction, the septum is concave toward the LV throughout systole and diastole with RV mass measuring roughly one sixth that of the LV. Orientation of myocardial fibres ensure direct mechanical interaction between LV and RV, termed ventricular interdependence. Superficial fibres lie circumferentially contiguous with the LV at the cardiac apex whereas deep fibres align longitudinally from base to apex. This causes a retained contribution from the LV towards RV ejection that can be up to 50% under certain loading conditions (Feneley et al., 1985).

Systolic ejection in the RV is sequential with approximately 50 milliseconds separating contraction of the inlet myocardium from contraction of the infundibulum (Dell'Italia, 1991). RV shortening is greater longitudinally than radially and in contrast to the LV, twisting rotational movements do not

make a significant contribution to the generation of forward flow. Volume rather than pressure work is performed during RV contraction producing shorter isovolumic contraction times with an early pressure peak and rapid fall off. In contrast to the LV, diastolic filling is more prolonged in the RV although the isovolumic phase of relaxation is shorter. The heightened sensitivity to changes in filling in the thin walled RV signifies its greater chamber compliance than the LV. Under conditions of pericardial constraint, this predisposes the RV to earlier decompensation.

In health and at sea-level, the pulmonary circulation has characteristic elastic properties that define its physiological behaviour. Small, thin-walled muscular arteries taper out to the pulmonary capillary level and ensure a high capacity, low resistance vasculature. The pulmonary circulation therefore remains relatively unpredisposed to a hypertensive state in comparison to the systemic circulation; indeed, in health, total vascular resistance is roughly 20% of that of the systemic circulation. The greater recruitable pulmonary vascular reserve also allows pulmonary arterial pressure to remain relatively unchanged despite large increases in circulating blood volume (cardiac output) such as at the onset of exercise. This property is used routinely in the clinical assessment of pulmonary circulatory function and is defined by the pressure flow relationship in the pulmonary vascular bed which describes the resistance to forward flow from the RV:

$$TPVR = mPAP / Q$$

where TPVR = total pulmonary vascular resistance and Q = RV cardiac output.

More frequently, the difference between the inflow and outflow pressure of the pulmonary vascular bed is calculated by subtracting mean left atrial pressure (LAP) from mPAP. LAP may be approximated through use of PCWP providing pulmonary vessels are fully recruited and pulmonary capillary pressure is higher than alveolar pressure. Thus, pulmonary vascular resistance (PVR) is given by:

$$PVR = (mPAP – PCWP) / Q$$

This calculation is governed by laws of laminar flow where resistance to flow is a function of the product of the length of the tube, l and viscosity constant, η divided by the internal radius of the tube to the power of four. PVR is derived most accurately by RHC and neatly describes the constriction and dilatation of pulmonary resistive vessels used most commonly in clinical monitoring.

1.3.2 Conductance Theory and Pressure Volume Loops

Haemodynamic parameters that assume laminar flow in the pulmonary artery form the backbone of clinical assessment in PH. However, no consensus exists on the optimal method of *RV* functional assessment which prognostically carries greater importance. In PH (and cardiac transplantation), flotation catheters represent the gold standard method of haemodynamic assessment but as far back as the 1970s, pressure volume (PV) RV catheterisation has been used as arguably a more sensitive indicator of RV function.

First applied in the human RV in 1984 by McKay (McKay et al., 1984), RV PV loop measurements are best generated by using conductance catheters. A typical PV loop obtained by a conductance catheter placed in the RV is shown in Figure 1.2. Conductance catheters are multipurpose catheters with platinum electrodes located at the distal end (Figure 1.3). Through simultaneous recording of pressure and volume, these catheters allow the construction of pressure volume loops throughout the cardiac cycle. This technique is currently unsurpassed by noninvasive imaging techniques due to the detailed beat to beat pressure and volume signals that describe ventricular responses to loading and unloading.

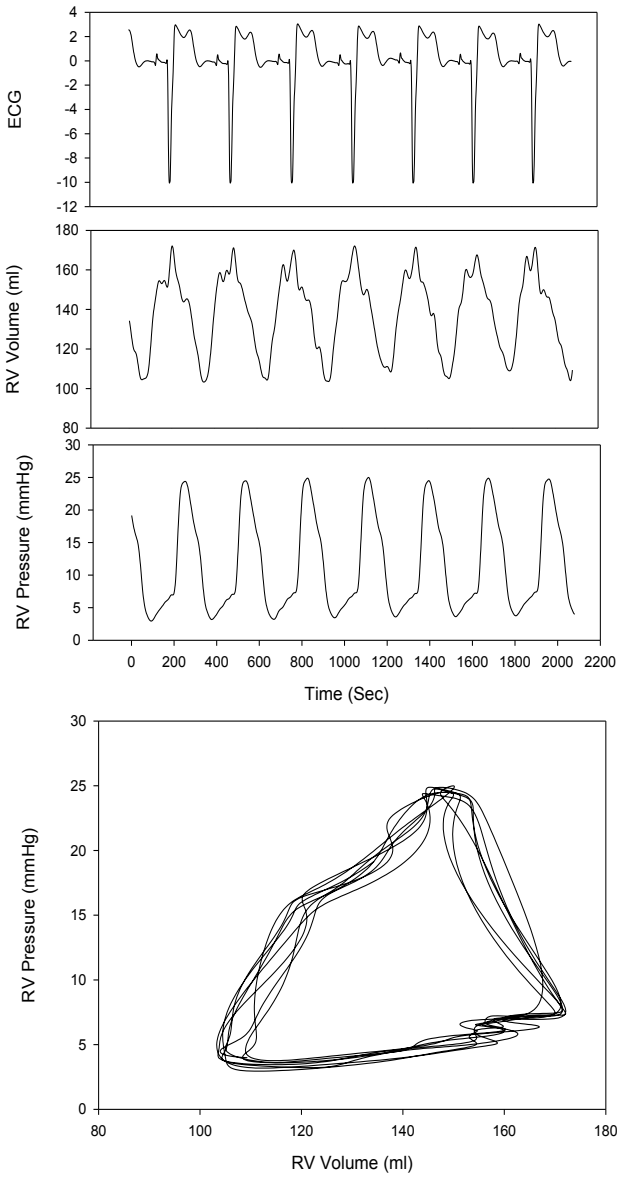

Figure 1.2

The normal RV pressure volume loop showing a typical RV triangular morphology. Continued Ejection (volume loss) during pressure decline is seen due to the highly compliant pulmonary vasculature and momentum of blood in the outflow tract. Separate RV pressure and volume signals coordinate with electrical activity on ECG.

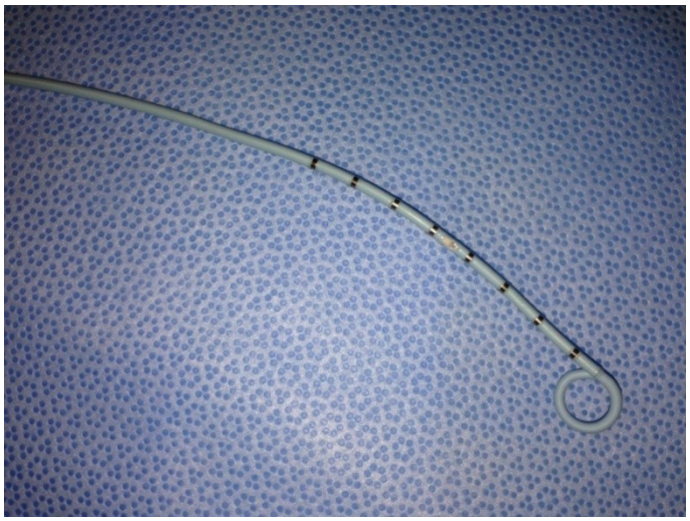

Figure 1.3

A custom built pigtail conductance catheter with platinum electrodes located on the distal end.

Conductance catheters generate intracardiac real-time blood volume via a technique exploiting the electrical conductivity of blood that emerged in the early 1980s. Conductance theory relies on direct measurement of change in intracardiac blood volumes based on the electrical impedance of the time-varying quantity of blood contained within the ventricular cavity. Blood is a good conductor of electricity and the ventricular wall relatively poor. Therefore, when the ventricle is full (at end-diastolic volume (EDV)), the conductance signal is high in contrast to the end-systolic volume (ESV) when conductance will be low.

Intracardiac blood volume-dependent electrical signals are generated using between seven and twelve equidistant cylindrical electrodes on the conductance catheter. Intervening electrodes are used to measure voltages generated by an alternating current between electrode pairs (30 μA at 20 kHz). The blood volume measured between two adjacent sensing electrodes may be considered to be a series of stacked cylinders of varying diameters with boundaries defined by the endocardial surfaces of the ventricle and equipotential surfaces of the catheter. A change in conductance during ventricular contraction in any one of these cylinders is brought about by a change in the resistance between two sensing electrodes as a result of the change in cross sectional area of each cylinder. The total

ventricular volume is therefore represented by the sum of stacked cylindrical volumes, similar to the Simpson's method used in echocardiography and CMR. The relationship between resistance and cross-sectional area of the cylinder is given by:

$$R = \rho L/A$$

where R = resistance, ρ = blood resistivity, L = interelectrode distance, A = cross-sectional area.

Conductivity (G) represents the reciprocal of resistance (G = 1/R) and therefore the time-varying conductance of the blood (Gt) within each of the ventricular segments is calculated from the applied current divided by the potential difference between consecutive electrodes. The relationship between the time-varying volume (Vt) between consecutive electrodes and time varying conductance (Gt) is given by the formula below:

$$Vt = 1/\alpha \,.(L2/\rho).(Gt - Gp)$$

where Vt = time varying interventricular volume, α = dimensionless slope factor (calculated using a reference cardiac output – this arises due to non-uniformity of the electrical field within the RV), L = inter-electrode distance, ρ = blood resistivity, Gp = conductance of structures outside the ventricular blood volume, Gt = time varying conductance.

Inevitable electric field dispersion extends beyond the RV boundary. To correct for this, parallel conductance (Gp) extending outside the ventricular blood pool has to be subtracted. Gp is best derived by the saline dilution technique whereby a brisk infusion of a bolus of 10% hypertonic saline is delivered to the RV to cause a brief increase in ventricular conductance (Baan et al., 1984). The apparent increase in RV volume whilst conductivity of surrounding structures remains constant (Figure 1.4) enables a theoretical point (A) to be plotted where ESV and EDV are equal and flow equals zero. The conductance signal at this point represents that attributable to structures outside the RV wall. The derived volume (Vc) is described by the intercept of the EDV/ESV regression against the line of identity and is subtracted to give absolute RV volume for each segment.

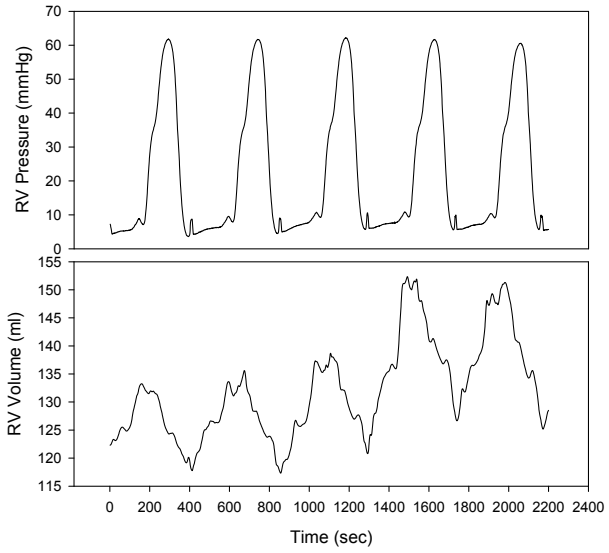

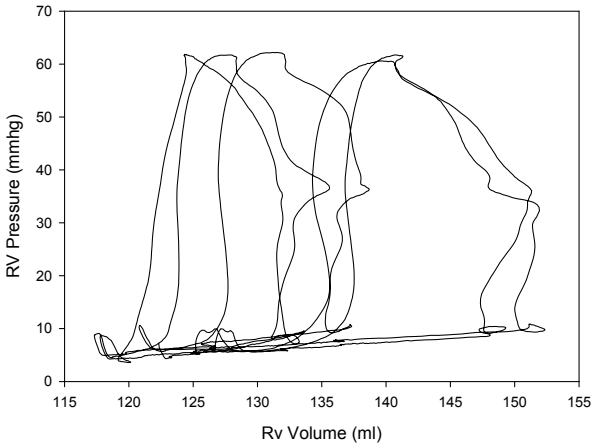

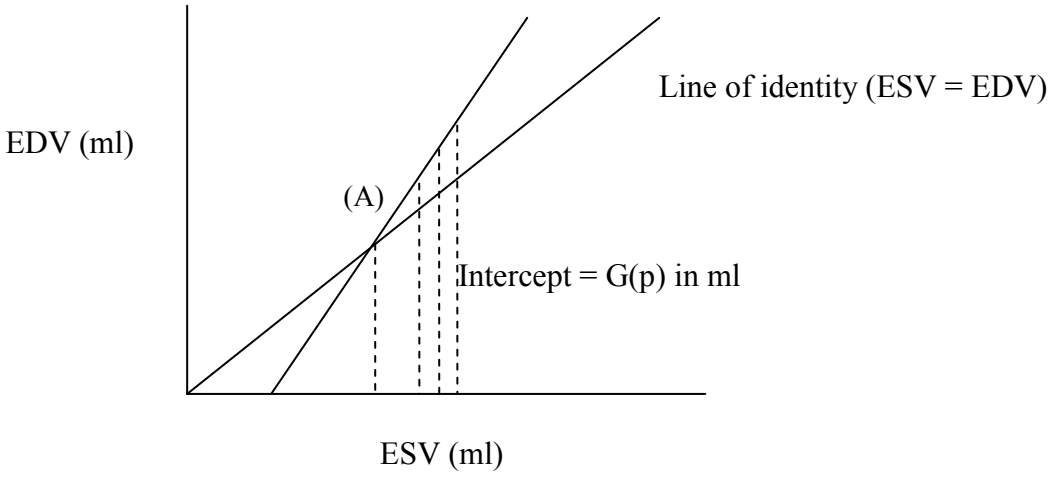

Figure 1.4

Calculation of parallel conductance; the catheter senses an increase in conductivity during hypertonic saline wash-in converting an electrical signal to change in V(t). EDV and ESV are then plotted for each beat. Linear regression of this line extrapolated to the line of identity intersects at a point where ESV = EDV. This volume is due to current conducted through structures surrounding the ventricle.

1.3.3 RV applications of Pressure Volume Catheterisation

Arguably the greatest strength of PV catheterisation is the capability to assess load-*independent* contractility of the RV. Contractility is defined by maximal end-systolic elastance (Ees) of the RV which is derived from the gradient of the end-systolic pressure volume relationship (ESPVR). This is best achieved by obtaining a family of PV loops during preload or afterload alteration (Figure 1.5). Frequently this has been achieved by Inferior Vena Cava balloon occlusion but an alternative method using single-beat estimation of Ees has emerged offering a less invasive approach (Figure 1.6). The single beat method however requires further validation in humans.

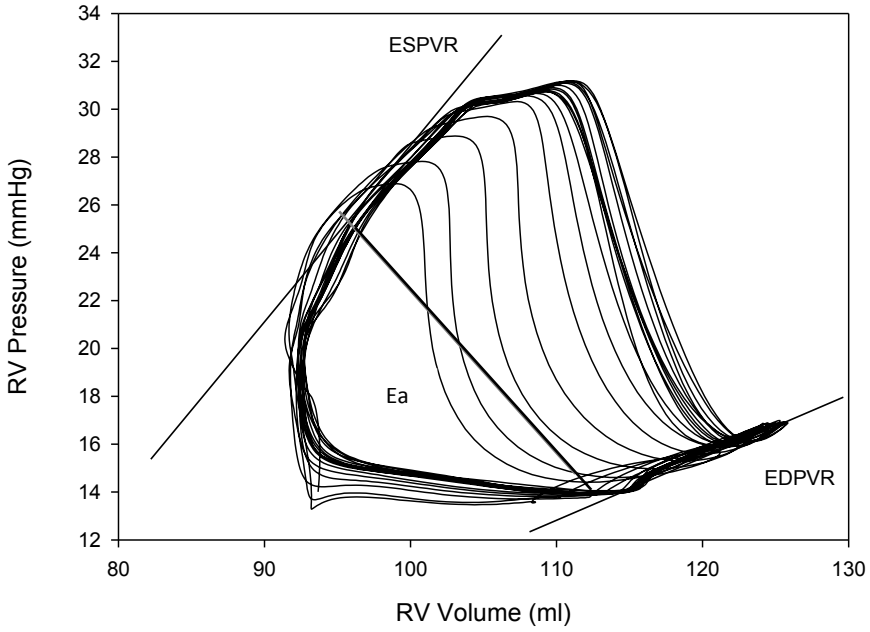

Figure 1.5

Pressure volume loops generated during preload reduction showing the derivation of ESPVR, the end diastolic pressure volume relationship (EDPVR) and Ea which is derived from the gradient of the line connecting the end-systolic point and end diastolic point of the PV loop.

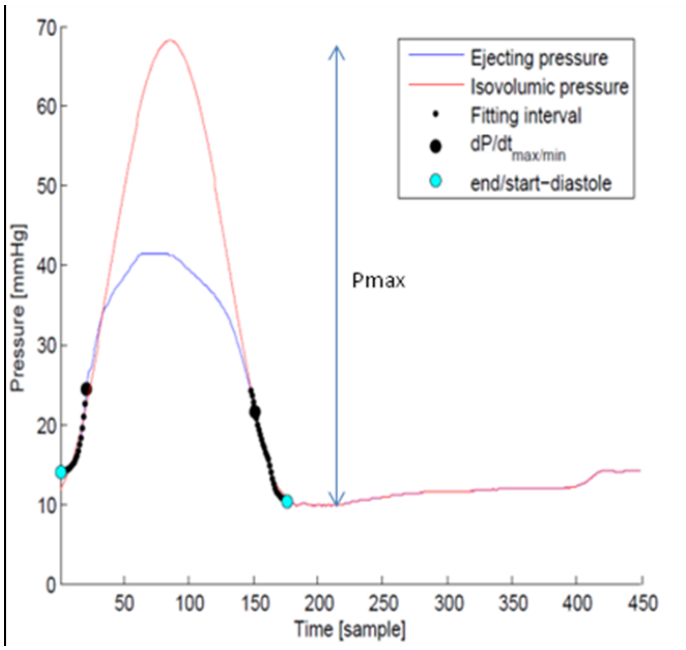

Figure 1.6

Single beat estimation of isovolumic Pmax using an extrapolated sinusoidal curve fit. The amplitude of the 'theoretical' pulmonary artery pressure wave is derived from non-linear extrapolation of the early and late systolic isovolumic portions of the RV pressure curve. This is calculated from dP/dt_{max} and dP/dt_{min} channels (black dots) with Pmax representing a theoretical pressure at maximum peak isovolumic contraction (against infinite resistance). The end systolic point (maximum P/V) is used with Pmax to derive the gradient Ees.

Effective arterial elastance of the pulmonary artery (Ea) is a parameter that offers a more complete assessment of RV afterload than PVR. Ea encompasses resistance, compliance and backward reflected waves from branch points in the pulmonary circulation. It is derived from the gradient of the line adjoining end-systolic and end-diastolic points of the PV loop (Figure 1.5) and is proportional to pulmonary artery wall stiffness (compliance (Ca)). Pulmonary artery compliance can be estimated from flotation catheterisation parameters using the pulse pressure method (Ca = stroke volume / pulmonary artery pulse pressure) although Ea is a more useful conglomerate of afterload.

The concept of 'matched' ventricular and vascular function, so called 'ventriculo-arterial (VA) coupling' has evolved since its first evaluation from PV loops in an isolated canine heart (Sunagawa et al., 1983). VA coupling may be derived by dividing Ees by Ea and describes the energetic efficiency of the RV- pulmonary artery interaction (Brimioulle et al., 2003; Maughan et al., 1979; Suga and Sagawa, 1974; Sunagawa et al., 1983). Optimal coupling ratios have been identified

between 1.0 and 2.0 (Sagawa, 1988) and this relationship demonstrates remarkable cross-species conservance (Wauthy et al., 2004). Uncoupling of Ees/Ea to values less than 1.0 is associated with high afterload states leading to RV inefficiency and inevitable RV dysfunction. In addition to VA coupling efficiency, the conductance technique also offers detailed functional analysis on the systolic and diastolic properties of myocardial performance. These are further outlined in Table 1.2.

Conductance parameter	Units	Definition	Significance	Notes
Systolic				
Stroke Work	mmHg.ml	Area enclosed by PV loop	Work performed by the ventricle to eject stroke volume into pulmonary/systemic circulation	Surrogate for kinetic energy within the RV
dP/dt $_{max}$	mmHg/s	Maximum rate of pressure change in the RV	Index of systolic contractility/performance – a higher value indicates better contractility	Strongly influenced by preload, afterload, heart rate and hypertrophy
Preload Recruitable Stroke Work (PRSW)	mmHg/ml	Linear regression of stroke work with EDV.	Slope of the PRSW relationship is highly linear and represents ventricular contractility.	*Independent* of preload and afterload. Reduced slope values signify reduced contractility
Ees (ESPVR)	mmHg/ml	End systolic elastance of the ventricle.	Describes the maximum pressure developed by the ventricle at any given volume. Shifts up and leftwards with increased inotropy.	Preload/afterload - *independent* measure of contractility. Unaffected by heart rate.
Diastolic				
dP/dt $_{min}$	mmHg/s	Maximum rate of pressure decline	Index of diastolic relaxation – a higher value indicates a more compliant ventricle	Strongly influenced by preload, afterload, heart rate.
Tau	ms	Time of exponential decay of pressure during isovolumic relaxation	Higher values imply prolonged relaxation/ impaired diastolic filling	Heart rate dependent with shortening at higher HR.
EDPVR	mmHg.ml	Slope of the EDPVR represents the reciprocal of ventricular compliance	Describes passive filling of the ventricle by slope of minimum EDP for given EDV.	Impaired ventricular filling results in smaller EDV for a given EDP.

Table 1.2

Parameters obtained by conductance catheter and their relative strengths and weaknesses. EDP = end diastolic pressure.

McKay used a conductance catheter to observe a beat by beat fall in stroke volume following Valsalva (McKay et al., 1984). Further early clinical application came in the optimisation of pacemaker device settings with description of RV volume in response to heart rate variation and arrhythmia control (Khoury et al., 1989; Maloney et al., 1992; Schaldach, 1990). The acute effects of RV ischemia on RV PV loop morphology were also derived from conductance (Bishop et al., 1997b). Bishop et al showed that right coronary artery occlusion caused an upward leftward movement of the end diastolic pressure volume relationship (EDPVR) that normalised on reperfusion thus intimately linking RV ischemia with reversible induction of RV diastolic dysfunction. Intra-operative evaluation of RV contractility during cardiopulmonary bypass using conductance was subsequently shown to be attenuated in the early postoperative phase highlighting important subclinical changes in perioperative RV performance (Brookes et al., 1998). The conductance catheter has also been applied to the study of valvular heart disease in a pediatric population showing pulmonary regurgitation can be quantified by the increase in RV volume during RV diastole (Chaturvedi et al., 1997). In this study, conductance showed good agreement with regurgitant fraction measured by magnetic resonance phase velocity mapping.

Human VA coupling mismatch has been observed in patients with Tetralogy of Fallot implicating a maladaptive RV response to chronic volume overload (Latus et al., 2013). Right to left resynchronisation of diastole has also been shown to improve RV stroke volume in a patient population with CTEPH, indicating dynamic ventricular interdependence communicating via the shared septum influences RV performance (Hardziyenka et al., 2011). Conductance catheterisation of non-sedated patients with scleroderma-related pulmonary vascular disease recently pointed to intrinsic RV systolic dysfunction in scleroderma. This is overlooked by routine haemodynamic assessment and suggests primary myocardial involvement in this disease that is not seen on echocardiography (Tedford et al., 2013).

1.3.4 Cardiac Magnetic Resonance

Cardiovascular magnetic resonance (CMR) is currently considered the non-invasive reference gold-standard for comprehensive assessment of global RV function. Its advantage over echocardiography is the ability to provide multiplanar high-resolution images unaffected by factors such as body habitus, concomitant lung disease, and chest wall deformity albeit with increased cost and reduced availability. The summation disc method used for calculation of RV volume, mass, and function are highly accurate, and reproducible, making CMR well suited for serial follow up (Grothues et al., 2004). Other parameters such as ventricular mass index (VMI): the ratio of RV to LV mass are less robust as the initial study demonstrating strong correlation with mPAP determined by RHC has not been consistently replicated (Roeleveld et al., 2005; Saba et al., 2002).

Velocity encoded phase-contrast sequence can provide reliable measurements of stroke volume, cardiac output and valvular regurgitation. A reduction in the average main pulmonary artery velocity to below 11.7 cm/sec has a sensitivity of 92.9% and specificity of 82.4% for detection of PH (Sanz et al., 2007). Pulmonary arterial distensibility index can predict the functional capacity with 100% sensitivity and 56% specificity when a cut- off value of 10% is used to assess response to vasodilator therapy (Jardim et al., 2007). Innovative real-time MRI-guided catheterisation has also been used to construct RV pressure-volume loops, which in combination with simultaneously measured pulmonary artery flow volumes derived from velocity-encoded cine MRI allows estimation of PVR (Kuehne et al., 2004).

CMR RV data can also be used for prognostication purposes. CMR-derived RV volumes predict mortality both at baseline and during follow-up in patients with PH, making CMR an invaluable tool for monitoring treatment response (van Wolferen et al., 2007). Other CMR based markers of prognosis include paradoxical septal motion which can be visually assessed on cine imaging. Myocardial tagging is employed for more objective evaluation of 3-dimensional motion and cardiac deformation. Although segmental functional quantification is feasible, it is technically demanding and

time consuming and hence not routinely performed. Likewise, it is possible to measure RV diastolic functional parameters such as isovolumic relaxation time and diastolic filling but large clinical trials are needed for validation.

Additional information on RV function is also available by studying patterns of delayed contrast enhancement using gadolinium. Typically, there is focal enhancement in the insertion of the RV free wall into the septum where there is increased mechanical stress (Figure 1.7) (Blyth et al., 2005). The extent of fibrosis correlates with RV dysfunction but its prognostic significance is less certain.

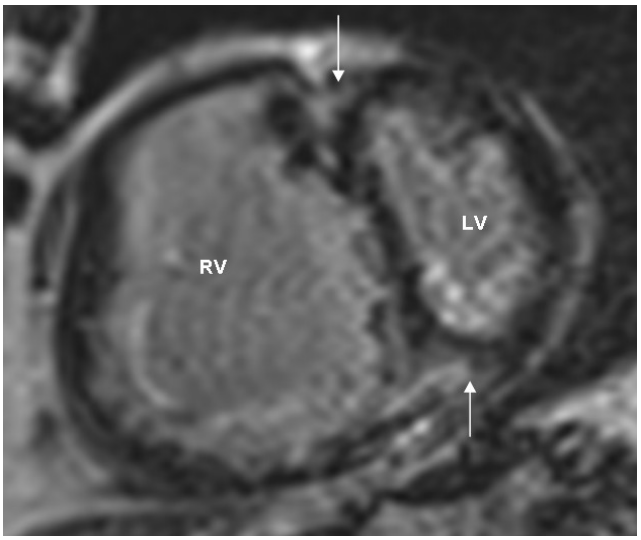

Figure 1.7

Short axis MR image from a late gadolinium sequence in a patient with pulmonary arterial hypertension demonstrating focal enhancement in the basal RV insertion sites (thin arrows). The right ventricle (RV) is enlarged and hypertrophied with flattening of the inter-ventricular septum.

In spite of its many advantages, the widespread adoption of CMR for routine clinical use is affected by reduced availability of equipment and expertise and high cost. Prolonged acquisition times with multiple breath-holds hinder its usage in very sick patients. Other pertinent limitations include the presence of CMR-incompatible devices such as pacemakers as well as claustrophobia.

1.3.5 Echocardiography

Echocardiography is often the first imaging modality to be used on any patient presenting with suspected PH. Echo is accessible, safe and cost effective and offers three important non-invasive aspects in RV assessment: RV dimensions, RV function and velocity-derived pulmonary artery pressures, thereby aiding in diagnosis, risk stratification and monitoring of therapeutic interventions. Two-dimensional (2D) imaging of the RV requires the integration of several imaging views due to the RV's complex 3D structure. Thus, calculation of RV volume using 2D echo is limited. 3D echo techniques continue to develop and are comparable with the CMR derived gold standard (Figure 1.8A) (Leibundgut et al., 2010; Niemann et al., 2007; van der Zwaan et al., 2010). Studies have consistently demonstrated that RV volumes are 20-34% smaller than MRI. This discrepancy may in part be due to limitations of endocardial border detection and tracking capabilities of current software.

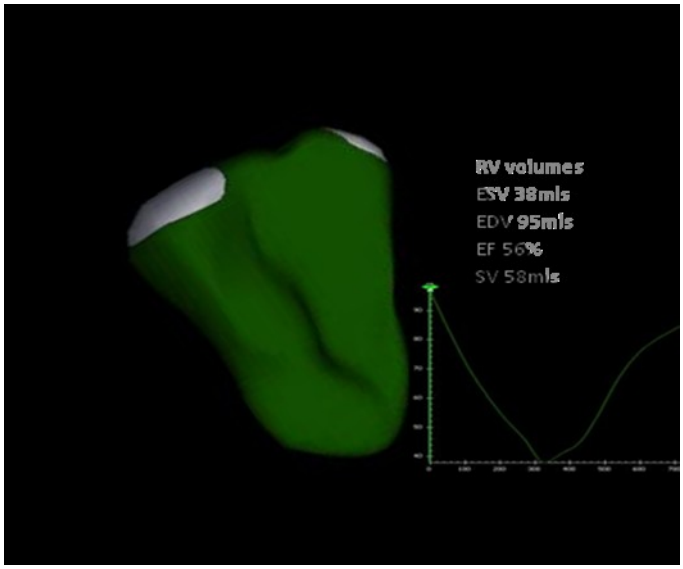

A

Figure 1.8

RV volumes measured by 3D echocardiography (TomTec (Unterschleissheim, Germany))

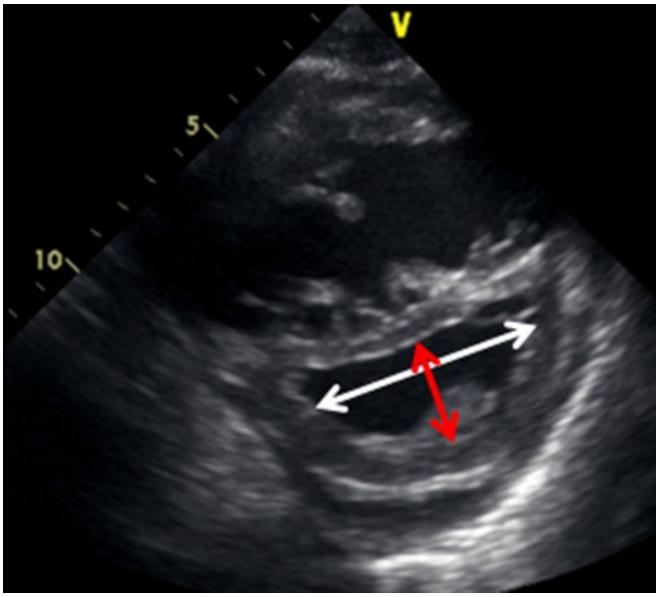

B

Figure 1.8

Eccentricity index measurement from a transthoracic parasternal short axis view in end systole. Red arrow (D1) measures left ventricular cavity dimensions and the white arrow (D2) measures dimension perpendicular to this plane. Ratio D2/D1 >1 is abnormal and represents RV overload (when in end systole, it indicates 'pressure' overload; in end diastole, 'volume' overload).

Abnormal RV-LV interaction can be assessed by detecting paradoxical interventricular septum (IVS) motion. This characteristic helps define the types of diseases that affect the RV. Pressure overload causes systolic septum flattening and volume overload causes diastolic septal flattening that can be quantified by the LV eccentricity index (LV EI) defined as the inferior-anterior free wall distance divided by the septum-lateral free wall distance measured in the short axis at the level of the mitral chordal transition. An abnormal EI value that is > 1 results in a D-shaped LV (Figure 1.8B).

Quantitative volumetric assessment of RV function by 2D echo modalities relies on surrogate markers and includes long axis function (M-mode and tissue Doppler imaging), fractional area change and RV index of myocardial performance, the latter providing a global estimate of both RV systolic and diastolic function since it includes isovolumic periods within its calculations. No single measurement has been validated in different conditions and hence a combined approach integrating several measurements is advocated (Rudski et al., 2010)

Similar to the LV, RV diastolic dysfunction lends important insight into early disease when abnormal contractility may not be evident. Diastolic dysfunction is a marker of poor prognosis in many RV pathologies and usefully reflects response to pharmacological interventions (Sadler et al., 1992; Turhan et al., 2006). Typically a combination of trans-tricuspid inflow Doppler pattern, TDI of the basal RV lateral wall and right atrial size helps describe the severity of RV diastolic dysfunction.

1.3.6 Multidetector Computed Tomography (CT)

Multidetector computed tomography (MDCT) is not a first line technique for RV assessment but can be an excellent substitute when echocardiography and CMR are suboptimal or contraindicated. Unlike CMR, CT data acquisition is fast and can be completed in a single breath hold, making it a more practical choice for sicker patients. The main limitations of CT are exposure to ionising radiation and the need for iodinated contrast medium that can be potentially nephrotoxic and may also influence preload and inotropy.

Non-gated CT pulmonary angiography permits simple structural evaluation such as the diameters of systemic veins and pulmonary arteries (indirect measures of preload and afterload), RV dilatation and hypertrophy, septal deviation and contrast reflux in the IVC. The addition of ECG-gating allows quantitative measurement of cardiac function. Retrospectively gated 3-dimensional CT data yields RV volumes, RV ejection fraction and myocardial mass that show good correlation with echocardiography, radionuclide scintigraphy and CMR (Coche et al., 2005; Dogan et al., 2006; Guo et al., 2010; Plumhans et al., 2008). 3D RV volume measurement on MDCT has been identified as a strong predictor of early death in acute PE (Kang et al., 2011) and an RV/LV score > 1.5 is highly suggestive of severe RV dysfunction and a poor prognosis (Ghaye et al., 2006; Quiroz et al., 2004). However, MDCT has a lower temporal resolution in comparison to CMR and echocardiography and

tends to overestimate RV end systolic volume, subsequently underestimating stroke volume and RV ejection fraction (Sugeng et al., 2010).

1.4 Human Genome Diversity and Genetic Susceptibility in Rare Disease

1.4.1 Background

The human genome consists of roughly 3.2 billion nucleotides, packaged inside cell nuclei as a polymer covered by octomeric units of histones. With the exception of identical twins, no two humans share identical genomes with on average 0.1% difference in genomic content between individuals. In every genome there are approximately 4 million variants termed DNA sequence variants (DSVs) which confer factors such as susceptibility to disease, clinical phenotype and treatment responses. DSVs can be subdivided into single nucleotide polymorphisms (SNPs) and structural variants (SVs) the latter tending to affect greater numbers of nucleotides. This occurs through rearrangements of large sections of DNA that may increase or decrease the number of copies of a particular gene. These are referred to as copy number variants (CNVs). There are estimated to be approximately 3.5 million SNPs per genome of which about 10,000 are likely to be non-synonymous, that is, encode for a change in amino acid (Marian, 2012a). A further two thirds of non-synomymous variants are predicted to exert deleterious effects on downstream protein products meaning they are of potential interest when looking for functionally important variants in complex phenotypes.

In addition to inherited variants, it is estimated that approximately 30 DSVs per whole genome arise *de novo* that is, not inherited from either parent (DePristo et al., 2011). These variants are responsible for the continuous introduction of new variants into the genetic pool. Recent rapid expansion of the human population within the last few centuries makes it likely that a large number of DSVs are relatively new (Tennessen et al., 2012). This is thought to occur because newer alleles have not been

subjected to the evolutionary filtering effect of purifying selection. The human genome therefore is likely to contain a large (and previously underestimated) number of new and therefore 'rare' DSVs. Their interaction with more common and by inference 'older' DSVs underpins the modern study of human genetic susceptibility in complex disease.

Complex phenotypes may result from the additive effects and interactions of both environmental factors and numerous causative alleles, each with variable genetic susceptibility effects. These effects are likely to range from miniscule to highly significant although the majority most probably lie somewhere in between and thus only harbour modest effect sizes (Marian, 2012b). It follows that alleles of more recent genetic origin are more likely to have greater effect sizes than older alleles as they have been spared selective filtration in successive populations.

By convention, alleles are categorised as common by minor allele frequency (MAF) > 5% , infrequent (1-5%) and rare (<1%) in terms of population prevalence. As observed for Mendelian disease, that is disorders arising due to a defect in a single gene, DSVs exerting large effects are expected to be rare (<1%) (Bamshad et al., 2011; Pritchard, 2001). However, considering rare DSVs as a whole, it has also been anticipated that the majority may have weak or no discernible effect. This is akin to the most common DSVs in the population which are also likely to harbour only negligible effects. The population distribution of rare and common alleles therefore has important bearings on the design of genetic studies of complex phenotypes.

Historically, candidate gene approaches based on *a priori* knowledge of specific genes involved in disease pathogenesis have been adopted to examine genetic susceptibility. In IPAH, linkage-based analyses of families with multiple affected family members have been able to pinpoint mutations in the BMPR2 gene that are responsible for a significant proportion of heritability (Deng et al., 2000; International et al., 2000). Where studies of affected family members have not been possible, a 'pathway-based' approach to the selection of candidate genes has been suggested as a potentially valuable sequencing strategy. This is based on the apparent clustering of causative variants in

different genes on the same or related pathways (Thusberg et al., 2011). Examples include rare mutations associated with autism and schizophrenia in multiple genes within neurosignalling pathways (Sebat et al., 2007; Walsh et al., 2008).

So called genome wide association studies (GWAS) typically depend on the common disease-common variant (CD-CV) hypothesis of genetic variation. This predicts that common disease-causing DSVs can be found across all human populations which manifest a given disease. The GWAS approach uses arrays that focus on common genetic alleles (MAF>5%). However, although GWAS have been highly successful in identifying novel disease-associated loci, most associated variants confer relatively small increments in risk (OR 1.1-1.5) and taken together explain only a small fraction of known disease heritability (Schork et al., 2009). Indeed, for the majority of complex traits studied to date, less than 10% of their genetic variance is explained by common polymorphisms identified through GWAS (Manolio et al., 2009). Further challenges have been the difficulty in identifying functional and causative variants in regions of association, and the uncertain biological significance of many variants detected by GWAS.

Attention has more recently shifted to the alternative common disease-rare variant (CD-RV) hypothesis which posits that multiple rare variants with larger effect sizes are the principle determinant of heritability in complex disease, thus accounting for the 'missing heritability' of common disease (Eichler et al., 2010; Manolio et al., 2009). These variants are not sufficiently frequent to be captured by current GWAS arrays, and their effect size is insufficient to be detected through linkage analysis of multiple affected family members. Examples of common conditions which have been described in association with multiple, rare large-effect mutations include breast cancer, inherited hearing loss, lipid metabolism and neuropsychiatric disorders (McClellan and King, 2010).

1.4.2 Whole exome sequencing

High throughput sequencing has emerged as the principle method of identifying rare variants which influence disease risk. High throughput sequencing uses simultaneous polymerase chain reaction (PCR) amplification of many hundreds of millions of DNA fragments, physically separated from one other, which are then attached to the flow cell of a sequencing platform. These fragments are then sequenced in parallel with the flow cell to determine the order of nucleotides in each separate fragment simultaneously. The last five years have seen widespread adoption of this technique as a novel approach in human complex disease genetics (Kiezun et al., 2012). This is in part due to the precipitous drop in the cost of DNA sequencing and the capability to identify all DSVs using this technique, with the possible exception of large CNVs. The approach of whole exome sequencing involves selectively sequencing only the complete *coding* regions of the genome - the 'whole-exome'. Although this strategy ignores potentially causative variants in *non-coding* regions, it is widely presumed that the majority of large-effect variants will be located in coding regions (Choi et al., 2009). This is supported by studies of monogenic conditions – in which approximately 85% of the underlying mutations are located in coding regions or canonical splice sites, as well as strong evidence for purifying selection acting most strongly against protein-coding polymorphisms (Tennessen et al., 2012). As coding regions comprise only 1-3% of the human genome, whole-exome sequencing is a potentially efficient strategy for the identification of rare variants underlying complex disease.

1.4.3 Case selection and sequencing strategy

In the last few years, the identification of homozygous or heterozygous mutations in plausible biological candidate genes has become possible even from small patient cohorts. This may be applied to the study of complex phenotypes with perhaps the most important step lying in the choice of samples to be sequenced. In most instances, the greatest potential lies in the sequencing of samples

with an extreme outcome, best defined as samples at the extremes of a trait distribution. By excluding known modifiers which may include age, sex or comorbidity, the potential genetic contribution to the phenotype can be maximised (Guey et al., 2011; Xu et al., 2011). A second approach is to sequence the exomes of large cohorts with complex disease, a method which may substantially increase statistical power (Kiezun et al., 2012). However, at present, the costs of such projects remain prohibitive and given the difficulty collecting sufficient sample numbers in rare conditions, this method is restricted to the largest centres.

1.4.4 Quality control and Variant Calling

The processing of high throughput sequencing data requires specialist expertise and computational biologists to handle the huge amounts of data generated. Figure 1.10 outlines the principle steps in this process.

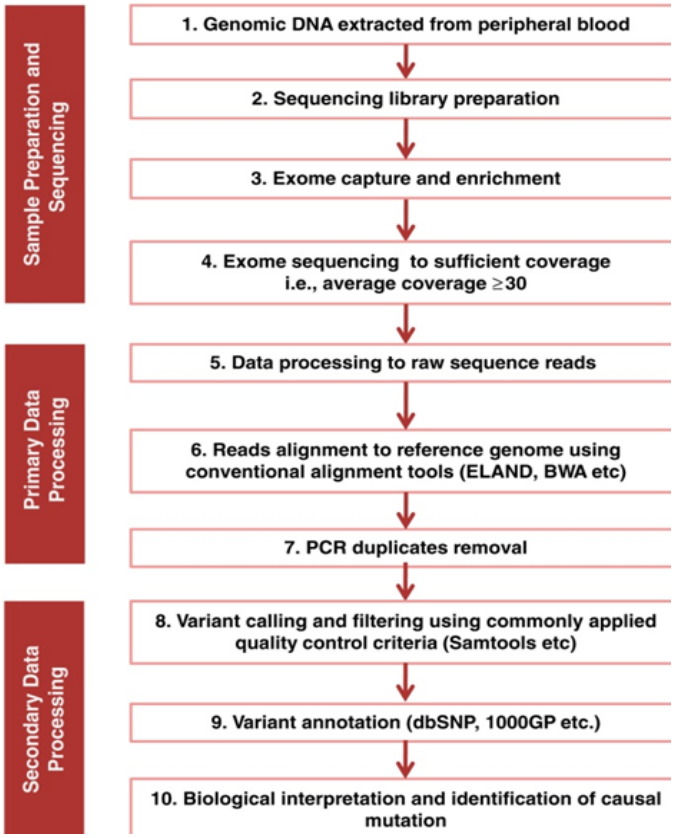

Figure 1.9

Typical exome processing pipeline (Ku et al., 2013)

Raw sequence reads undergo processing first to ensure that read sequences can be translated into high quality genotypes for each sequenced sample. Secondly, filtration of DSVs narrows down the list of candidates to more manageable numbers. Numerous methods are available to filter DSVs and typically depend on the trait under study, inheritance pattern and study population. However, a common goal with each filtration strategy is the aim of pinpointing clusters or even single DSVs that lead to pathological protein mutation. One of the most common and powerful filtration steps used in familial sequencing involves prioritisation by mode of inheritance. Figure 1.11 shows that heterozygote and homozygote DSVs vastly reduce DSV number and can segregate in roughly equal numbers.

DSV quality control involves application of bioinformatic steps initially to establish thresholds for optimal base calling that assign a confidence that base quality is reliable. Following several quality control filters for DNA contamination, short sequence reads are aligned to a reference genome allowing calibration of base-quality scores and removal of duplicate reads. This stage allows regions that are either poorly mapped or that have low base quality readings to be reprocessed computationally. Once overlapping reads have been aligned, variant sites are analysed for differences from the reference genome. Machine-learning based classifiers distinguish variants likely to be polymorphic from those that represent base call artefacts. Alternatively, a manual approach using predetermined quality cut-offs can be used in studies with smaller numbers.

Mapping quality metrics and depth of sequence coverage ultimately determine whether DSVs constitute true genetic variation or false positive variation. Further checks are made to ensure the number of DSVs per individual are as expected. This may include the number of synonymous and non-synonymous variants and the proportion of stop or splice-site variants per individual. Transition-transversion ratios describe the number of transitions (A to G, G to A and C to T, T to C) in relation to the number of transversions (A to C, A to T, G to C, G to T) and should lie over 2.0 for non-synonymous variants with values over 5.0 expected for synonymous variants (Carr et al., 2013; Isakov et al., 2013).

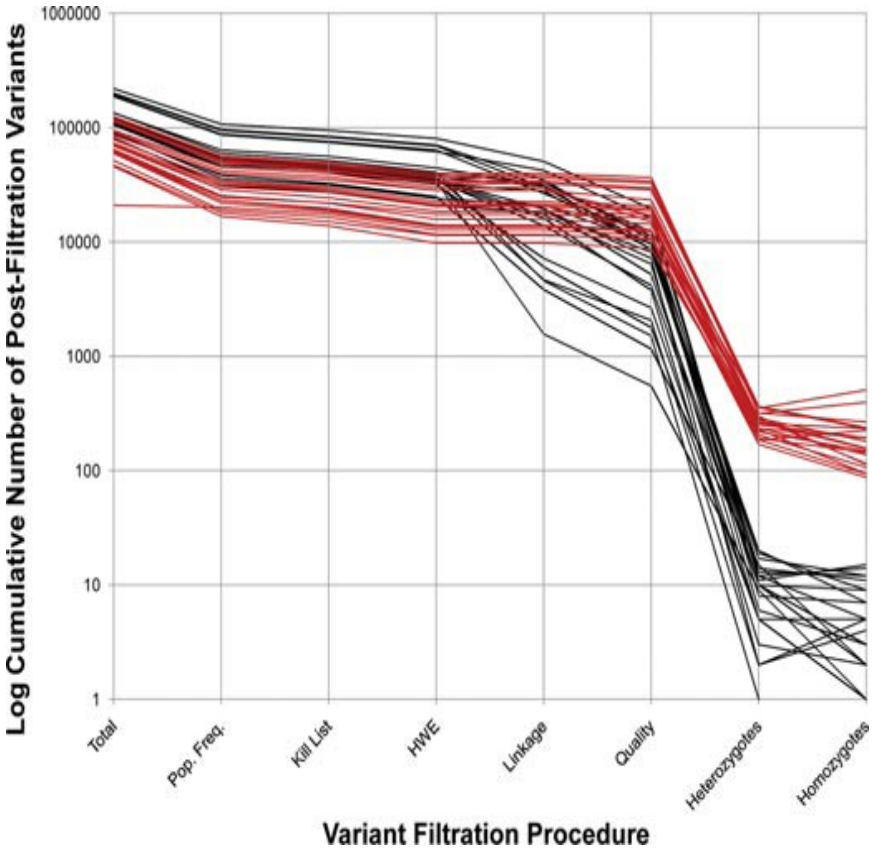

Figure 1.10

Filtration by mode of inheritance acts as a powerful tool to narrow down the genetic target (Majewski and Rosenblatt, 2012)

1.4.5 Statistical association analysis relating to rare DSVs

Analysis of rare variants poses challenges and several strategies have been proposed in the recent literature (Stitziel et al., 2011). These include aggregation of variants, identification of variants that have a causal effect on disease, prediction of their functional consequences, and evaluation of their individual and joint contributions to disease. Unlike common polymorphisms, which have typically been analysed individually, analysis of rare and unique alleles requires their aggregation as a class and then comparison of 'mutational load' within the same gene for a given individual. Combining results at the gene level, even if different loci are genotyped, can therefore be applied to increase statistical power. Bioinformatic tools such as *Polyphen* are available to classify variants on the basis of likely functionality and select variants for statistical analysis that are more likely to have deleterious functional effects (Adzhubei et al., 2010).

1.7 Aims

This thesis approaches CTEPH from a physiological perspective focusing on early RV adaptation and clinical outcome measures in real patients. The genetic architecture of CTEPH is also interrogated using a mutliparalleled sequencing approach that stresses the role of rare genetic variation at phenotypic extremes in this disorder. The genetic study in Chapter 5 contains preliminary data and the discussion places emphasis on data quality rather than raw sequencing output. Two principle objectives of the work at outset were as follows:

1. To interrogate the performance of the RV and pulmonary circulation in CTEPH at different stages of pathological adaptation using pressure volume assessment of RV function and exercise assessment.
2. To employ a novel methodology to the study of genetic predisposition in CTEPH in attempt to further the biological understanding of its aetiology.
3. To improve prognostic prediction tools in CTEPH using a patient centred approach.

Chapters 1 and 2 include the Introduction and Methods and Materials. Chapter 3 describes an invasive catheterisation study of RV function examining the effect of thromboembolic obstruction on pulmonary artery and RV performance. The effects of thromboembolic obstruction in patients with exercise limitation and normal haemodynamic profiles are further interrogated in chapter 4 using cardiopulmonary exercise testing (CPET) to evaluate mechanisms of exercise limitation. In this study, the presence of haemodynamically-confirmed PH is shown to be predicted through use of non-invasive exercise assessment, which may have value in the serial assessment of younger patient populations. Exome sequencing data in CTEPH is presented in chapter 5 in a study attempting to uncover novel and potentially damaging genetic variation in this disease. Finally, chapter 6 focuses on patient-centred outcomes, increasingly relevant to the management of chronic lung disease, which are shown to have predictive value on prognosis in two subtypes of PH.

Chapter 2. Material and Methods

2.1 Conductance Catheterisation and Catheter Calibration within the RV

Chapter 3 involves conductance catheterisation of the RV to determine parameters of systolic and diastolic RV function and contractility. Conductance catheterisation of the human RV is a challenging technique and has been more commonly employed in the study of LV function. RV geometric characteristics challenge the assumption that its internal dimensions can be approximated to a series of stacked cylinders. However, conductance theory has been extrapolated to the RV (Dell'Italia and Santamore, 1998) although to date the majority of clinical RV studies have taken place under general anaesthesia. This affords investigators greater control of breathholding required for volume measurements during the ventilatory cycle and minimises artifact arising from chest wall movements in the awake patient.

2.1.1 Method of RV Conductance Catheterisation

Conductance catheterisation of the RV was undertaken immediately following routine Swan-Ganz catheterisation (7Fr) via a femoral or jugular approach. Swan Ganz catheterisation was required in all study participants as part of their clinical assessment. To calibrate for cardiac output, thermodilution was used as the reference derived from the Swan-Ganz catheter. All study participants undergoing conductance studies were non-sedated and no haemodynamically altering medications were given during any procedure. Prior to placement of the conductance catheter, blood resistivity was determined by Rho cuvette. A 6 Fr 8-electrode conductance catheter (Millar Instruments; Houston, TX) was inserted through the vascular sheath then advanced under fluoroscopic guidance across the tricuspid valve towards the RV apex. Catheters were placed along the longitudinal axis of the ventricle to optimise the pressure volume signal. Correct placement was confirmed fluoroscopically

(Figure 2.1) and by monitoring segmental volume phase relationships and counter-clockwise pressure volume loop genesis. Catheter calibration was performed according to the technique described by Baan et al (Baan et al., 1981). Parallel conductance volume (Vc) was measured using the hypertonic saline injection technique through a side-channel port. At least two measurements of Vc were made using 5mls 10% hypertonic NaCl and the results averaged. The coefficient α was calculated as the ratio between conductance catheter-derived cardiac output and the reference cardiac output. Pressure volume recordings were acquired at end-expiration during breath hold and only steady state measurements were analysed. The proximal end of the conductance catheter was connected to an MPVS Ultra signal-conditioning unit (Millar Instruments) and Labchart 7 Pro was used to calibrate the conductance signal through a Powerlab 16/30 A-D converter (AD Instruments).

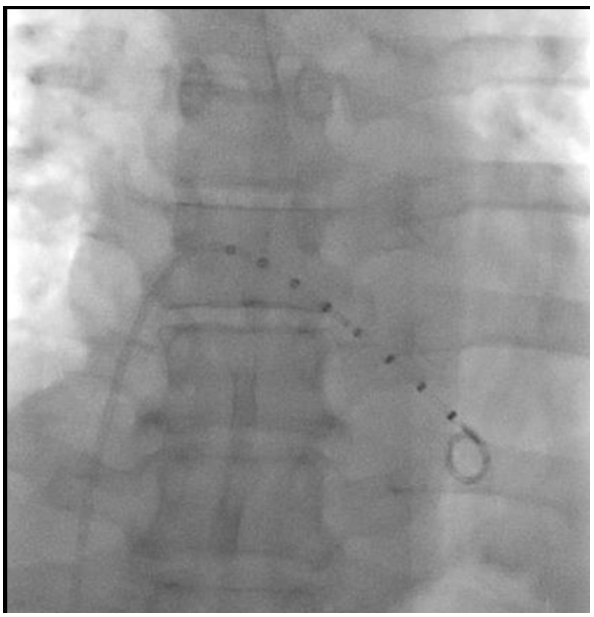

Figure 2.1

Conductance catheter placed via the femoral vein under fluorscopy into the RV

2.1.2 Conductance Output Parameters

Conductance catheter data were analysed off line by reviewers blinded to patient's diagnostic group. Conductance signals were calculated using the conventional single field excitation which assumes homogeneity in the RV electric field. Systolic function was assessed by RV stroke work index (RVSWI), dP/dt_{max} (maximum rate of isovolumic pressure increase) and Ees. Diastolic function was assessed by dP/dt_{min} (maximum rate of isovolumic pressure decline) and Tau (τ), the time constant of isovolumic relaxation. Tau (τ) represents the time constant of isovolumic pressure decay and is measured during active myocardial relaxation. It is calculated as a fitted parameter that is exponential to the pressure channel data (Weiss' method), using the following equation: $p(t)= A.\exp(-t/\tau)$ where t is time and A is the 'fitted parameter'. Compliance was calculated using the pulse pressure method: conductance-derived stroke volume/pulmonary artery pulse pressure). Single beat estimation of Ees was carried out in all study participants using a Matlab sinusoidal curve fit algorithm written to estimate theoretical maximum isovolumic pressure from dP/dt_{max} and dP/dt_{min} during ventricular ejection (Chapter 1, Figure 1.3) (Brimioulle et al., 2003). This program was originally written by Professor Anton Vonk Noordegraaf's research group in Amsterdam and then adapted locally to extrapolate from a personalised channel set-up in Labchart 7 Pro.

Ees was taken as the gradient from theoretical maximal isovolumic pressure (Pmax) to the end-systolic point. Ea was taken as the gradient from the end-systolic to end-diastolic points of the pressure volume loop (Figure 2.2). End-systole was defined as the point of maximum pressure/volume toward end-ventricular ejection. Pulmonary valve opening was taken at the onset of ventricular ejection following isovolumic contraction.

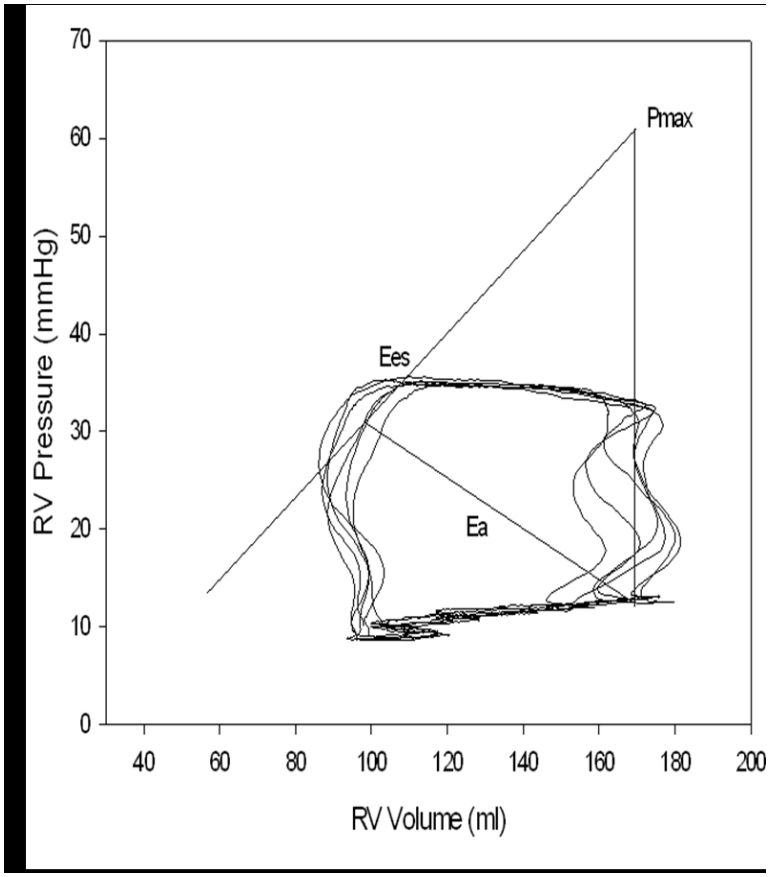

Figure 2.2

RV pressure volume loop showing parameters of RV – pulmonary arterial coupling, Ees and Ea. The ratio Ees/Ea provides an index of the mechanical efficiency of the interaction between RV and pulmonary artery.

2.2 Cardiac Magnetic Resonance

Chapter 3 involves a volumetric comparison between RV volumes obtained by conductance catheter and CMR. CMR imaging was performed on a 1.5-T system (MAGNETOM Avanto®, Siemens Healthcare, Erlangen, Germany). Images were acquired using a phased-array torso coil with retrospective cardiac gating achieved with a vector-ECG system. After initial localiser sequences, standard steady-state free-precession (SSFP) technique was used to obtain a contiguous stack of 14-18 transverse slices (dependent on the size of the heart) covering the RV from the base to apex during

breath-holds at end-expiration. The following scan parameters were used: slice thickness 8 mm with 2 mm slice gap, scan matrix = 200 x 240, flip angle $\alpha = 68°$, repetition time (TR) 42.6 ms with 15 segments giving effective TR of 2.84 ms and echo time (TE) of 1.2 ms (iPAT factor 2). The CMRs were stored on a Cambridge Computed Imaging (CCI, Cambridge, UK) picture archive and communication system (PACS) for subsequent recall and analysis. Measurement of ventricular volumes was performed using a certified software package (Q mass ® MR 7.5, Medis Medical Imaging system, The Netherlands). Endocardial contours were drawn manually for the RV at end-systole and end-diastole in each data set as defined by the smallest and largest endocardial areas. The method of disk summation was then employed to provide volumetric data for the RV in the axial and short axis plane. The moderator band and large trabeculae were included in the myocardial volume area with time varying volumes computed at end-systole and end-diastole.

2.3 Cardiopulmonary Exercise Testing

Chapter 4 evaluates outcome variables from cardiopulmonary exercise testing. The CPET protocol consisted of 1) 2 minutes rest 2) 3 minutes of unloaded pedalling 3) a symptom limited incremental exercise protocol using a 5 to 20W/min work ramp on an electronically braked cycle ergometer. Gas exchange variables were measured breath by breath and averaged over 20 second intervals (Oxycon^{TM} Pro, Carefusion, UK), in accordance with the American Thoracic Society/American College of Chest Physicians Statement on Cardiopulmonary Exercise Testing (Ross, 2003). Work ramp was estimated from anthropometric data and patients' functional impairment so as to attain an incremental exercise time lasting 8 to 12 minutes. All patients had to maintain a pedaling frequency of 60–65 revolutions per minute. Flowmeter and mouthpiece volumes were calibrated prior to each test (Bi-directional DVT, Carefusion). Participants were continuously monitored by a 12-lead electrocardiogram and pulse oximeter (Radical-7^{R}, Masimo). Blood pressure was measured at rest, peak exercise and during recovery. Peak aerobic capacity was recorded as the mean value of oxygen uptake during the last 30 seconds of the test. Anaerobic threshold (AT) was determined by the V-

slope method, the lowest ventilatory equivalent for oxygen and end tidal oxygen partial pressure. As for peak VO_2, AT was averaged over 30 seconds. Vd/Vt was calculated by the Bohr equation (Vd/Vt = $(P_aCO_2 – P_eCO_2)/P_aCO_2$, where P_aCO_2 is the arterial partial pressure of CO_2 and P_eCO_2 is the mixed expired partial pressure of CO_2). CPET parameters were analysed at rest, unloaded cycling, anaerobic threshold (AT) and peak exercise. Arterial blood gases were all drawn at peak exercise. CPET was led independently by a technician who had no knowledge of the results of the RHC used to determine a diagnosis of PH.

2.4 Whole Exome Sequencing

Chapter 5 involves whole exome sequencing of twenty patients in attempt to uncover novel DNA variation that accounts for an underlying genetic aetiology in CTEPH. During this two year period of work, rapid developments in sequencing techniques have presented continual challenges to the processing, analysis and interpretation of results. These have included improved measures of quality control of raw sequence data, resequencing of DNA samples found initially to be of inadequate quality and a bioinformatic re-analysis based on several different alignment algorithms. This work was undertaken jointly between an external sequencing provider and more recently the Cambridge BioResource that runs larger sequencing projects of patients with rare diseases. Following sample preparation and DNA extraction, sequencing was initially outsourced to the East Anglia Sequencing and Informatics Hub (EASIH) who offer a full DNA quantification and sequencing service. At outset in October 2011, 20 patients with CTEPH were sequenced using Agilent's Version 1.3 exome capture kit. It was subsequently decided to extend these results by sequencing parents of CTEPH probands in cases where parental DNA was available. This was again undertaken by EASIH and began in December 2012.

2.4.1 DNA extraction and Exome Capture

Genomic DNA from twenty patients with CTEPH was obtained from frozen whole blood samples stored in Papworth tissue bank. Whole blood was transferred from the EDTA tube to a corresponding 50ml centrifuge tube. The EDTA bottle was rinsed with lysis buffer and contents collected to make up a total volume of 40mls. Tubes were spun at 2500 rpm for 10 min following which the supernatant was discarded into Trigene solution retaining the white blood cell pellet. The pellet was broken with repeat vortexing and re-centrifuged at 2500 rpm for 10 min. Samples were stored at -20C overnight. 24 hours later, 3.5 ml 6 M GuHCl, 7.5M NH_4Ac, 20% Na Sarcosyl and 50 µl 10 mg/ml Proteinase K was used to dissolve the pellet and tubes were incubated in a water-bath overnight. After addition of 2ml chloroform, samples were centrifuged and the superficial aqueous layer removed with addition of a further 2ml of chloroform. Tubes of 10 ml HPLC Grade Ethanol containing the DNA were re-incubated at -20C overnight and washed for one further cycle. DNA was resuspended in 400µl TE buffer depending on pellet size.

Parental DNA was obtained through remote collections of saliva which were returned by post. DNA from the saliva was obtained using the Oragene OG-500 DNA self collection system (Genotek Inc., Ontario Canada). DNA extraction form saliva was carried out according to the manufacturer's protocol (http://www.dnagenotek.com/ROW/pdf/PD-PR-015.pdf).

DNA was quantified using a Nanodrop spectrophotometer (Nanodrop, Delaware, USA). Quality was verified on 0.75% agarose gels. For the Nanodrop, the sample application area was cleaned and initialised with 1µl water. 1µl of DNA was applied and the DNA concentration and 260:280 ratio determined. (Nucleic acids and proteins have absorbance maxima at 260 and 280 nm, respectively). Historically, the ratio of absorbencies at these wavelengths has been used as a measure of purity in both nucleic acid and protein extractions. A ratio of ~1.8 is generally accepted as "pure" for DNA; a ratio of ~2.0 is generally accepted as "pure" for RNA. As this method does not distinguish between

double stranded DNA or single stranded DNA/RNA therefore, further quantification was undertaken using Qubit by EASIH.

EASIH provided sequencing library construction, exome capture, sequencing, and the initial bioinformatic analysis of our study. Following library construction, whole exome enrichment was undertaken using the Agilent Sureselect V1.3 sequence capture system which uses custom-designed, biotinylated RNA oligonucleotides for hybridization to the target sequence (Figure 2.3) and the Human All Exon kit uses 120-mer baits designed to tile across more than 37 Mbp of human genomic sequence.

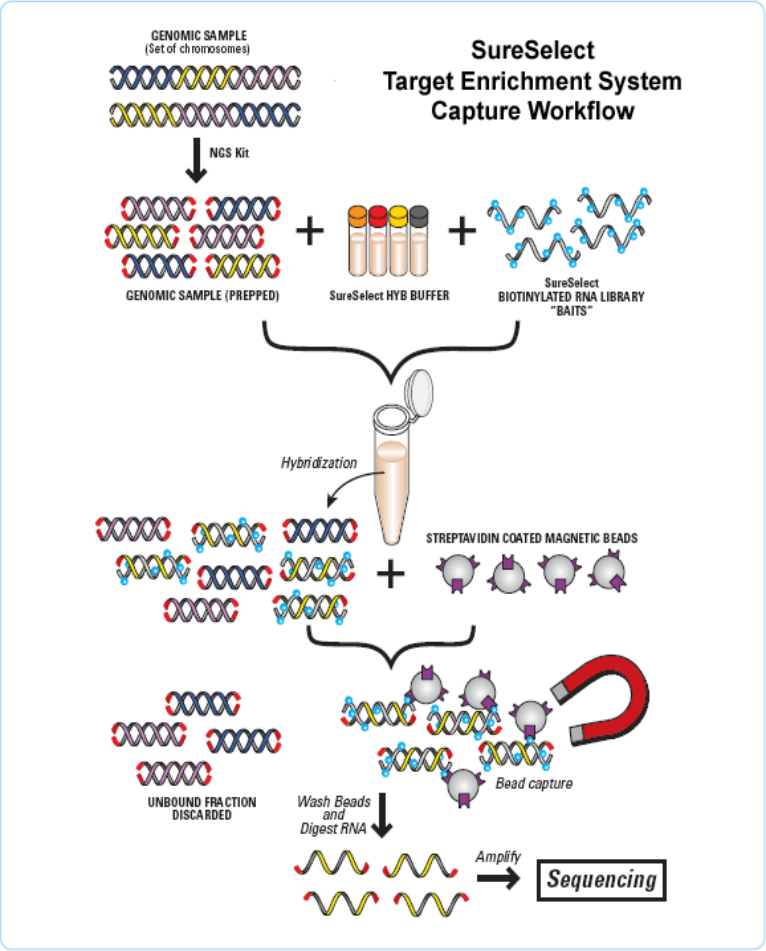

Figure 2.3

Overview of Agilent's SureSelect exome capture http://cp.literature.agilent.com/litweb/pdf/5990-3532EN.pdf).

Following hybridization of library fragments to RNA baits, the bound fragments are captured by streptavidin-coated magnetic beads, and unbound fragments are washed away. After washing to remove unbound DNA, targeted fragments are eluted, amplified and requantified prior to cluster generation and sequencing on an Illumina HiSeq 2000 flowcell in 75bp paired-end runs (Figure 2.4).

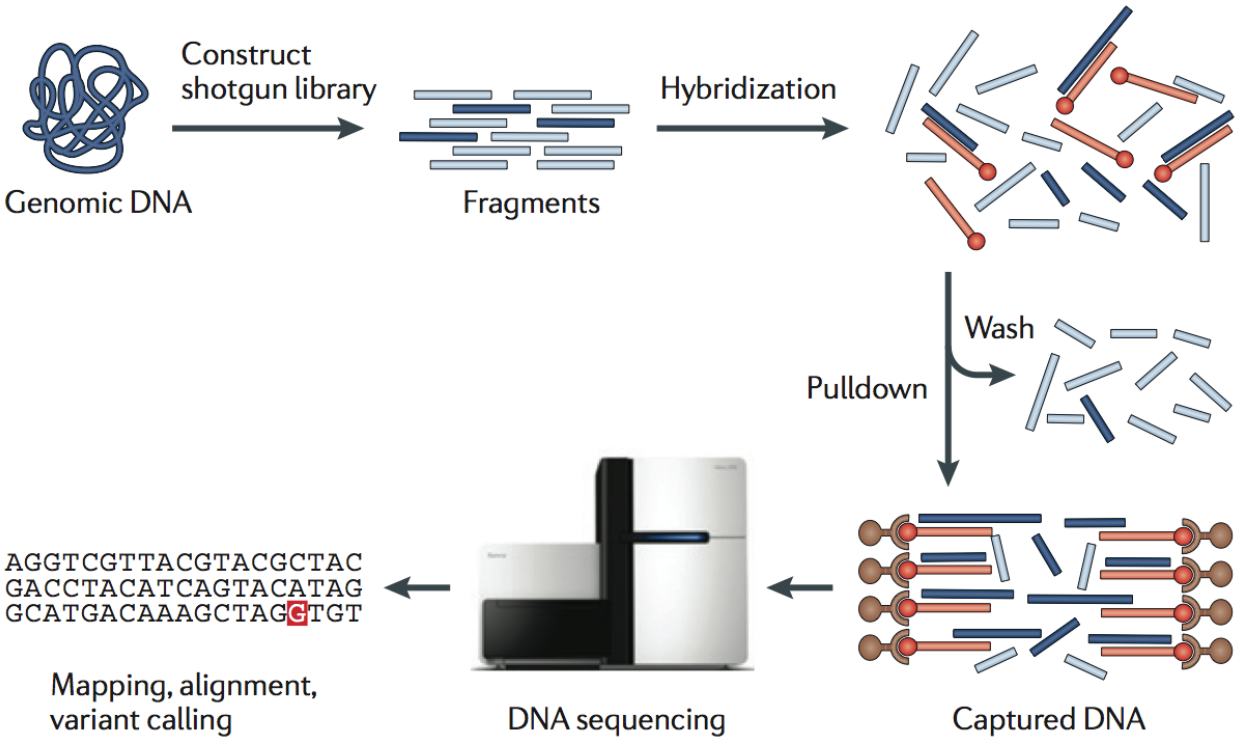

Figure 2.4

Overview of the sequencing workflow. Exome capture takes place following construction of DNA library, prior to the hybridisation stage.

2.4.2 Bioinformatics

In addition to performing targeted exome capture and sequencing, EASIH contributed to bioinformatics analysis. This analysis was largely automated from established workflows set up to

uncover germ line mutations. Within this, raw sequence data was processed using Illumina's RTA and CASAVA pipeline software, which includes image analysis, base calling, and sequence quality scoring. Sequencing reads were aligned to human genome assembly GRCh37 using the short read aligner, Burroughs Wheeler Aligner (BWA). Read mapping statistics describing capture efficiency were derived using GATK. This includes absolute number and percentage of mapped reads on and off-target, target region coverage and the percentage of targeted regions that met coverage criteria (20x depth). Duplicated sequence reads were marked by GATK and removed in Binary Alignment Map (BAM) file format. PCR duplication was quantified for all samples as this can increase the rate of false positive variant calls as well as falsely elevating the degree of target coverage. GATK was used to perform local realignment and quality recalibration relative to the reference genome. This includes corrections of misalignments particularly around insertion/deletion sites which reduces errors in downstream DSV calling.

DSVs were called with the Unified Genotyper following variant quality score calibration in GATK. Only DSVs with a VQSLOD >/= 5 were taken forward to reduce the false discovery rate. DSVs within targeted regions were stored in VCF format and annotated according to variant classification to assess function effects on downstream proteins products. This classification included non-synonymous coding, missense, nonsense, intronic, UTR 5' and 3'. Analysed datsets were examined using the Broad Institute Integrated Genomics Viewer (http://www.broadinstitute.org/igv/) allowing visual and comparative analysis of samples. The process of preferentially selecting pathological DSVs is described in further detail in Chapter 6.

Chapter 3. Right Ventricular Dysfunction in Chronic Thromboembolic Obstruction of the Pulmonary Artery

3.1 Introduction

RV function remains the single most important determinant of patient outcomes in PH with description of changes in RV volume related to time and pressure arguably the most fundamental method of assessment (Champion et al., 2009). The conductance catheter offers simultaneous acquisition of pressure and volume on a beat to beat basis (Baan et al., 1981; Baan et al., 1984; Kass et al., 1986; Suga et al., 1973) and integrates load-independent indices of forward flow with measurement of afterload, a technique widely employed in RV animal models (Brimioulle et al., 2003; Dell'Italia and Walsh, 1988a, b; Leeuwenburgh et al., 2002; Pagnamenta et al., 2010; Solda et al., 1992; Tabima et al., 2010; Wauthy et al., 2005). Ventricular end-systolic (Ees) and effective arterial (Ea) elastance may be derived from RV pressure volume loops and a small number of clinical studies have suggested predominant homeometric (systolic) RV adaptation in response to high afterload (Dell'Italia and Walsh, 1988a; Kuehne et al., 2004; Tedford et al., 2013; Wauthy et al., 2005). In PH, reduced ventriculo-arterial coupling efficiency (Ees/Ea) has also been estimated non-invasively using cardiac magnetic resonance (CMR) (Sanz et al., 2012). The assessment of adaptive ventricular responses relies on accurate determination of cardiac volume and this study uses beat-to-beat changes in RV volume derived from a conductance catheter to describe changes in RV performance not detectable through use of routine haemodynamics.

CTEPH is characterised by an elevated mPAP due to endothelialised thrombotic obstructions of the pulmonary vascular bed that persist despite anticoagulation. However, a proportion of patients presenting with chronic thromboembolic obstructions suffer symptomatic limitation despite a resting mPAP reading below the diagnostic cut-off for PH (mPAP < 25mmHg). These patients are labeled as having chronic thromboembolic disease (CTED) and frequently present with preserved resting RV

contractility and near normal cardiac chamber morphology. Routine RHC conducted at rest yields limited insight into symptom origins in this disease which may originate in part from early RV dysfunction and impaired RV adaptation on exercise (Castelain et al., 2001; Gan et al., 2007). We hypothesised that conductance catheter-derived PV loops could expose different resting RV mechanics in patients with CTED, specifically arising from subclinical RV dysfunction due to 'latent' elevation in RV afterload, not incorporated within routine haemodynamics discerned from fluid-filled catheters. To reassess the accuracy of RV volumes measured by the conductance catheter, we compared conductance catheter-derived volumes in a subset of patients with contemporaneous CMR, widely considered to be the current gold-standard method for measurement of RV volume.

3.2 Methods

Twenty four patients referred to our Pulmonary Vascular Disease Unit were recruited over 15 months for the conductance catheter study. In total, seventeen patients with exertional breathlessness and chronic thromboembolic obstruction of the pulmonary artery underwent conductance catheterisation, 10 of whom fulfilled diagnostic criteria for CTEPH. The remaining 7 had a resting mPAP < 25mmHg despite substantial thrombotic burden (Figure 3.1). These patients were labeled as having CTED and all had sufficient burden of thromboembolic obstruction to justify invasive haemodynamic assessment as judged by their responsible clinician.

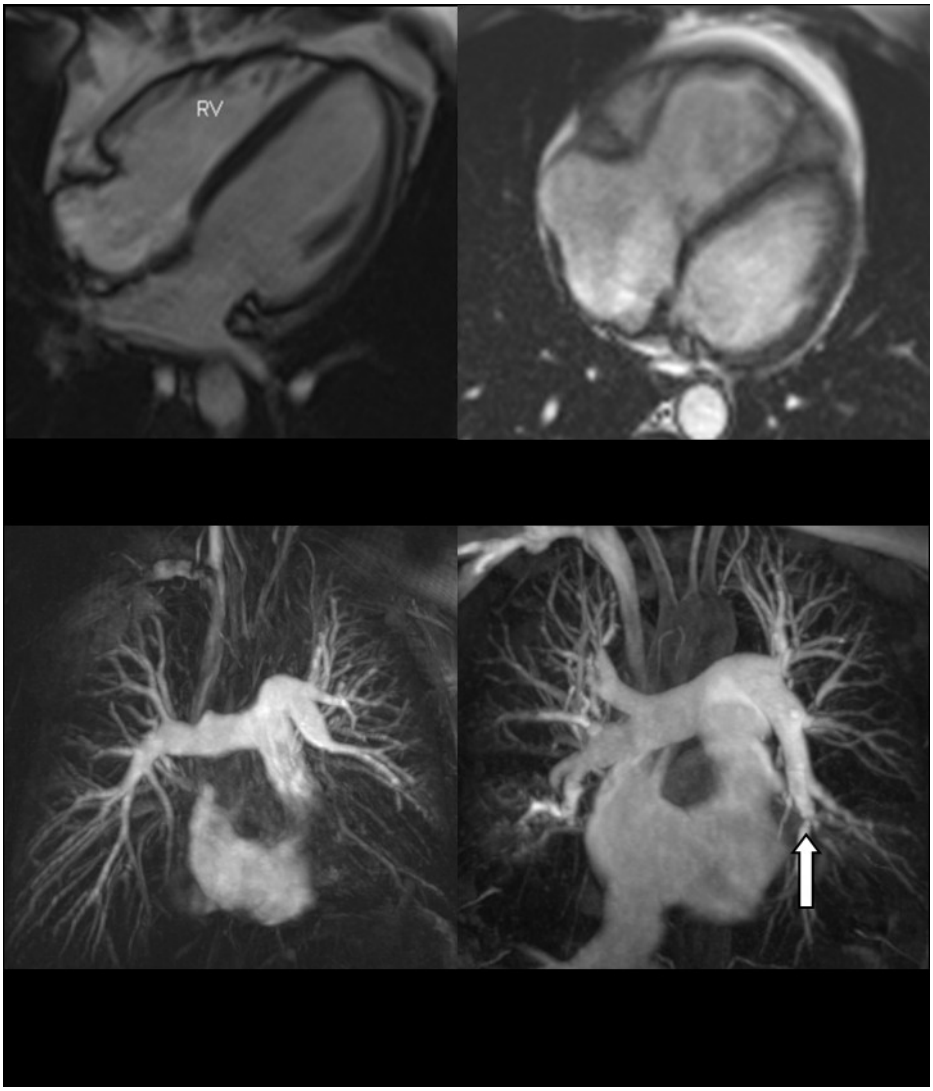

Figure 3.1

CMR images in CTED and CTEPH. A: Four chamber still images from a gradient echo sequence in a patient with CTED (left) and CTEPH (right). The left hand image displays a normal sized RV in comparison to the right hand image showing dilated right heart chambers, RV hypertrophy and septal straightening. B: Maximum intensity projection images from a MR pulmonary angiogram from the same patients with CTED and CTEPH. Left hand image shows proximal occlusion of left lower lobe and segmental middle lobe disease on the right. Right hand image shows proximal web in right upper lobe, complex web in right lower lobe and complex web in proximal left lower lobe with attenuated anterior segment (block arrow).

A further 7 patients who were undergoing closure of a patent foramen ovale (PFO) for prior occurrence of minor neurological deficit were used as controls. These patients had an otherwise structurally normal heart. 8 patients with either CTEPH or CTED were entered into a sub-study comparing RV volumes measured by conductance catheter and CMR performed immediately prior.

No control patients underwent CMR. In CTED and CTEPH groups, in order to exclude RV functional effects beyond those attributable to thromboembolic obstruction, patients clinically limited by other factors were excluded. This was determined on the basis of the following criteria: FEV_1 < 70% predicted, FEV_1/FVC ratio < 70%, suspected intracardiac shunt, BMI > 30kg/m^2, history of angina, evidence of LV systolic or diastolic dysfunction on screening echocardiogram.

Patients with suspected CTEPH and CTED were all in WHO functional Class II/III. Patients undergoing closure of PFO were all assessed as WHO Class I. All patients were admitted to the Pulmonary Vascular Disease Unit over a three to four day period during which time baseline investigations were made and invasive procedures performed. Anticoagulation was discontinued prior to the patient's scheduled admission. On the day of the RHC, patients eligible for CMR underwent scanning as per the protocol described in Chapter 2. Immediately following this, patients were brought to the cardiac catheterisation laboratory to undergo RHC in order to match the preload status and heart rate as closely as possible between procedures. All patients approached for CMR and conductance studies completed both procedures and no patients were withdrawn. Routine blood tests including serum NT-proBNP were drawn and a 6MWD was performed in all study participants within 24 hours of RHC. All patients were in sinus rhythm.

The principles of the conductance technique and catheterisation methods are described in full in Chapters 1 and 2. In patients with CTEPH and CTED, vascular sheaths were removed at the end of the procedure. In control subjects undergoing PFO closure, a general anaesthetic was administered to complete the PFO closure according to local protocols. The study was approved by the local research ethics committee (Cambridge South REC: 12/EE/0085) and the protocol complied with the guidelines of the amended Declaration of Helsinki. All participants gave fully informed written consent.

3.2.1 Statistical Analysis

Stata software (Version 12; Stata Corp, College Station, Texas) was used for statistical analysis. Conductance data was calculated as the mean values of at least 5 cardiac cycles. Continuous data is presented as means ± sd. Comparison between conductance and CMR was assessed by Bland-Altman plots. Prior to group comparison, distribution normality of haemodynamic and conductance parameters was satisfied by the Kolmogorov-Smirnov test. Conductance data was analysed by patient group using repeated measures analysis of variance (ANOVA). When the F ratio of the ANOVA reached a critical p value < 0.05, modified T-tests (Scheffe) were used to compare between groups. To estimate required group sizes, a minimum clinically important inter-group difference in Tau of 10ms (sd 8 ms) was used which, at outset, required 11 subjects in each group ($\alpha = 0.05$, $\beta = 0.20$) (Hoole et al., 2010).

3.3 Results

3.3.1 Intergroup demographics and haemodynamics

Patient demographics and clinical characteristics were well matched between groups and are shown in Table 3.1. Exercise capacity assessed by 6MWD was reduced in CTEPH and CTED groups but not in controls. 6MWD showed no relation to mPAP ($r=-0.03$, $p=0.97$) although mPAP and serum NT-proBNP were strongly related ($r=0.72$, $p<0.001$). Oxygen saturations across right heart chambers and atrial pressures at RHC confirmed no inter-atrial shunting was present in patients with PFOs prior to the conductance study and closure of the PFO. Statistically significant differences were observed between the CTEPH group and the CTED and control groups for mPAP, RV end diastolic pressure (RVEDP) and PVR (Table 3.1). However CTED and control groups were indistinguishable by routine RHC data.

	Controls N = 7	CTED N = 7	CTEPH N = 10
Age, yr	48 ± 10	51 ± 16	50 ± 12
Sex	3F:4M	4F:3M	4F:6M
BMI, Kg/m^2	24.3 ± 1.3	26.2 ± 1.9	26.9 ± 2.9
WHO Class I/II/III	7/0/0	0/7/0	0/7/3
6MWD, m	556±98	411 ± 62*	393 ± 121*
Hb, g/dl	14.0±0.9	14.0±1.4	14.8±0.6
Cr Cl, ml/min	91±13	102±37	99±18
NT proBNP, pg/ml	21 ± 17	57 ± 23	679 ± 1105
Concomitant disease			
-Systemic hypertension	1 (17%)	1 (13%)	2 (20%)
-Diabetes	-	-	-
-Ex Smoker	2 (33%)	1 (13%)	2 (20%)
RHC haemodynamics			
-RA mean	5 ± 2	5 ± 2	7 ± 2
-RV EDP	5 ± 2	5 ± 3	8 ± 2*†
-mPAP	15 ± 3	17 ± 5	43 ± 10*†
-PCWP/LAP	7 ± 2	7 ± 3	8 ± 3
-SvO_2, %	76 ± 3	75 ± 4	72 ± 6
-CI, l/min/m^2	3.2 ± 0.5	2.9 ± 0.3	2.5 ± 0.3*
-SV (td), ml	87 ± 6	80 ± 6	74 ± 5
-PVR, dyn/s/cm^5	110 ± 43	124 ± 39	547 ± 242*†

Table 3.1

Demographic and Haemodynamic data from RHC prior to conductance study. All pressures in mmHg. * $P < 0.05$ compared with Controls, † $P < 0.05$ compared with 'CTED.' Td = thermodilution

3.3.2 Conductance catheter study of CTED, CTEPH and control patients

Typical morphologies of RV pressure volume loops by group are shown in Figure 3.2. Control patients displayed triangular loops with poor distinction of the end-systolic point compared to patients with CTED and CTEPH. During systolic ejection (from pulmonary valve (PV) opening to end-systole (ES)), the pressure differential (δP) discriminated controls and CTED groups (mean δP = -6.3 ± 3.0 (controls), 3.2 ± 3.5 (CTED) and 20.4 ± 18.4 (CTEPH) mmHg respectively), (controls vs CTED, p =

0.03). δP significantly correlated with mPAP (r = 0.61, p < 0.01), PVR (r = 0.63, p < 0.01), serum NT-proBNP (r = 0.70, p < 0.001) and pulmonary artery compliance (r = -0.55, p = 0.01).

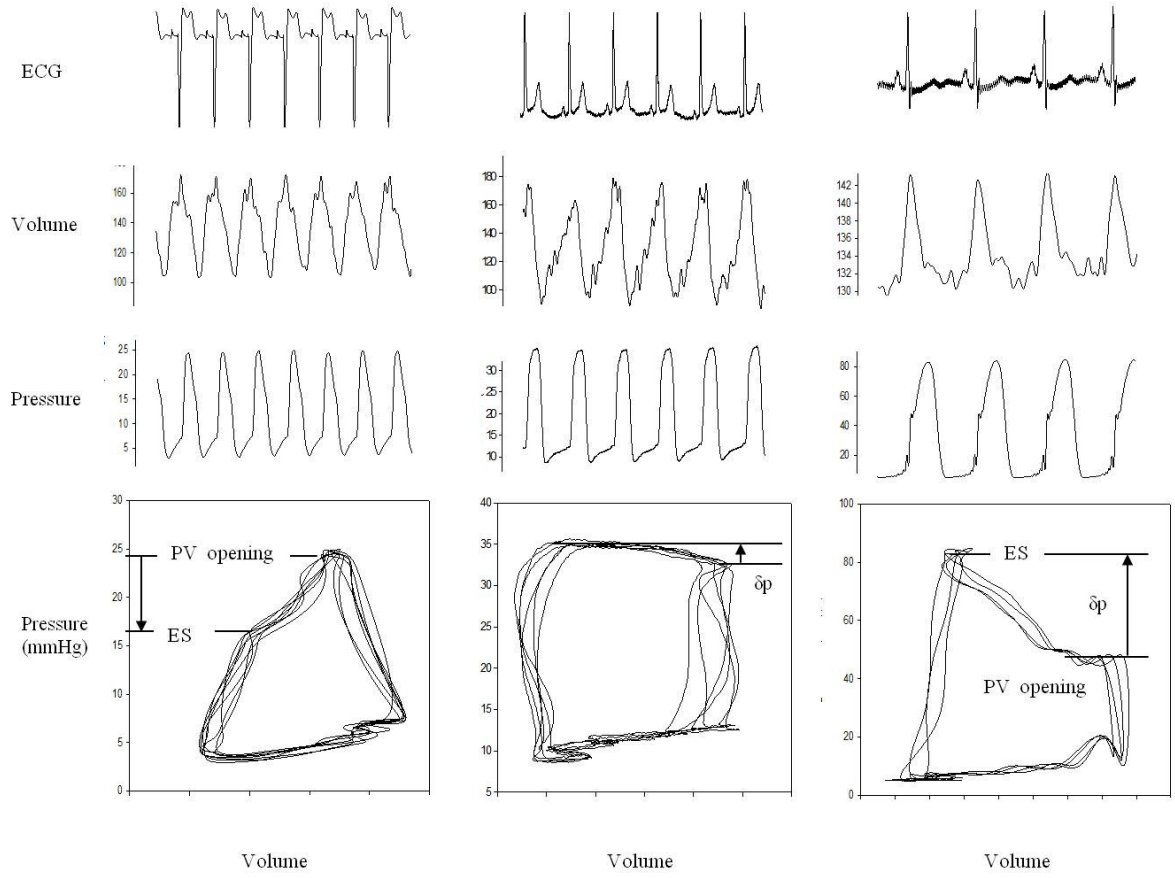

Figure 3.2

A Typical pressure volume loops generated by conductance catheter in the RV during end-expiratory breathhold. Control patients (left) demonstrate triangular RV loop morphology in comparison to CTED (middle) and CTEPH (right) groups. B Pressure differential (δP) during systolic ejection from pulmonary valve (PV) opening to end systole (ES) discriminates disease groups. PV = pulmonary valve, ES = end-systole.

Numerical conductance data is displayed in Table 3.2. RV diastolic parameters showed that Tau was significantly prolonged in patients with CTED and CTEPH compared to controls (p = 0.02). Absolute dP/dt_{min} was highest in patients with CTEPH. dP/dt_{min} showed strong correlation with serum NT-proBNP (r = -0.61, p<0.01). In the CTEPH group, systolic contractility was higher as defined by RVSWI, dP/dt_{max} and Ees. Higher Ees was linearly related to elevated Ea (R^2 = 0.73, p < 0.001) and

inversely correlated to pulmonary artery compliance (r = -0.58, p = 0.01) and 6MWD (r=-0.47, p = 0.03). VA coupling index (Ees/Ea) was lowest in patients with CTEPH and showed a strong inverse relationship to mPAP and PVR (r = 0.75, p < 0.001). Ees/Ea also showed modest but significant correlation with serum NT-proBNP (r = -0.54, p = 0.01). The coefficient of variation for estimated values of Pmax in each patient used to determine Ees lay within a 10% limit.

Conductance Parameter	**Controls (n = 7)**	**CTED (n = 7)**	**CTEPH (n = 10)**
Haemodynamic Indices			
RV Pressure (sys), mmHg	31.0 ± 5.6	35.4 ± 3.4	77.2 ± 11.8*†
RV Pressure (edp), mmHg	4.8 ± 1.4	5.0 ± 1.3	7.6 ± 1.6*†
Pmax (est. using sb model)	43.1 ± 10.4	52.9 ±6.7	98.6 ± 19.6*†
Heart rate, beats/min	71.4 ± 11.7	72.2 ± 8.6	72.0 ± 11.0
Volumes			
End systolic volume, ml	(80 ± 41)	(55 ± 43)	(60 ± 30)
End diastolic volume, ml	(165 ± 39)	(127 ± 55)	(143 ± 38)
Stroke Volume, ml	83 ± 20	74 ± 21	69 ± 17
Systolic Indices			
RVSWI, mmHg.ml/m^2	603 ± 179	653 ± 209	1114 ± 402*†
dP/dt$_{max}$, mmHg/s	394 ± 52	423 ± 124	638 ± 235*†
Ees, mmHg/ml	0.44 ± 0.20	0.59 ± 0.15	1.13 ± 0.43*†
Diastolic Indices			
dP/dt$_{min}$, mmHg/s	-265 ± 40	-435 ± 79	-733 ± 143*†
Tau, ms	56.2 ± 6.7	69.7 ± 10.0*	67.9 ± 6.2
Pulmonary arterial afterload			
Ea, mmHg/ml	0.30 ± 0.10	0.52 ± 0.24	1.92 ± 0.70*†
PA compliance, ml/mmHg	5.7 ± 1.5	4.7 ± 1.6	1.76± 1.05*†
Ventriculo-arterial coupling			
Ees/Ea	1.46 ± 0.30	1.27 ± 0.36	0.60 ± 0.18*†

Table 3.2

Conductance Catheter data by patient group. * P < 0.05 compared with Controls, † P < 0.05 compared with CTED. Bracketed values subject to inaccuracy (see Discussion). sb = single beat.

3.3.3 Conductance and CMR subgroup analysis

RV volumes for individual patients undergoing both CMR and conductance are shown in Table 3.3.

				Haemodynamics							RV volumes (ml)					
ID	**Sex**	**Age**	**Diagnosis**	**RA mean**	**RV EDP**	**mPAP**	**PCWP**	**SvO2 %**	**CI L/min/m^2**	**PVR Dyn/s/cm^5**	**EDV CMR**	**EDV C**	**ESV CMR**	**ESV C**	**SV CMR**	**SV C**
1	M	28	CTEPH	6	7	32	8	71.7	2.2	419	208	123	101	24	107	99
2	F	64	CTEPH	12	12	46	9	58.9	1.8	928	285	283	219	242	66	42
3	M	34	CTEPH	6	8	41	6	73.6	2.6	622	274	106	189	50	85	56
4	F	48	CTEPH	6	6	51	12	71.8	2.5	700	150	135	78	75	72	61
5	F	52	CTEPH	4	5	44	6	76.3	2.6	661	146	171	101	117	45	53
6	M	57	CTED	5	4	15	7	78.0	2.3	157	189	101	105	23	84	78
7	F	69	CTED	5	6	16	10	72.9	2.5	133	88	87	31	36	57	52
8	M	42	CTEPH	9	11	27	10	74.5	2.9	289	148	-	60	-	88	88
				Mean ± sd							186±68	144±67	111±63	81±78	76±20	66±20

Table 3.3

Patient diagnosis, haemodynamics and RV volumes by CMR (Axial plane) and conductance catheter (C)

CMR volumes from axial and short axis planes showed strong correlation for end-diastolic (r=0.98), end-systolic (r=0.97) and stroke volume (r=0.96). Mean heart rates during CMR and conductance catheterisation were not significantly different: 73.2 vs. 75.4 beats per min respectively (p = 0.75). Stroke volume between CMR and conductance catheter showed a mean difference of +9ml (95% CI -1 to 19ml) (Figure 3.3, top), indicating that conductance stroke volume was smaller than CMR stroke volume. Larger biases of +48ml (95% CI -16 to 111ml) for EDV and +37ml (95% CI -21 to 94ml) for ESV were observed (Figure 3.3, middle and bottom). Markedly lower values for EDV and ESV were observed in CTED and CTEPH groups compared to controls. In one patient (ID 8, Table 3.3), significant overestimation of Vc resulted in a negative absolute ESV although stroke volume was still determinable. Mean Vc and α across our 8 patient subset was 86 ± 14mls and 0.35 ± 0.08 respectively.

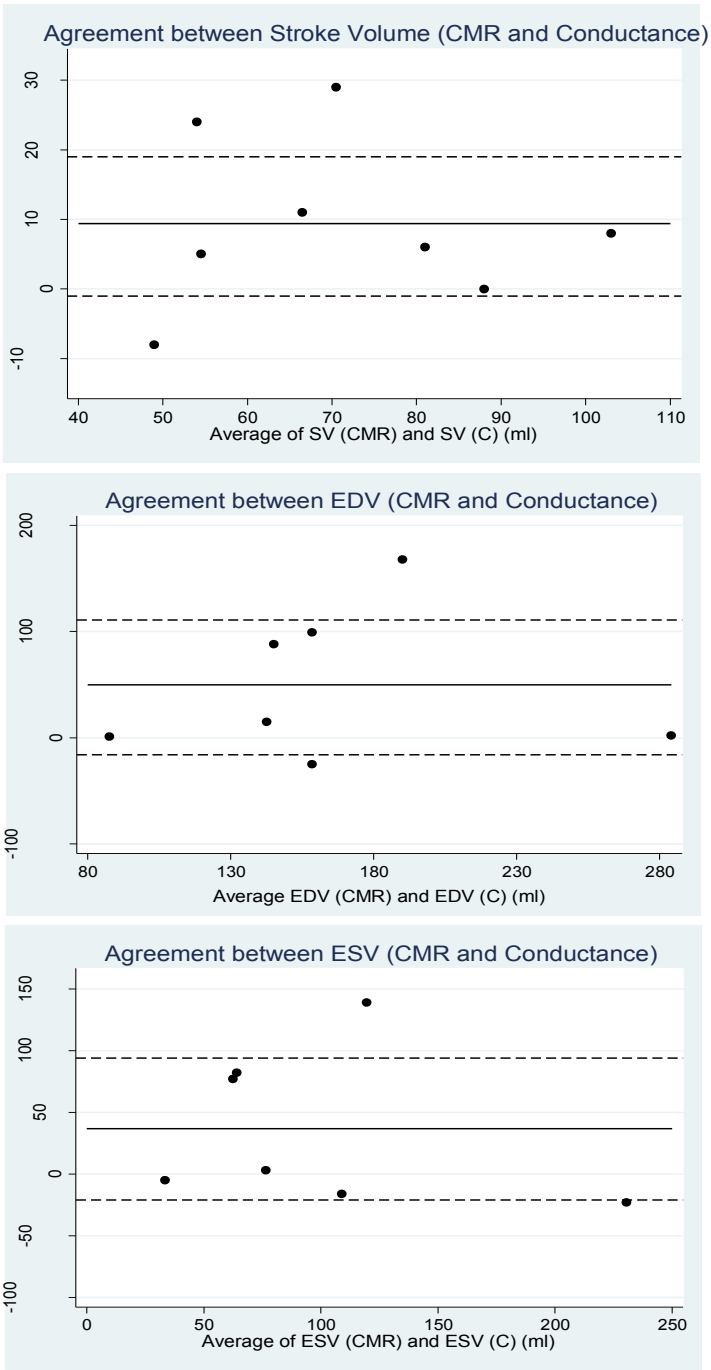

Figure 3.3

Bland-Altman plots of CMR RV volume measurements vs Conductance measurements. Top: stroke volume (SV), Middle; EDV, Bottom; ESV. Thickened black line indicates bias, dashed lines indicate 95% confidence interval. Conductance underestimated EDV and ESV in comparison to CMR whereas SV showed better agreement.

3.4 Discussion

Our results yield novel insight into the RV's dynamic performance in response to chronic pulmonary thromboembolic obstruction. Changes in PV loop morphology in CTED, most notable during systolic ejection, result from elevated RV afterload that develops exclusive of haemodynamic definition of PH. In addition, the RV relaxes more slowly in patients with CTED and CTEPH as defined by Tau. Discrimination in RV diastolic performance between CTED and controls potentially signifies diastolic maladaptation in the RV which in tandem with decreased pulmonary artery compliance may contribute to symptom origins in this condition. Our data for the first time describes homeometric RV adaptation in response to high afterload in CTEPH. This reaffirms the association between elevated RV haemodynamics and reduced ventriculo-arterial coupling efficiency found in previous clinical PH studies (Kuehne et al., 2004; Sanz et al., 2012; Tedford et al., 2013).

3.4.1 Intergroup conductance study

Conductance catheterisation showed 'left ventricularisation' in PV loop morphology in CTED and CTEPH compared to controls; patients with CTED continue to develop RV pressure during systolic ejection similar to CTEPH where increased resistance and lower arterial compliance is exposed to the RV early after pulmonary valve opening. By contrast, control subjects show rapid dissipation in pressure during systole with ejection into a more compliant pulmonary circulation. This may be explained by abnormal afterload elevation in CTEPH and to a lesser extent in CTED (Bishop et al., 1997a). Ea did not statistically differ between CTED and controls which may in part be due to small numbers in each group and its wide standard deviation. However, the trend towards higher Ees in CTED suggests early systolic adaptation in response to higher afterload. We quantified RV performance during systolic ejection using δP which is a function of Ea and demonstrated a relationship to disease severity across all patients (NT-proBNP). δP significantly correlated with PVR

and pulmonary artery compliance which reinforce its association with RV afterload in our patient cohort.

In CTEPH, slower RV relaxation measured by Tau can be attributed to chronic elevation in RV afterload and lower arterial compliance. The RV in CTEPH is stiff which is in keeping with steepening of the end-diastolic pressure volume relationship in experimental models of heart failure and following pulmonary artery banding (de Man et al., 2012; Leeuwenburgh et al., 2002). Notably, Tau was also prolonged in the CTED group. This is unlikely to be entirely explained by RV afterload given broadly similar Ea values in CTED and controls. RV diastolic function may be functionally sub-classified by either a decrease in passive myocardial diastolic compliance or impairment in active RV relaxation. These phases are inter-related and normal diastolic function is dependent on both (Tabima et al., 2010). Given statistically similar values for Ea and pulmonary artery compliance between control and CTED groups, we speculate that our CTED group harbour intrinsic RV diastolic dysfunction in addition to 'latent' elevation in afterload suggested by δP. This is further supported by borderline elevation in absolute dP/dt_{min} in CTED compared to controls, groups that were well matched by preload. The markedly elevated absolute dP/dt_{min} in CTEPH, suggesting more rapid dissipation in RV pressure at onset of diastole, is likely attributable to elevated preload (RVEDP) in this group, as dP/dt_{min} is known to be load-dependant (Leeuwenburgh et al., 2002).

3.4.2 RV Volume physiological analysis

Our data suggest poor determination of absolute EDV and ESV using a conductance catheter in the human RV, but more accurate determination of stroke volume was achieved. Previously, considerable attention has been placed on the accuracy of conductance-derived RV volumes due to increased myocardial trabeculation and its crescentic short-axis shape. Both of these factors can disrupt the uniformity of the conductance field. The observed underestimation of EDV and ESV may be attributable to Vc calculation which appeared overestimated in our patient subset. This results in

inappropriate leftward displacement of the PV loop along the volume axis resulting in underestimation of absolute volumes. However, stroke volume remains relatively unaffected by Vc.

Higher absolute volumes in control subjects may have arisen from volume variation due to catheter position using either the jugular or femoral approach. Catheter insertion from an internal jugular approach results in closer catheter opposition to the RV free wall compared to a femoral approach where the catheter lies more central to the RV long axis (Figure 3.4). Out of clinical necessity, control patients were exclusively studied via a femoral approach compared to only one patient in CTED and CTEPH groups. Dual jugular and femoral approaches have not been previously reported in humans and we speculate that a more centrally placed catheter may offer improved interrogation of the RV outflow tract resulting in improved 'capture' of the RV geometry (Brookes et al., 1998; Kornet et al., 2000). Although not tested in our setting, it has also been suggested dual-field excitation catheters improve the electric field uniformity (Danton et al., 2003), but, to our knowledge, this has not been substantiated in the human RV.

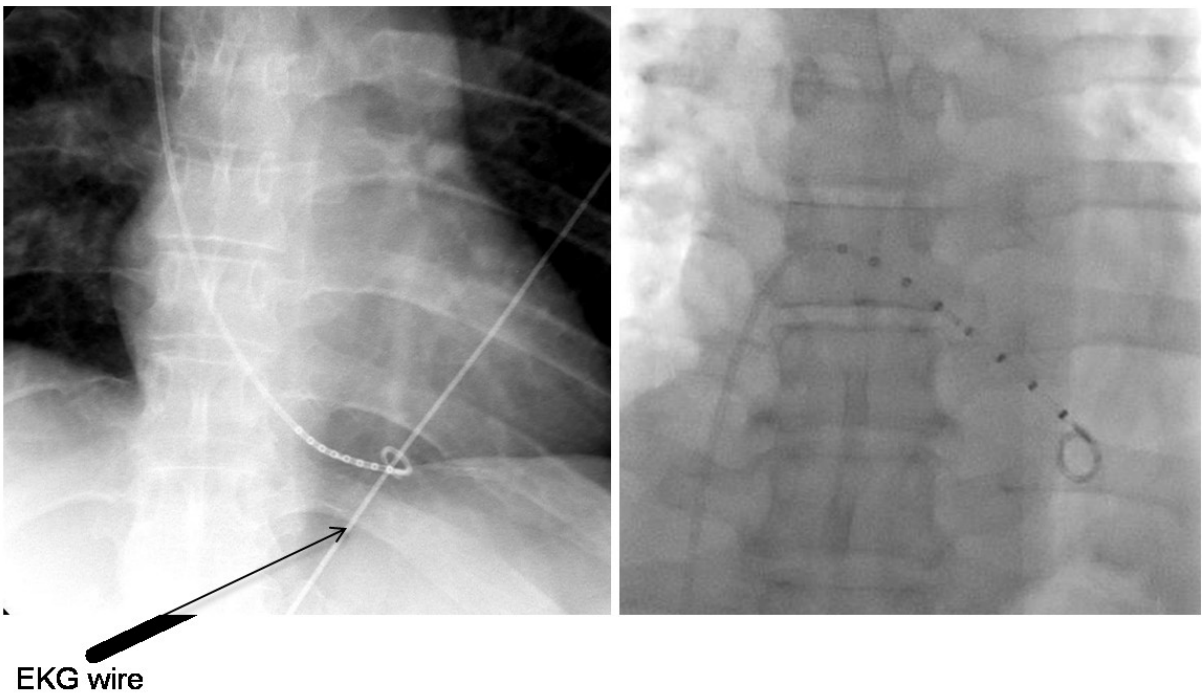

Fig 3.4

Jugular insertion (left) results in closer apposition of the conductance catheter to the RV free wall compared to use of the femoral approach (right).

3.4.3 Mechanisms of impaired diastolic relaxation

One possible origin of diastolic impairment in CTED and CTEPH may be RV ischaemia. Akin to the ischaemic cascade in the LV, RV diastolic impairment may be induced by right coronary artery occlusion and so may be driven by a myocardial oxygen supply demand imbalance (Bishop et al., 1997b). In support of our findings, isolated RV diastolic dysfunction has been purported in a connective tissue disease population with normal resting haemodynamics through stress-induced effects on subendocardial fibres (Faludi et al., 2008). Animal models of early RV dysfunction have also been associated with metabolic remodeling in the RV myocardium where myocardial genetic profiling points to abnormal energy substrate use that is partly independent of chronic pressure overload (Gomez-Arroyo et al., 2013). Very recently, increased collagen and stiffening of RV cardiomyocyte sarcomeres have been implicated in diastolic dysfunction in the human RV in PH (Rain et al., 2013). Future investigations detailing RV functional assessment with tissue gene expression and metabolomics may perhaps offer clearer explanation of our findings.

3.4.4 Clinical implications

Currently the natural history of CTED is poorly defined and it is unproven that patients with CTED deteriorate over time. However, a predisposition to RV diastolic dysfunction observed in our study offers novel insight into the clinical trajectory of patients with chronic thromboembolic obstruction who may be at risk of deterioration. A normal/near normal resting haemodynamic profile fails to account for symptom limitation in this condition suggesting haemodynamic abnormalities may only manifest on exercise. This has to date been investigated in a similar patient population who demonstrate reduced exercise pulmonary arterial compliance following pulmonary endarterectomy despite normalisation of PVR (Bonderman et al., 2011). Pulmonary endarterectomy is an established treatment for CTEPH and almost universally leads to reverse remodeling of the RV. However, this is often incomplete suggesting additional mechanisms of RV dysfunction beyond an increase in

afterload may be contributory. Our data suggest a predisposition to primary diastolic RV dysfunction in CTED and we speculate that patients with CTED may derive uncertain benefit from pulmonary endarterectomy which is currently offered for symptomatic benefit (van der Plas et al., 2010).

3.4.5 Limitations

Our study population derives from a pool of highly selected individuals referred to a tertiary centre for invasive haemodynamic investigation. Therefore, although the dataset is small and carries risk of Type II error, groups were necessarily selected to minimise confounding effects on RV mechanics from conditions such as COPD, LV dysfunction and obesity. Caution should nevertheless be exercised in extrapolating our results to a 'real-world' population with CTED in whom comorbidities may be prevalent. Secondly, RV volume determination using a conductance catheter is challenging with potential error arising from a non-uniform electric field due to fall off in equipotential planes at the extremes of the ventricular boundary. However, our study attempts to address the accuracy of conductance RV volumes in humans using temporal comparison with the most up to date gold-standard method, CMR. In doing so, we have shown acceptable agreement between conductance and CMR techniques for stroke volume determination suggesting conclusions drawn from PV loop dimensions are robust.

Simultaneous right and left ventricular haemodynamic and volume indices were not measured during conductance meaning we cannot comment on ventricular interdependence. However, no patients in our study had echocardiographic evidence of LV systolic or diastolic dysfunction and all had normal pulmonary capillary wedge pressures making a LV contribution to our diastolic findings unlikely. We employed a single beat methodology to derive an estimated Pmax, which relies on mathematical assumptions derived from a large mammal model. To date, this method remains unvalidated in the RV of patients with PH although with use of a Valsalva manoeuvre to alter cardiac load, Ees has recently been generated by a family of loops (Tedford et al., 2013). Lastly, our protocol did not enable wave reflection measurement which may have been contributory to our observations on RV afterload.

3.5 Conclusions

Comprehensive RV assessment by conductance catheterisation detects novel alteration of PV loop morphology and delayed RV relaxation in patients with CTED. However, when referenced to CMR, our method provides suboptimal determination of absolute RV volume. Abnormal resting RV mechanics demonstrated by conductance signify functional adaptation in the RV in thromboembolic obstruction which warrants further evaluation in future studies to establish downstream clinical effects.

Chapter 4. Inefficient exercise gas exchange identifies pulmonary hypertension following pulmonary embolism in patients with chronic thromboembolic obstruction

4.1 Introduction

Chronic thromboembolic pulmonary hypertension (CTEPH) is an uncommon sequela of acute pulmonary embolism (PE) (Becattini et al., 2006; Dentali et al., 2009; Klok et al., 2010; Miniati et al., 2006; Pengo et al., 2004; Poli et al., 2010) although within a CTEPH patient population, antecedent PE may be present in up to 75% (Fedullo et al., 1995; Pepke-Zaba et al., 2011). Patients present with effort dyspnoea predominantly related to incapacity of the RV to increase cardiac output on exercise. Untreated this condition typically leads to progressive RV dysfunction so early detection, ideally using non-invasive methods, prior to physiological decompensation may be advantageous.

Patients with CTEPH present with effort dyspnoea however, a proportion demonstrate mPAP values < 25mmHg at rest despite the presence of persistent chronic pulmonary thromboembolic obstructions. As described in Chapter 3, these patients may be labelled with CTED and usually present with preserved resting RV contractility and normal cardiac chamber morphology. Hence, investigations conducted at rest such as echocardiography may lack power to detect changes suggestive of progression to CTEPH. Assessment of potential attenuation in cardiac output on exercise therefore requires an exercise-based assessment method.

Cardiopulmonary exercise testing (CPET) demonstrates a characteristic profile in PAH (Hansen et al., 2004; Sun et al., 2001). However patients with chronic thromboembolic obstruction are less well described. 6MWD reflects haemodynamic severity in CTEPH but does not inform on mechanisms of exercise limitation (Reesink et al., 2007). Therefore, we hypothesised that CPET could be used to differentiate the exercise profiles of patients with CTED and CTEPH compared to sedentary controls. Following this, we aimed to establish which exercise parameters were predictive of a diagnosis of

CTEPH and potentially therefore of value in the follow up of patients with unresolved PE who are at risk of deterioration. To account for a potential association between proximal thrombotic burden and pulmonary haemodynamics, we quantified thrombotic obstruction in these groups to evaluate for any effect of greater thrombotic load.

4.2 Methods

Patients underwent incremental symptom-limited CPET and RHC within 72 hours. Radiological evaluation with CT pulmonary angiogram was carried out prior to RHC in patients with CTED and CTEPH to confirm a radiological pattern consistent with chronic thromboembolic obstruction. Patients with chronic thromboembolic obstruction were grouped by diagnosis following RHC: mPAP >= 25mmHg (CTEPH), mPAP < 25mmHg (CTED) and compared with age and sex-matched sedentary controls (Controls). Eligibility for study enrolment was determined following patient referral to our unit with a suspected diagnosis of CTEPH. As a prerequisite, study patients had to be symptomatically limited with evidence of chronic thromboembolic obstruction on CT pulmonary angiogram after PE despite at least 6 months anticoagulation with documented treatment compliance. CT pulmonary angiography was undertaken in either the patient's local institution or our own and in all cases was preceded by at least 6 months anticoagulation. All patients were anticoagulated at study entry.

In total, thirty patients were recruited over thirteen months. 5 patients were not enrolled due to screening failure (see Figure 4.1). One such patient was not enrolled due to lack of thromboembolic disease on CT pulmonary angiography following repeat CT scan at our institution. All patients enrolled completed the CPET and RHC and no patients were withdrawn. Asymptomatic age and sex matched sedentary controls underwent incremental CPET only. The CPET protocol is as described within the Methods: Chapter 2. The study was approved by the local research ethics committee

(Cambridge South Ref 12/EE/0085) and the protocol complied with the amended Declaration of Helsinki. All study participants gave written informed consent prior to study enrolment.

Patients clinically limited by factors other than chronic thomboembolic obstructions were excluded. This was determined on the basis of the following factors: FEV_1 < 70% predicted, FEV_1/FVC ratio < 70%, suspected intracardiac shunt, BMI > 30 kg/m^2, history of angina, evidence of LV systolic or diastolic dysfunction on echocardiogram. In addition patients unable to perform cycle ergometry were excluded. The enrolment pathway of patients is summarised in Figure 4.1.

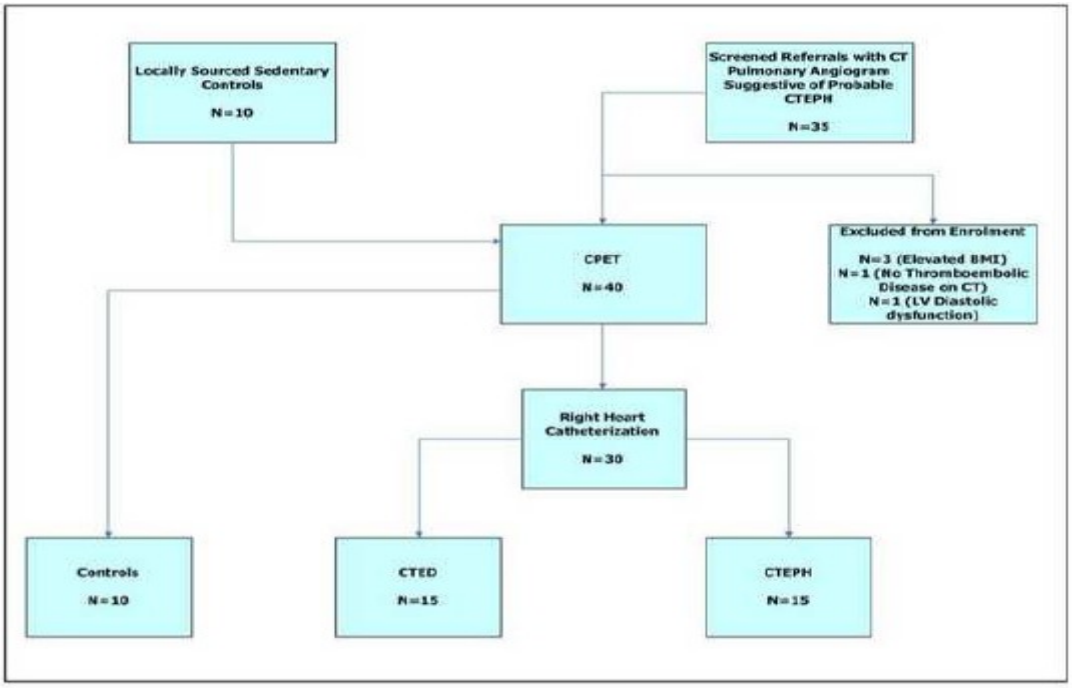

Figure 4.1

Patient enrolment pathway: exercise study

4.2.1 Radiological evaluation

We used a modified Qanadli Index to quantify proximal chronic thromboembolic obstruction as previously described (Hoey et al., 2011). Briefly, a maximal score of 2 was assigned for a patent

segmental artery and its first order subsegmental branches, giving a total possible score of 40 (three branches to both upper lobes, two branches to the middle lobe and lingula, and five branches to both lower lobes). One point was subtracted if there was clear evidence of subsegmental disease, a segmental web stenosis, or segmental partial occlusion. If two or more of these abnormalities were present, a score of 0 was assigned to that segment. Segmental total occlusion was also assigned a score of 0. Laminated thrombus of the main or lobar arteries that exceeded 50% of luminal reduction necessitated the subtraction of 1 from the scores for all segmental arterial branches distal to this point. Total vascular obstructive (TVPO) index was calculated by dividing the patient score by 40 and multiplying the result by 100. Scores therefore represent a percentage of normal (patent) segmental arteries in that patient.

4.2.2 Statistical Analysis

Averaged data are presented as mean ± sd (parametric variables) and unpaired Student's t-test was used to compare between parametric datasets. Non-parametric data was summarised as median and interquartile range. Mann-Whitney test was used to compare non-parametric data. Values of $p < 0.05$ were considered significant. The capacity of CPET parameters to predict a diagnosis of CTEPH was analysed using univariate and multivariate logistic regression. Variables demonstrating discriminatory value between CTED and CTEPH groups with biological plausibility were analysed. A threshold of $p < 0.10$ was set prior to logistic post-estimation receiver operating characteristics (ROC) analysis. In all cases the area under the curve (AUC) was compared with a value of 0.50 and the highest sensitivity and specificity of the predictor variables determined. Statistical analysis was performed using Stata Version 12 (Stata Corp, College Station, TX).

4.3 Results

4.3.1 Patient characteristics

Demographics and RHC data are shown in Table 4.1. At RHC, 15 patients fulfilled diagnostic criteria for CTEPH. A further 15 had a resting mPAP < 25mmHg despite substantial thrombotic burden. Compliance, estimated using the pulse pressure method, was lower in CTEPH. There were 12 ex-smokers in total although none had greater than a 10 pack year smoking exposure. No patients with CTED or CTEPH were taking supplemental oxygen. Patients with CTED and CTEPH suffered both acute and recurrent PE in our cohort. This is further described in Table 4.2. No control subjects reported symptoms consistent with cardiopulmonary disease. 6MWD performed was not different between patients with CTED or CTEPH (p = 0.22).

	Controls N = 10	**CTED N = 15**	**CTEPH N = 15**
Age	46 ± 11	53 ± 17	54 ± 13
BMI	25.1 ± 2.6	26.5 ± 2.7	26.8 ± 3.3
Female/Male	6:4	8:7	7:8
NYHA Class I/II/III	10/0/0	0/14/1	0/13/2
Haemoglobin (g/dl)	-	14.4 ±1.7	14.7±1.9
Cr Clearance (ml/min)	-	100 ± 17	103 ± 23
Comorbidities			
-systemic hypertension	0	2	0
-diabetes	0	0	0
-smoking history	2	6	4
FEV1 (%)	97 ± 10	97 ± 15	89 ± 18
FVC (%)	105 ± 16	104 ± 14	102 ± 16
KCO (%)	-	88.0 ± 18.7	86.8 ± 12.1
RA mean (mmHg)	-	4.5 ± 2.5	7.1 ± 1.9*
RV EDP (mmHg)	-	5.1 ± 2.9	8.5 ± 2.0*
mPAP (mmHg)	-	18 ± 5	40 ± 8*
PCWP (mmHg)	-	7.6 ± 3.1	9.6 ± 2.4
PVR ($dyn.s^{-1}.cm^{-5}$)	-	169 ± 80	541 ± 237*
CI ($L/min/m^2$)	-	2.7 ± 0.5	2.5 ± 0.4
SvO_2 (%)	-	75 ± 5	71 ± 5
Compliance (ml/mmHg/Kg)	-	0.04 ± 0.02	0.02 ± 0.01*
6MWD	-	413 ± 86	368 ± 108
Min SpO2 (6MWD)	-	93 ± 4	92 ± 3
NT-pro BNP (pg/ml)	-	182 ± 349	789 ± 1046*

Table 4.1

Demographics of patients studied with both CPET and RHC. Data presented as mean ± sd * p < 0.05, unpaired Student's T test (CTEPH vs CTED)

	Single/Recurrent PE	Plasmatic factors conferring risk of thrombosis
CTED (N = 15)	12/3	Idiopathic (N = 7) Factor II heterozygosity (N = 1) Low Protein C/S (N = 4) Factor V Leiden (N = 2) APC resistance (N = 1)
CTEPH (N = 15)	9/6	Idiopathic (N = 8) Low Protein C/S (N = 6) Anticardiolipin IgG positive (N = 1)

Table 4.2

Modality of PE presentation and plasmatic risk factors by CTED and CTEPH groups. 'Idiopathic' describes no identified cause on plasmatic screen. APC = activated protein C.

4.3.2 Exercise responses

All patients exercised to symptom limitation and AT was confidently detected in all patients. Exercise capacity assessed by peak VO_2 and peak workload was lower in the CTEPH group compared to the CTED group and in the CTED group compared to controls. The CTEPH group also demonstrated higher Vd/Vt, greater hypoxaemia, higher Ve/VCO_2 slope value, steeper HR/VO_2 slope and lower end tidal-CO_2 (AT) (Table 4.3). At AT, Ve/VCO_2 ratio was higher in the CTEPH group compared to the CTED group and controls (Table 4.3, Figure 4.2). End-tidal CO_2 was lowest in patients with CTEPH with the greatest differentiation between groups seen at AT. Peak O_2 pulse was attenuated in patients with CTED and CTEPH compared to controls (Figure 4.2). Arterial blood gases were obtained in 24/30 (80%) of patients with CTED and CTEPH. For similar pH and serum lactate, $PaCO_2$ did not differ between CTED and CTEPH groups. Analysis of Ve/VCO_2 ratio by end-tidal CO_2 and $PaCO_2$ at peak exercise suggested that Vd/Vt was accountable for the difference in ventilatory efficiency in CTED and CTEPH (Figure 4.3). Systemic BP did not differ between groups at rest, peak exercise or during recovery.

Peak Exercise Parameter (unless stated)	Controls N = 10	CTED N = 15	CTEPH N = 15
VO_2 (ml/Kg/min)	31.6 ± 10.7	20.1 ± 5.8†	15.7 ± 3.7*
VO_2 (% pred)	113 ± 35	94.1 ± 26	74.2 ± 16*
Load (W)	186 ± 62	122 ± 34†	107 ± 37*
RER	1.22 ± 0.10	1.15 ± 0.10	1.13 ± 0.10
Ve (/min)	89 ± 27.5	80 ± 27	75 ± 26
BR (%)	35 ± 22	27 ± 25	27 ± 29
HR (/min)	169 ± 19	155 ± 20	150 ± 15
HRR (%)	5.4 ± 17	12 ± 14	15 ± 11
O_2 pulse (ml)	13.1 ± 4.0	10.3 ± 3.5†	8.5 ± 2.6
HR/VO_2(/litre)	44 ± 12	59 ± 22†	84 ± 27*
Ve/VCO_2 slope	29.25 ± 6.3	37.6 ± 11.2†	46.8 ± 12.2*
Ve/VCO_2(at)	27.0 ± 4.4	37.1 ± 8.0†	45.8 ± 7.4*
End tidal-CO_2(at)(mmHg)	42.8 ± 4.5	31.4 ± 6.9†	26.5 ± 4.3*
pH	-	7.33 ± 0.07	7.34 ± 0.07
pO_2 (mmHg)	-	89 ± 14	75 ± 15*
pCO_2 (mmHg)	-	34 ± 6	35 ± 4
Lactate	-	9.7 ± 3.7	9.4 ± 3.1
Vd/Vt (%)	-	34.5 ± 11.4	50.8 ± 6.6*
Aa O_2 gradient (mmHg)	-	29 ± 16	46 ± 12*

Table 4.3

Exercise response variables for patients studied by RHC and CPET and sedentary controls (no RHC undertaken). Data presented as mean ± sd. RER = respiratory exchange ratio, Ve = minute ventilation, BR = breathing reserve, HR = heart rate, HRR = heart rate reserve, CI = chronotropic index, Vd/Vt = dead space fraction, Aa gradient = alveolar arterial gradient, (at) = anaerobic threshold * $p < 0.05$, CTEPH vs CTED, † $p < 0.05$, CTED vs Controls

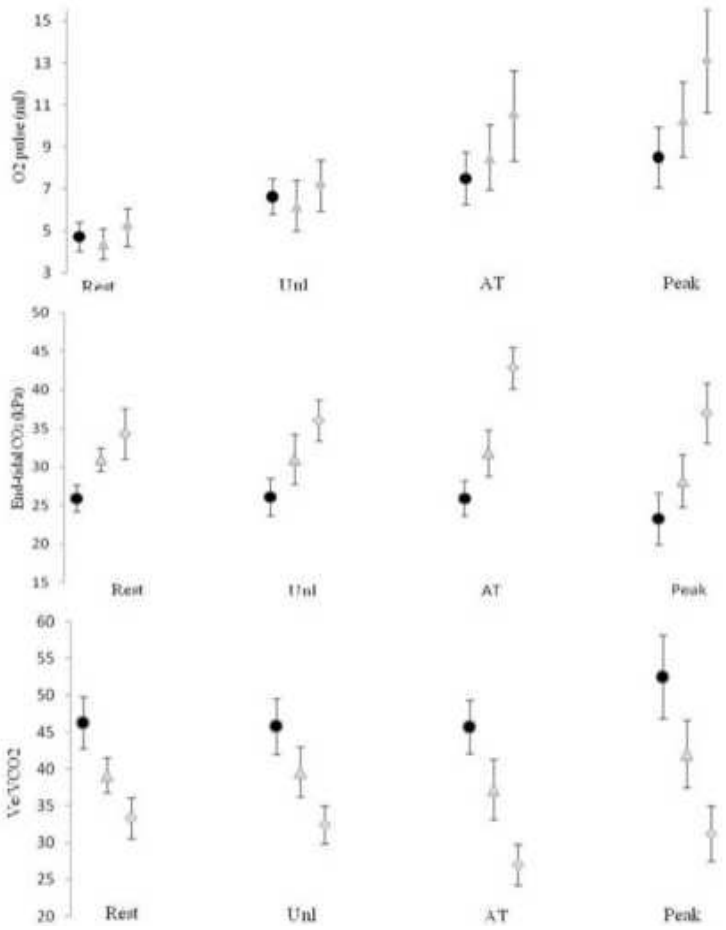

Figure 4.2

Ve/VCO_2, end tidal CO_2 and O_2 pulse through phases of exercise. Black circles – CTEPH, Clear triangles – CTED, Clear circles – Controls

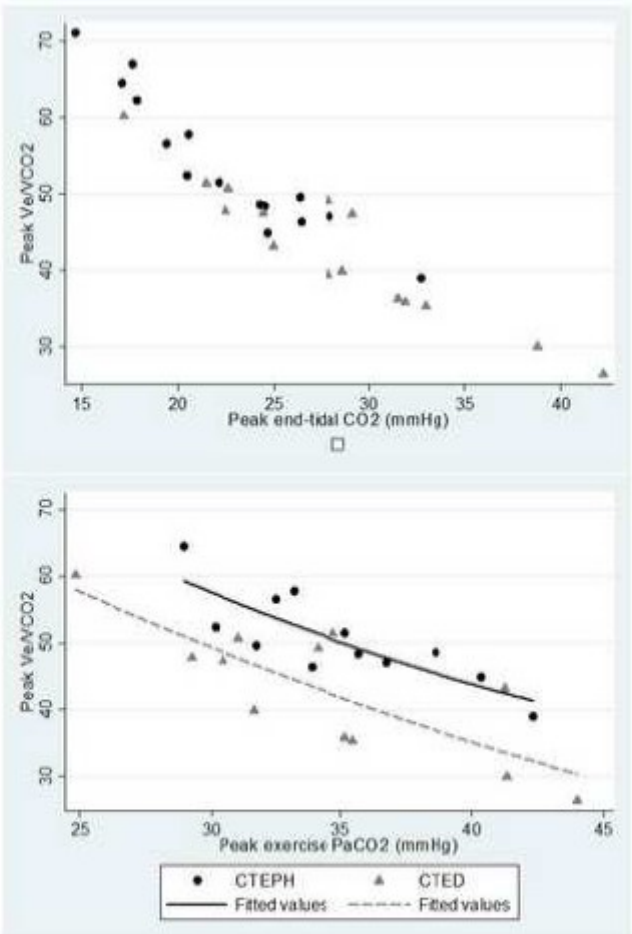

Figure 4.3

Responses in Ve/VCO_2 in relation to end tidal CO_2 and $PaCO_2$ at peak exercise

4.3.3 Prediction of a CTEPH diagnosis

Peak exercise Vd/Vt and Aa gradient, HR/VO_2 slope, Ve/VCO_2 slope, Ve/VCO_2(AT) and end-tidal-CO_2(AT) discriminated strongly between CTED and CTEPH groups (Table 4.3, all $p < 0.01$). Vd/Vt showed good correlation with mPAP ($r=0.66$, $p < 0.01$). Serum NT pro-BNP had weaker discriminatory value ($p = 0.04$). Univariable predictors of a CTEPH diagnosis where the area under the ROC curve was significantly different from 0.50 were peak exercise Vd/Vt, Aa gradient and Ve/VCO_2 (AT) (Figure 4.4). In a multivariate model comparison of Vd/Vt, Aa gradient and Ve/VCO_2(AT) with serum NT pro-BNP and HR/VO_2 slope, only Vd/Vt retained a significant predictive effect ($p = 0.03$ (Vd/Vt) vs $p = 0.09$ (Aa gradient) vs $p = 0.08$ (Ve/VCO2(AT)). A peak

exercise Vd/Vt > 45 % had a sensitivity of 92% and specificity of 83% in predicting a diagnosis of CTEPH. A peak exercise Aa-oxygen gradient > 32 mmHg had an equivalent sensitivity of 92% and specificity of 67%.

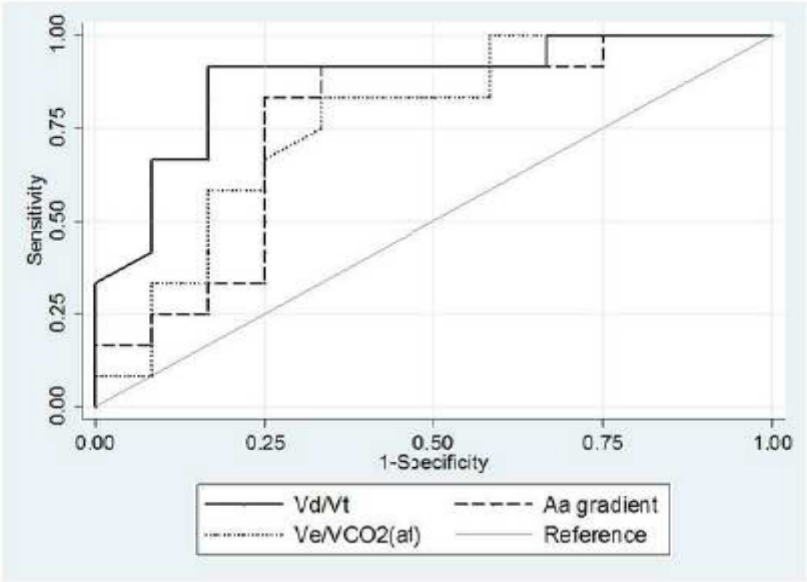

Figure 4.4

ROC analysis of exercise parameters comparing predictive effect for a diagnosis of CTEPH: Vd/Vt AUC 0.88 (CI 0.67 – 0.97), Aa gradient AUC = 0.76 (CI 0.53 – 0.90), Ve/VCO_2 (at) AUC = 0.77 (CI 0.61 – 0.92)

4.4.4 Pulmonary Vascular Obstruction

Total pulmonary vascular obstructive indices for CTED and CTEPH groups were 72.5% (60 – 80%) and 67.5% (55 – 70%) respectively (Table 4.4). The trend towards a lower Total Pulmonary Vascular Obstruction Index (indicating more obstructed vessels) in patients with CTEPH did not meet statistical significance (p=0.08). No patients suffered from isolated unilateral obstruction suggestive of an alternative diagnosis to CTED and CTEPH.

	Right Lung	Left Lung	Total	TPVO Index
CTED (N = 15)	196/300	229/300	425/600	72.5% (IQ 60 – 80)
CTEPH (N = 15)	180/300	208/300	388/600	67.5% (IQ 55 – 70)
			p value	0.08

Table 4.4

Quantification of pulmonary vascular obstruction in patients with CTED and CTEPH. Total score per patient = 40 including both lungs (see Chapter 2: Materials and Methods for detailed explanation of Total Pulmonary Vascular Obstruction (TPVO) Index)

4.4 Discussion

Our results describe changes in peak exercise gas exchange and ventilatory efficiency in patients with confirmed chronic thromboembolic obstruction following PE stratified by haemodynamic criteria diagnostic of PH. Vd/Vt at peak exercise predicts a diagnosis of CTEPH in this setting with acceptable sensitivity and specificity. Furthermore, Aa gradient at peak exercise and Ve/VCO_2 (AT) harbour similar predictive value. Reduced exercise capacity in CTED and CTEPH and elevated Ve/VCO_2 ratio compared to controls appeared attributable to elevated Vd/Vt. In keeping with its strong predictive effect, Vd/Vt correlated well with the severity of haemodynamic derangement. On CT evaluation, resting haemodynamics appeared not to be influenced by the extent or distribution of proximal thromboembolic obstruction. This supports an additional contribution from a small vessel vasculopathy in patients with CTEPH and to a lesser extent in patients with CTED.

Patients in CTED and CTEPH groups showed a similar diffusion capacity (KCo) (88 vs 87 %). This may be explained by the relatively mild phenotype of the CTEPH group. Different resting ventilatory responses in CTED and CTEPH are supported by the high discriminatory value of capillary to resting end-tidal CO_2 gradients in CTEPH above other forms of PH (Scheidl et al., 2012). Exploring the origins of ventilatory inefficiency requires multiple inert gas elimination studies which were not available in this setting. However, at peak exercise, different $VeVCO_2/PaCO_2$ alignment between CTED and CTEPH groups was noted (Figure 4). This appeared to be accounted for by higher peak

exercise Vd/Vt although increased chemosensitivity in the CTEPH group may have contributed to this difference. Increased chemosensitivity has been postulated as a stimulus of exercise hyperventilation in PAH and chronic heart failure although its importance in CTEPH remains subject to debate (Chesler et al., 2009; Deboeck et al., 2004).

The relative contributions of V/Q mismatch, inadequate cardiac output and exertional hypoxaemia that contribute to exercise limitation may differ between PAH and CTEPH. Vd/Vt in our study predicted haemodynamic outcome, a finding that persisted in a multivariable model. Accounting for this, it has been suggested Vd/Vt may contribute more towards ventilatory inefficiency in CTEPH than in other forms of PH (Zhai et al., 2011). Gas exchange in CTEPH is likely characterised by a shift towards higher ventilation-perfusion ratios which may give rise to increased Vd/Vt (West, 1969). The normal exercise response is associated with a fall in Vd/Vt to values < 20% (Balady et al., 2010), hence we suggest that patients with CTED suffer a failure of adequate recruitment of the pulmonary vascular bed on exercise. This may occur through impaired cardiac output adaptation and ventilation perfusion inequality. Importantly, increased shunting was not attributable to flow through a patent foramen ovale in our study using criteria defined by Sun et al (Sun et al., 2002).

In the CTED group, mild elevation in serum NT-pro BNP supports an underlying impairment in RV adaptation. This is also suggested by their low/normal cardiac index at RHC (2.7 ± 0.5, Table 2). Elevation in Ve/VCO_2 ratio was noted which although milder than in the CTEPH group, closely mirrors the CPET response of congestive heart failure (Hollenberg and Tager, 2000). High Aa oxygen gradient has been shown to be explained by mild disturbance in ventilation/perfusion ratios amplified by a low SvO_2 at rest and during exercise secondary to a low cardiac output (Dantzker and D'Alonzo, 1985). This is in keeping with higher Aa-gradient values in our CTEPH group and values in the upper limit of normal in patients with CTED.

Elevated RV afterload is also relevant to impaired RV adaptation on exercise. RV afterload encompasses components of resistance, compliance and wave reflection. Persistent exercise intolerance post pulmonary endarterectomy has been attributed to lower exercise pulmonary arterial

compliance despite normalisation of PVR post-operatively (Bonderman et al., 2011). In our study, persistent thrombus may adversely affect compliance conferring higher total afterload that is not incorporated by measurement of PVR. This could potentially blunt the exercise cardiac output response in patients with CTED. In spite of this, compliance showed no relationship to exercise capacity. An increase in the mPAP/cardiac output (CO) slope which relates to dyspnoea symptoms may perhaps have offered clearer insight (Naeije, 2013). Although not investigated, it is probable that the CTED group demonstrate higher than normal slope values. In future this may be best approached by echocardiographic measurements (Argiento et al., 2012).

Non-invasive methods that suggest the presence of chronic thromboembolic obstruction in an 'at-risk' population are potentially advantageous. In CTEPH, exercise may be especially valuable given recent evidence suggesting resting echocardiographic estimation of PVR incorporating measurement of TR velocity may not be entirely robust (Xie et al., 2014). Although routine screening with resting echocardiography for CTEPH has been recommended six weeks after PE, echocardiography data carries little predictive value and the optimal timing of scans in symptomatic patients is yet to be established (Ribeiro et al., 1999). Our study is notable in that all patients with CTED and CTEPH had suffered prior acute PE, none were taking pulmonary vasodilator therapy and groups were age matched. Age-related differences in RV remodelling in CTED and CTEPH are therefore unlikely. Although the ideal control cohort for this study would have been a population being followed up for exercise limitation post-PE *without* chronic thromboembolic obstruction, such a group was not available for study. Nevertheless, we have characterised CPET responses in two conditions (CTED and CTEPH) that should alert clinicians to the possible presence of chronic thromboembolic obstruction in this clinical setting.

Differentiation of chronic thromboembolic obstruction by haemodynamic outcome may be especially pertinent given surgical treatment with PEA is recently being considered for symptomatic benefit in patients with CTED. Following PE, exercise limitation in this group has a less clear causal relationship to chronic thromboembolic obstruction (Gotthardt et al., 2002). Therefore CPET may

help guide selection for surgery to offer maximal patient benefit by providing surrogate assessment of exercise cardiac adaptation. We have shown that exercise parameters inform on disease severity in our cohort and CPET has already been used in patients with CTEPH in the assessment of response to therapy (Mereles et al., 2006; Nagel et al., 2012; Pepke-Zaba et al., 2013). Further evaluation of exercise responses in patients with chronic thromboembolic obstruction is warranted irrespective of resting haemodynamics.

Finally, in roughly one half of all patients, no prior thrombotic predisposition could be identified. This finding is broadly consistent with a recent international CTEPH registry (Pepke-Zaba et al., 2011). Biological mechanisms that predict the degree of persistent vascular obstruction following PE are incompletely understood. Our findings on CT reinforce the hypothesis that the extent of residual pulmonary vascular obstruction does not appear to be the sole mechanism responsible for the development of CTEPH. Impaired 'in vitro' fibrinolysis has been suggested as a possible mechanism for persistence of thrombotic material (Miniati et al., 2010; Morris et al., 2006). Furthermore, wide variation exists between the degrees of pulmonary vasculopathy in small vessels which, left untreated, may increase over time (Moser et al., 1990). Currently, definitive evidence of clinical progression from CTED to CTEPH is lacking. The abnormal exercise response observed in this study suggests patients with CTED may harbour subclinical changes in the distal pulmonary vasculature in addition to impaired exercise cardiac reserve. This should be evaluated in longitudinal studies.

Despite the prospective nature of the study, there are limitations, in particular our small and highly selected patient group which excluded patients with COPD, LV systolic dysfunction and obesity. Despite CTED being a rare entity, this was necessary as these comorbidities can colour the CPET interpretation of exercise intolerance. Caution should therefore be exercised in extrapolating our results to all patients with CTED. Second, we did not measure simultaneous exercise haemodynamics and thus cannot comment as to whether CPET findings represent changes of exercise-induced PH. At present however, the prognostic significance of exercise-induced PH remains unclarified in chronic thromboembolic obstruction. Lastly, our study was not designed to detect the presence of persistent

thromboembolic obstruction following PE. Whilst modalities that avoid the use of ionising radiation may be clinically attractive, especially in younger populations, this would require more substantial patient numbers assessed at stratified intervals during anticoagulation for PE that to our knowledge has so far not been achieved.

4.5 Conclusions

The major finding of this study was the distinction on CPET between patients with chronic thromboembolic obstruction with and without PH compared to sedentary controls. The mechanism of exercise impairment in CTED centres on impaired RV adaptation on exercise without apparent significant influence from the degree of proximal thromboembolic obstruction. CPET, unlike routinely employed exercise assessments such as 6MWD, offers diagnostic insight into patients suffering persistent symptoms after acute PE. This is particularly relevant to patients with preserved RV function on resting echocardiography whose symptoms are rarely present at rest.

Chapter 5: Whole exome sequencing in Chronic Thromboembolic Pulmonary Hypertension

5.1 Introduction

Recent advances in next generation DNA sequencing technology have greatly reduced the costs and feasibility of sequencing the entire genome in relation to Sanger sequencing (Metzker, 2010). Exome sequencing concentrates on the 5% of the genome that encodes for proteins and requires no prior assumptions or knowledge about the genes predisposing to the disease thus allowing unexpected genetic predisposition to be uncovered. Since the seminal study by Ng, this approach has led to a rapid expansion in the identification of genetic mutations in Mendelian disease in the last five years (Bamshad et al., 2011; Biesecker, 2010; Ng et al., 2010; Ng et al., 2009; Yang et al., 2013).

Application of exome sequencing in complex disease has progressed more slowly. Unlike conditions exhibiting Mendelian inheritance, it is hypothesised that multiple DSVs contribute interactive effects on the phenotype. This suggests that, in complex disease, individual DSVs may have near negligible effects. Nevertheless the identification of homozygous and heterozygous DSVs with predicted deleterious effects remains possible and strategies to enrich the phenotype under investigation may increase the likelihood of identifying a causative genetic defect (Cole et al., 2012). A key factor in increasing this likelihood is to define as closely as possible an extreme phenotype within a trait. CTEPH is itself an extreme phenotype but this can be further refined by identifying patients with a similar clinical course, and by excluding known risk factors.

Mechanisms of development of CTEPH are unclear but may centre on the interplay between vascular inflammation, aberrant cellular proliferation and endothelial dysfunction. In a small minority of patients suffering PE, this leads to persistence of organised thrombotic tissue within the pulmonary artery (Fedullo et al., 2000; Pengo et al., 2004). In up to 30% of cases, CTEPH is diagnosed at a

young age with no identifiable predisposing genetic factor (Morris et al., 2006; Pengo et al., 2004). In these cases, a inherited predisposition towards disordered clot resolution may exist in a significant proportion.

To date, CTEPH has not demonstrated heritable transmission and no single genetic or biological factor has been pinpointed to account for its epidemiology. Based on its extremely low population prevalence and low incidence following PE, it may be hypothesised that a proportion of cases result from rare genetic variation that confers a pathological effect. By exome sequencing DNA from unrelated individuals with a similar (and extreme) phenotype of CTEPH, all of whom have suffered inadequate thrombus resolution following PE, it may be possible to enrich for mutations predisposing to disordered clot resolution. This is in keeping with proposed mechanisms of disordered fibrinolysis (Morris, 2013). The finding of commonly mutated genes in unrelated individuals might therefore point to novel disease mechanisms.

A complimentary approach is the further analysis of parental-child trios. This involves sequencing parental DNA of CTEPH probands in an effort to uncover *de novo* genetic variation (new germ line variants arising from the gametes of the parents). *De novo* DSVs have been hypothesised to harbour more damaging effects (Veltman and Brunner, 2012) and are subjected to less stringent evolutionary selection. They are therefore prime candidates for causing sporadically occurring disease such as CTEPH. Parental child trio analysis has been successfully used in families with Mendelian neurological disease to pinpoint disease causing mutations (Hamdan et al., 2013; Rosewich et al., 2012) but is not yet established in complex phenotypes. Nevertheless, given availability of parental DNA in ten out of twenty CTEPH probands, *de novo* mutation analysis was also undertaken.

This chapter presents preliminary results from whole exome sequencing experiments in twenty individuals with CTEPH and 10 parental child trios. All CTEPH probands were diagnosed at a young age following acute PE to maximise the potential genetic contribution to disease. In addition, heritable and environmental factors known to predispose to CTEPH were excluded as far as possible as

unknown genetic variation was hypothesised to be important. This Chpater's results are presented chronologically as refinement of mutation analysis pipeline is under ongoing review within the Papworth Pulmonary Vascular Disease research group at Papworth and aspects of the analysis are perhaps better understood in this way.

5.2 Case Selection

Patients with CTEPH were selected for sequencing based on phenotyping that aimed to enrich for mutations lying within fibrinolytic pathways. This was in part based on our previous group's experience suggesting fibrinolytic factors may explain a proportion of cases of CTEPH (Suntharalingam et al., 2008) as well as established *in vitro* data suggesting an association between dysfibrinogenaemia and CTEPH (Morris et al., 2009). Inclusion and exclusion factors are listed in Table 5.1 and 5.2 respectively.

- Diagnosis of CTEPH as per PAH Dana Point 2008 guidelines -Age < 50 -Same sex/ethnicity (European Caucasian) -History of acute PE treated with anticoagulation -Absence of known clinical, biochemical or genetic risk factors for venous thromboembolism or significant co-morbidity

Table 5.1

Inclusion criteria

-Splenectomised
-Antiphospholipid Antibody/lupus anticoagulant positivity
-Protein C and S deficiency
-Prothrombin gene mutation
-Antithrombin III deficiency
-Factor V Leiden mutation positive
-Other defined heritable defect in coagulation pathway
-Myeloproliferative disease
-Active or past history of neoplasia
-(Use of HRT/oral contraceptive pill)
-(Pregnancy or breastfeeding)
-Congenital heart disease
-HIV positivity
-History of intravenous drug use
-USS evidence of liver cirrhosis (Alcoholic or non-Alcoholic)
-Presence of haemoglobinopathy/chronic haemolysis
-Other factors contributing to pulmonary hypertension
- Moderate to severe obstructive or restrictive spirometry (FEV1/FVC < 50% or FVC <50%)
- Severe congenital abnormalities of the thorax, diaphragm or lungs
- Evidence of interstitial lung disease on HRCT Chest
- History of OSA/sleep disordered breathing/pre-existing abnormal sleep study
- Congestive cardiac failure defined as impaired LV systolic/diastolic function on echocardiography

-Chronic renal impairment (Cr clearance < 30ml/min/h)
-History of pulmonary, renal or systemic vasculitis
-Evidence of connective tissue disease from history or examination
-All other classifications of pulmonary hypertension within Dana Point classification other than chronic thomboembolic pulmonary hypertension

Table 5.2

Exclusion criteria

Samples meeting inclusion and exclusion criteria were obtained from Papworth Hospital Tissue Bank which is a frozen storage facility containing whole blood samples of patients under the care of the Pulmonary Vascular Disease Service at Papworth Hospital since 2005. Patients were selected by

casenote review with selection, phenotyping and whole exome sequencing of samples beginning in November 2011.

5.3 Results

5.3.1 DSV filtration – CTEPH probands

Table 5.3 outlines age, sex and DNA concentrations of the 20 CTEPH probands undergoing exome sequencing. This included 9 males and 11 females. All patients were of European Caucasian ancestry and under 50 years of age at the time of blood donation. None had a positive family history for VTE. DNA extraction and quantification were performed as per the methods described in Chapter 2 prior to sample handover to EASIH for DNA sequencing.

Identifier	Sex	Age	DNA concentration (ng/µL)	OD260/OD280
1	M	32	72.2	1.77
2	M	38	78.4	1.85
3	M	39	125	1.78
4	M	42	51.2	1.73
5	M	47	156.6	1.72
6	M	48	64.9	1.78
7	M	50	58.5	1.81
8	M	50	75.7	1.82
9	M	44	125.1	1.80
10	F	21	114.1	1.88
11	F	23	115	1.78
12	F	23	213.9	1.76
13	F	26	123.5	1.78
14	F	28	202.6	1.79
15	F	34	63.6	1.79
16	F	38	141.7	1.74
17	F	39	144.6	1.73
18	F	43	165.1	1.78
19	F	43	250.2	1.75
20	F	50	115.4	1.79

Table 5.3

Age, sex and DNA concentration of CTEPH probands

20 CTEPH probands were sequenced in a single dataset generated using the Agilent 50Mb All Exon target enrichment kit. Sequencing was undertaken on the Illumina HiSeq2000 platform by EASIH using a single flowcell lane on a 75 bp paired-end Illumina run. The coverage and capture efficiency of this dataset are shown below in Table 5.4. This highlights acceptable levels of read mapping as well as a degree of non-specific capture. Generally, in using Illumina short-read sequence data, a rate > 80% of targeted exons that exceed 20x depth coverage serves as a typical lower limit for high-confidence DSV calls. The equivalent rate of coverage for 20 CTEPH probands was 66.5% for this sequencing run.

	CTEPH probands (20 samples)	
	Average	**Percent**
Mapped Reads	$1.24x10^8$	98.9
Unmapped Reads	$1.58x10^6$	1.1
Reads aligned to reference genome	$4.92x10^7$	87.5
On bait bases	$2.19x10^9$	-
Off bait bases	$4.02x10^8$	-
Baits with 10x coverage	-	82.5
Baits with 20x coverage	-	66.5
Baits with 30x coverage	-	51.3

Table 5.4

The average coverage in the target region is defined as the total number of bases mapped within the target region

The finding of common DSVs in multiple unrelated probands was the final goal of the initial analysis. To this end, several bioinformatic filters were applied through GATK to prioritise DSVs by pathogenicity, inheritance and novelty. DSVs were filtered for pathogenicity by first selecting only protein-encoding DSVs. As target bait coverage incorporated within Agilent's exome capture technology is known to include intronic regions, protein-coding regions of the genome were prioritised at outset. Secondly, only those protein-encoding DSVs with predicted deleterious effects (though to be pathological) were taken forward. These DSVs were defined by the following classifications of transcript variant: splice site, frameshift coding, non-synonymous coding, NMD

transcript, within-mature miRNA, STOP-codon gained, STOP-codon lost and essential splice site. Pathological DSVs were subsequently grouped by heterozygosity/homozygosity under an autosomal dominant/autosomal recessive model of inheritance respectively.

Further filtration was undertaken to prioritse *novel* DSVs that is, those DSVs not present within publically available genetic databases. The rationale for this step was that CTEPH is currently unaccounted for by existing DSVs. Three databases were used for screening DSVs: dbSNP137, Exome Sequencing Project 6500 and the 1000 Genomes Project (1Kg) and population prevalences of DSVs, where known, were established across all databases.

Table 5.5 shows DSV numbers categorised by classification, inheritance and MAF. Rare DSVs were those present in 1Kg at low population frequency (MAF < 1%) based on European Caucasian ancestry. DSVs were labelled 'novel' if not present in the latest version of dbSNP 137.

		QC filtered		**Rare (MAF < 0.01) known and novel variation**	
		Het	**Hom**	**Het**	**Hom**
SNP	**Known**	387887	262811	48874	38368
	Novel	4111	130	4052	88
INS	**Known**	1476	676	657	329
	Novel	15	2	15	1
DEL	**Known**	2045	786	802	451
	Novel	17	0	17	0

Table 5.5

Number of total and 'rare' DSVs passing quality control (QC) appearing in all 20 CTEPH probands. Results are then segregated by Heterozygosity (Het), homozygosity (Hom) and novelty. Note the same DSV may be present in multiple probands hence the large absolute number in each class.

This table demonstrates that numerous rare DSVs are undescribed within dbSNP137 and therefore novel by our definition. This included > 4000 rare SNPs under an autosomal dominant model and

over 80 under an autosomal recessive model. This list was long to be able to select candidate DSVs for further analysis. To concentrate results at the gene rather than the DSV level, a list of commonly mutated genes arising from CTEPH probands is also presented in Table 5.6. This list was obtained by filtration for pathogencity and comparison against dbSNP137 to exclude previously described DSVs with subsequent omission of genes containing those DSVs. Results are split by heterozygous and homzygous alleles.

RSS1	14	APOBEC3H	5	SLC25A6	3	PRSS3	3
TRBV6-5	12	MPP4	5	BCORL1	3	KRBA1	3
PRIM2	10	FAM163A	5	EPDR1	3	GPER	3
BRD8	9	MUC1	5	PRSS2	3	ZAN	3
ATP6V1A	9	NR4A3	5	TRBV4-2	3	IGLV3-22	3
RETSAT	9	TRBC2	5	GPR98	3	SPEG	3
SGK2	8	NEFH	5	TMEM161B	3	PRDM15	3
FRG1B	8	RIMS4	5	ENSG00000205785	3	KRTAP29-1	3
ENSG00000186399	8	KIR3DX1	4	MAGI1	3	KRTAP4-5	3
KRT75	7	PPCS	4	YEATS2	3	B4GALT2	3
MUC6	7	FAM194B	4	ATP9B	3	ATP8A2	3
MUC5	7	ANO4	4	APCDD1	3	SRGAP1	3
TTN	7	ENSG00000215615	4	MRC2	3	USH2A	3
C12orf51	7	FAM120A	4	TMEM132E	3	SLC45A3	3
FOXRED1	7	FOXK1	3	COTL1	3	ENSG00000179571	3
ENSG00000239262	7	TRBV6-7	3	ENSG00000138600	3	PRDM2	3
RABGAP1	7	BRD8	3	MEF2A	3	ATXN7L2	3
BZRAP1	7	CACNA1I	3	HOMEZ	3	EIF2S3	3
DMXL2	7	CSF2RB	3	GAS6	3	AKAP17A	3
C1orf163	7	VWA3A	3	ITPKB	3	P2RY8	3
IPO5	6	FMR1	3	TNN	3	MPP1	3
MCM8	6	PION	3	TCP11L1	3	ASMTL	3
GRIK3	6	GIMAP6	3	PPP2R3B	3	ERMP1	3
ZNF706	6	EPHA1	3	ARSD	3	MTUS1	3

(Heterozygous)

STM1	7	PPCS	5	CRIPAK	5
KRTAP5-7	6	RPF1	5	ENSG00000229924	5
ENSG00000251537	6	OR6M1	5	FOXF2	5
TSPYL6	6	HNRNPA1P30	5	PIP5K1P2	5
PRPF4B	6	RBM23	5	TUSC3	5
C6orf138	6	CACNA1G	5	LCN1P2	5
BZW2	6	BAIAP2L2	5	ENSG00000212857	4
PIP5K1P2	6	PLA2G6	5	ENSG00000212847	4
TUSC3	6	PDE6B	5	MXRA5	4
KIR2DL5B	6	FAM153A	5	ITGB1BP2	4
LPCAT1	6	CAMK2B	5	PABPC5	4

(Homozygous)

Table 5.6

Genes containing common DSVs with predicted pathological effect (heterozygous and homozygous allele models). The columns (left to right) represent the affected gene and the number of samples in that gene which contain one or more novel, pathogenic variants. This analysis focuses on variation at the gene level rather than on specific DSVs. Ensembl references (ENS) are given where no gene nomenclature has been defined.

No further analysis of individual DSVs from CTEPH probands was proposed at this stage; instead, further sequencing of parental samples was undertaken. This decision was supported by a number of factors. As previously discussed, recent literature highlighting a relative excess of rare genomic variation (due to recent population expansion) suggested exome sequencing in complex disease with a rare population frequency (<10 cases/100,000) may require in excess of 1000 samples to achieve statistical significance at the individual DSV level (Tennessen et al., 2012). This suggested our small sample (n = 20) was likely to be underpowered in its ability to statistically segregate DSVs. Secondly, our read alignment tool, BWA, pointed towards several DSVs with predicted damaging effects that were not reproduced using other read aligners. In particular, a known limitation of BWA is its weak annotation of copy number variations (CNVs) despite it reporting mapping quality scores that can be used to discard unsupported mappings. Realignment with another alignment tool, Novoalign (Novocraft, 2010), suggested several DSVs may have been been incorrectly called. Finally, and perhaps most significantly, raw sequencing data from the 20 CTEPH probands suggested a relatively

low read depth coverage (20x coverage depth in 66.5% of exons) meaning the power of our analysis to call *all* functionally relevant DSVs may be significantly reduced.

Sequencing of DNA from the parents of 10 of 20 CTEPH probands was therefore undertaken. Ten sets of both parents were consented under a Rare Disease Cohort study (Bioresource, Cambridge) which allows the collection of volunteer samples. Samples were anonymised so as to prevent tracking of familial genetic predisposition not relevant to CTEPH. Importantly, all sequenced parents of affected probands had no history of thromboembolic disease (acute or chronic). This is consistent with the lack of heritibility in CTEPH and absence of pro-thrombotic risk factors in CTEPH probands. DNA was extracted from saliva samples donated by parents and sequenced in December 2012. The exome capture kits (Agilent V1.3), enrichment techniques and sequencing platform were the same as were used for proband sequencing. Parental sequencing was completed in January 2013.

5.3.2 Quality Control and Read Mapping Statistics

Pooled coverage and capture efficiencies of both cohorts are shown in Figure 5.1.

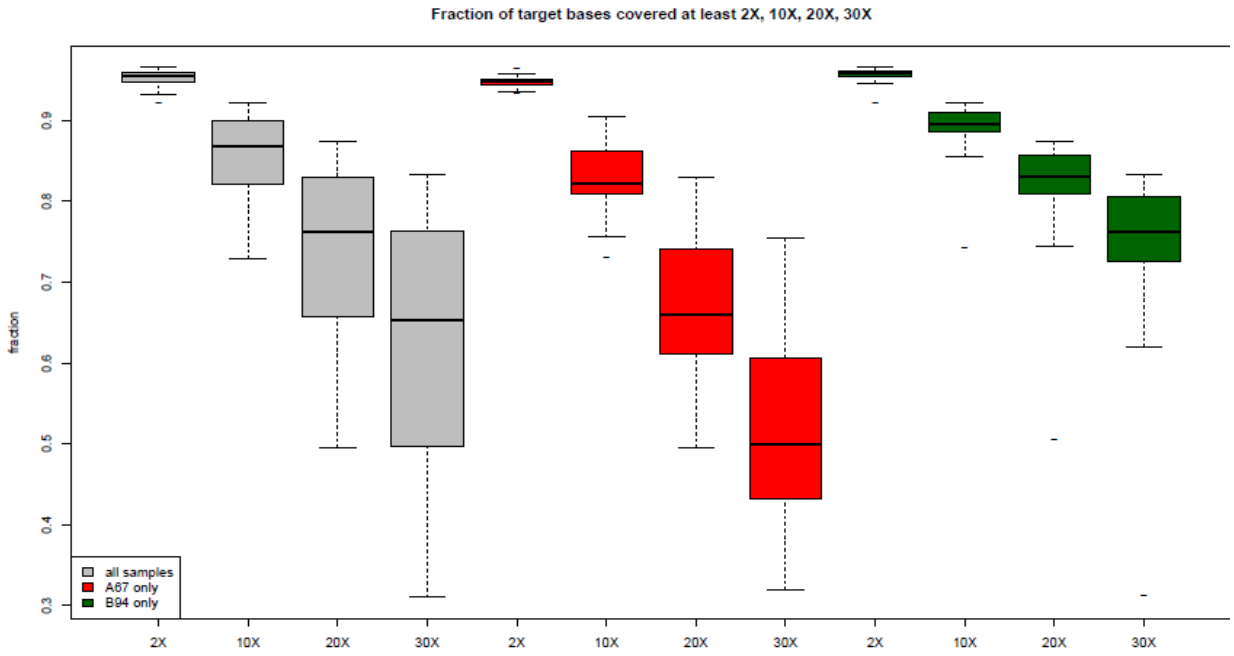

Figure 5.1

Mean target coverage for CTEPH probands (A67 red) and parents (B94 green) with pooled datasets (grey).

This data shows a comparison of target capture between index cases and parental cohorts and highlights a significant discrepancy. In index cases, an inadequate depth of coverage (mean 66.5% 20x depth) has been achieved potentially limiting variant calling. Figure 5.2 shows the number of total and mapped reads for CTEPH probands (left half - A67) and twenty parents (right half - B64). This shows, in all but one case (sample B640014), greater than 50 million mapped reads per run which is the minimum acceptable threshold for exome analysis. Sample B640014 was re-sequenced following this finding.

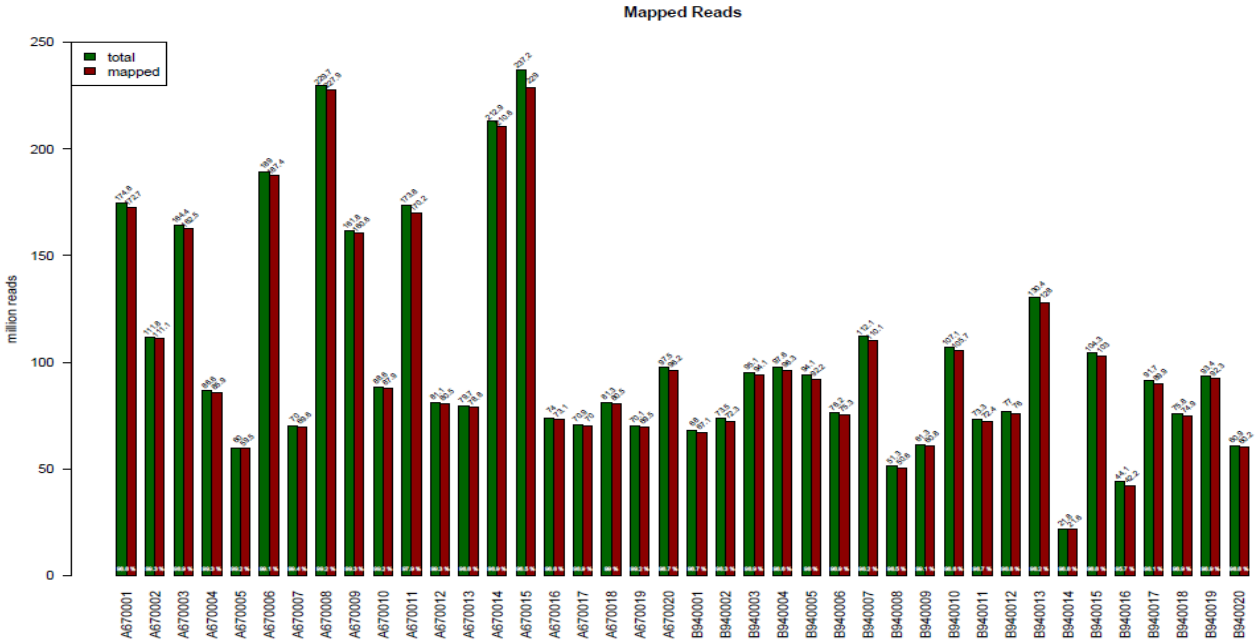

Figure 5.2

Mapped reads (millions) across all 40 sequenced individuals. Left half – CTEPH probands, right half parental samples

The discrepancy in read mapping statistics between index cases and parents (Table 5.7), on more detailed exploration was explicable by a higher fraction of PCR duplicates in CTEPH probands (Figure 5.3). PCR duplicates are produced during PCR amplification in DNA library preparation and occur because the same reads are overamplified. Although an imbalance in PCR duplicates may arise from deeper sequencing in one cohort compared to another, the marked discrepancy was thought to be attributable to PCR slippage. PCR slippage is encountered particularly in areas of the genome rich in repetitive sequences of adenine-thymine (AT) or guanine-cytosine (GC) base pairs. These base pair

combinations produce low thermodynamic stability resulting in the polymerase being less able to anneal to a template. PCR duplicates may be removed bioinformatically from the final analysis but represent a large fraction of non-informative sequencing data resulting in significant limitations in the dataset.

	CTEPH index cases (20 samples)		CTEPH parents (20 samples)	
	Average	**Percent**	**Average**	**Percentage**
Mapped Reads	$1.24x10^8$	98.9	$7.92x10^7$	98.5
Unmapped Reads	$1.58x10^6$	1.1	$1.21x10^6$	1.5
Reads aligned to reference genome	$4.92x10^7$	87.5	$6.51x10^7$	90.1
On bait bases	$2.19x10^9$	-	$4.31x10^9$	-
Off bait bases	$4.02x10^8$	-	$8.32x10^8$	-
Baits with 10x coverage	-	82.5		88.9
Baits with 20x coverage	-	66.5		81.6
Baits with 30x coverage	-	51.3		74.2
Bases aligned to reference in reads mapped at high quality	$8.34x10^9$	-	$7.10x10^9$	-

Table 5.7

Comparison of read mapping statistics for CTEPH probands and parental samples. The target coverage and depth was markedly better for parental samples.

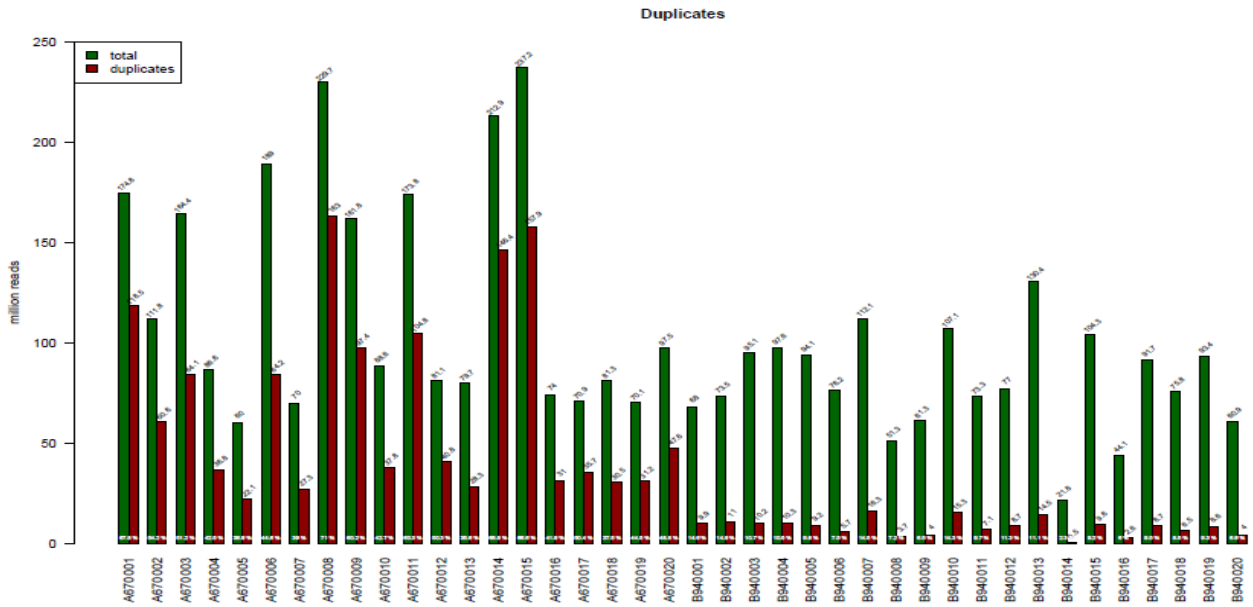

Figure 5.3

PCR duplication rates across index cases (A67 samples – left side of graph) and parents (B64 samples- right side)

5.3.3 Variant Calls

De novo DSVs arising from the parental child sequencing are shown in Table 5.8.

6	ZNF678	**2**	GLTSCR1	**1**	SARDH	**1**	LILRB5	**1**	CEL
6	SRP68	**2**	ESPNP	**1**	RYR1	**1**	LILRA6	**1**	CDC42EP1
6	ANKRD36	**2**	CYP26B1	**1**	RSPH4A	**1**	LCP2	**1**	CCNC
5	SPI1	**2**	CPSF1	**1**	RGSL1	**1**	LCNL1	**1**	CAPZA3
5	HLA-DRB5	**2**	CIC	**1**	RBMX	**1**	KPTN	**1**	C17orf70
4	KRI1	**2**	CCDC85B	**1**	RBM15B	**1**	KIAA1715	**1**	C17orf100
4	AK128833	**2**	BCLAF1	**1**	RBKS	**1**	KIAA0125	**1**	BRD4
3	TTC21B	**2**	BAI1	**1**	PP14571	**1**	KCNK15	**1**	ATP4A
3	SOGA2	**1**	ZSCAN10	**1**	PLEC	**1**	KCNJ12	**1**	ARIH2OS
3	SAMD4A	**1**	ZNF83	**1**	PLCH1	**1**	ITGB2	**1**	ANKS3
3	MUC6	**1**	ZNF703	**1**	PLCB3	**1**	IL33	**1**	ANGPTL4
3	ITGAE	**1**	ZBTB46	**1**	PKM	**1**	HLA-H	**1**	ALG3
3	HOOK1	**1**	WNT10B	**1**	PIGQ	**1**	HLA-DQB1	**1**	AHRR
3	HLA-B	**1**	WDR81	**1**	PHLPP1	**1**	GPR20	**1**	ADCY5
3	ANO8	**1**	VWA5B2	**1**	PER1	**1**	GPHN	**1**	ADCY10
3	AHNAK2	**1**	VWA3B	**1**	PDZD4	**1**	GABRA3	**1**	ADAMTS9
2	TTC9B	**1**	UNC13D	**1**	PDDC1	**1**	FUK	**1**	ADAMTS7
2	TARBP1	**1**	UBXN11	**1**	OTOG	**1**	FIBP	**1**	ABCA13
2	SNAPC4	**1**	UBE2C	**1**	OR4C3	**1**	FCGBP		
2	SCN7A	**1**	TTN	**1**	OR12D3	**1**	FBXO2		
2	SCAPER	**1**	TRPM2	**1**	NYAP1	**1**	FBRSL1		
2	RETSAT	**1**	TRAPPC12	**1**	NTN3	**1**	FAM46C		
2	POLDIP2	**1**	TRABD2B	**1**	NR4A3	**1**	ERI3		
2	MYRF	**1**	TRA	**1**	NPHP4	**1**	DUSP2		
2	MUC12	**1**	TP73	**1**	NOTCH2	**1**	DRD4		
2	MICA	**1**	TMPRSS13	**1**	MYO9A	**1**	DOCK7		
2	MAMDC4	**1**	TMEM145	**1**	MUC4	**1**	DOCK2		
2	LRP5	**1**	SSH2	**1**	MRGPRX3	**1**	DNAH7		
2	LONP2	**1**	SPTA1	**1**	MFRP	**1**	DLGAP1		
2	LINC00273	**1**	SPSB4	**1**	MCM3AP	**1**	DBX2		
2	KRT18	**1**	SPON1	**1**	MAP1S	**1**	CUX1		
2	KCNB1	**1**	SPEG	**1**	MAG	**1**	COL18A1		
2	ICOSLG	**1**	SORBS3	**1**	LRSAM1	**1**	CHD5		
2	HLA-DRB1	**1**	SKA3	**1**	LRFN2	**1**	CFHR5		
2	HLA-A	**1**	SELPLG	**1**	LOC653513	**1**	CELA1		

Table 5.8

List of genes containing *de novo* DSVs arising from the analysis of ten parental-child trios under and autosomal dominant model. The number associated with each gene corresponds to the number of *de novo* DSVs within that gene appearing in the ten CTEPH probands.

Some *de novo* mutations were shared across multiple unrelated samples (for example ZNF678, SRP68 and ANKRD36). In total, 158 genes containing *de novo* DSVs emerged from 10 parental child trios giving 15.8 genes per trio. The absolute number of *de novo* DSVs was 232 and not in keeping with previous trio analyses which more commonly quote between 0 – 3 *de novo* DSVs arising per trio. Reasons for this discrepancy in output are discussed further below.

As well as grouped data, individual genetic targets were interrogated by visual inspection with a genome browser (Integrated Genomics Viewer, IGV). For example, read depth coverage of the angiogenic factor, Vascular Endothelial Growth Factor A (VEGF-A) is shown in Figure 5.4. This demonstrates maternal inheritance of a single DSV lying within an intronic region q16.1. Although VEGF-A is intimately linked to angiogenesis, this variant transpired to be neither pathogenic nor novel.

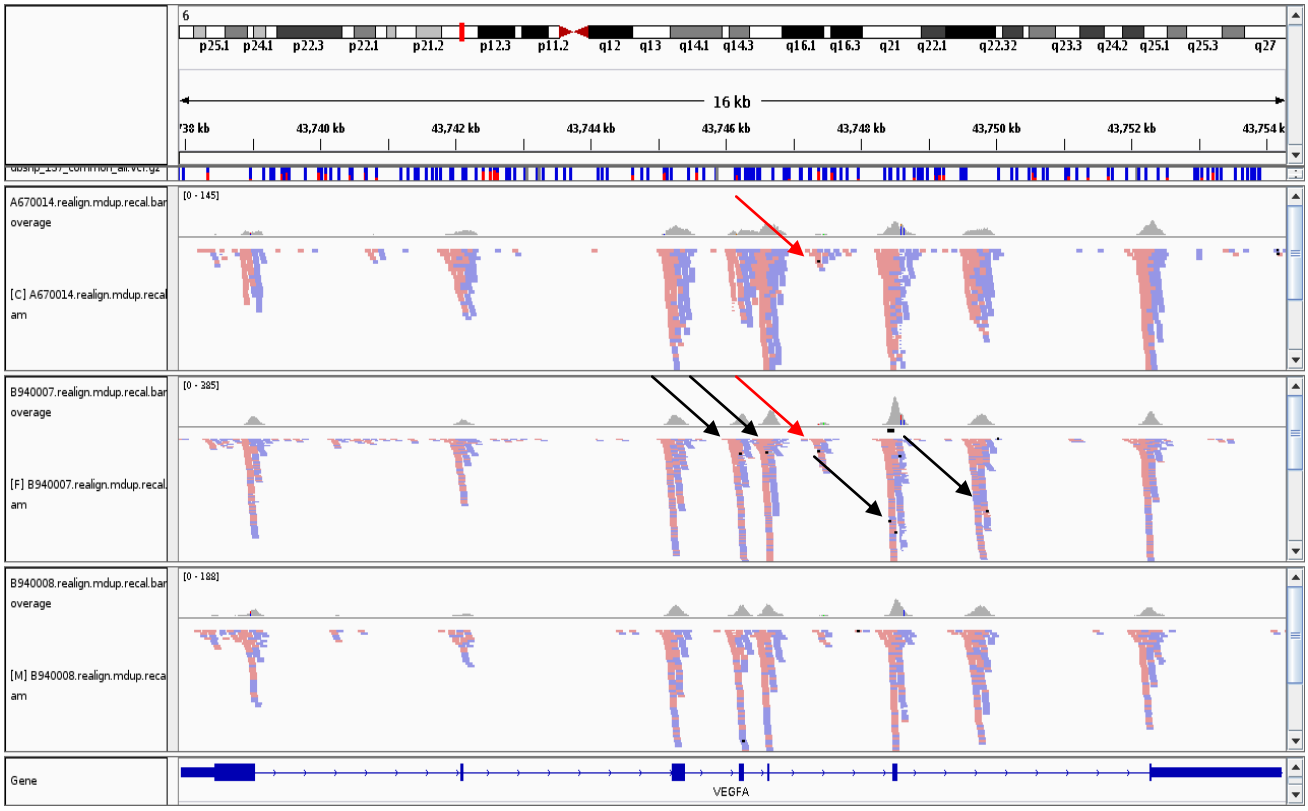

Figure 5.4

IGV screenshot of a parental-child trio genotypes in VEGF-A. Proband (top), maternal (middle) and paternal (bottom) genotype suggest a maternal variant (lower red arrow) differing from the reference genome that is inherited in the proband (top red arrow). Other variants in the maternal copy are not inherited (black arrows).

Vascular Endothelial Zinc Finger – 1 (VEZF-1) (Figure 5.5), also related to angiogenesis, was also found to contain a 6 base pair insertion that resulted in an extension of a polyglutamine (Q) tract. Polyglutamine extensions in large number have been commonly associated with inherited movement disorders such as cerebellar ataxia and Huntingdon's chorea. However, this variant despite being annotated as novel, was not reproduced with Novoalign suggesting it had been called artefactually.

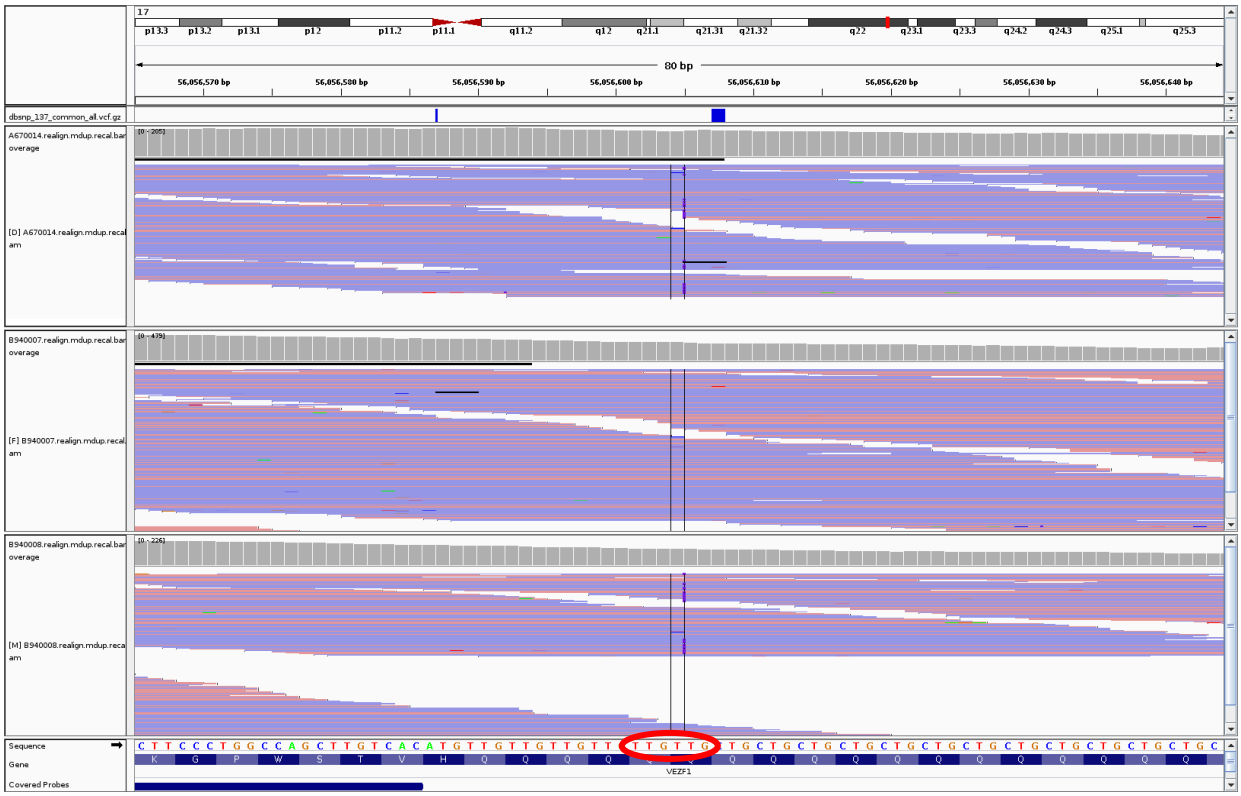

Figure 5.5

IGV screenshot of parental-child trio genotypes in VEZF-1, important to angiogenesis and cellular proliferation. Despite good target coverage, placement of a 6 base pair extension (TTGTTG - red circle) in different locations of a polyQ tract within this gene results in different DSV calls using alternative alignment tools.

5.3.4 Grouped analysis of fibrinolytic genes

In further attempt to support or refute a fibrinolytic origin in CTEPH, an analysis was undertaken looking at numbers of DSVs lying within genes known to lie within fibrinolytic pathways in probands

and parents. These genes were identified by a keyword search for "fibrinolysis" in Genecards, (Weizmann Institute of Science) which is an online searchable, integrated, database of human genes that provides concise genomic related information, on all known and predicted human genes. This resulted in 140 candidate genes against which the list of DSVs from probands and parents could be cross-referenced (Appendix 5.1). No discrimination was made between common or rare DSVs in this analysis. Simply, the number of DSVs was calculated as a proportion of the total number of DSVs passing QC for probands and parents. The rationale for this was that an excess proportion of deleterious DSVs in fibrinolytic genes in probands compared to parents would support a preponderance of risk in CTEPH lying within fibrinolytic genes. Results are shown in Table 5.9.

DSVs sequenced	CTEPH probands	Parents
All genes	25292	25466
Fibrinolytic genes	1153 (4.6%)	1145 (4.5%)
Fibrinolytic and Damaging	114 (9.9%)	110 (9.6%)
Pearson X^2	1.39	p = 0.49

Table 5.9

Comparison of DSVs in proband and parental samples for all genes as well as for 'fibrinolytic' and 'fibrinolytic and damaging' subsets. Boxes describe the number of DSVs in each category with the percentage of the total number of DSVs in brackets. Note, in this representation, DSVs are shared between probands and between parents and are therefore not shown in absolute number. Polyphen was used to predict downstream damaging effects on proteins and DSVs classified as 'possibly' and 'probably' damaging were included. Chi-square test for univariate frequency distributions was used to compare an expected frequency of DSVs (parents) with the observed frequency (CTEPH probands) across all groups.

These results show broadly similar DSV numbers in probands and parents for all genes and genes lying within fibrinolytic pathways. CTEPH probands and parents also harbour similar numbers of fibrinolytic DSVs that are predicted to be damaging to downstream proteins – roughly 10% of the 'fibrinolytic' DSV pool.

5.4 Discussion

The use of whole exome sequencing is at an early stage in complex disease genetics. Although prioritised to targeting coding regions of the genome where sequence variation is assumed to have more important effects, this technique has a high potential for false positive and false negative results. Sequence data quality was suboptimal in this study with an inadequate depth of coverage in CTEPH probands most likely attributable to a high proportion of duplicated reads. This places non-trivial restrictions on the robustness of conclusions despite DSV numbers broadly reflecting those achieved in exome sequencing studies with similar designs (Cole et al., 2012).

The selection of candidate DSVs through bioinformatic filtration requires assiduous care. In particular, prioritisation of 'pathogenic' and 'novel' DSVs by the exclusion of those appearing within common databases of genetic variation (dbSNP) is controversial; dbSNP is known to include both common and rare 'pathological' DSVs. Furthermore, complex phenoypes are less well defined with their genetic contribution unestablished within public databases. This study hypothesised the aetiology of CTEPH to be attributable to rare genetic variation given its low population prevalence and extreme nature of the phenotype. However, the assumption that rare variants (prioritised by MAF < 0.01) carry greater pathogeneic potential stems from predictive modelling and to date has not been validated within complex phenotypes. In addition, the role of rare DSVs is highly likely to vary by disease (Carr et al., 2013; Larson and Schaid, 2014; Stitziel et al., 2011). Following on from this, methods to statistically segregate DSVs are non-standardised and no formal consensus exists on the best method to define statistical association in complex disease. This study did not incorporate a large control or replication cohort as there were doubts over sequencing data quality. For similar reasons, adjustment for gene size which has strong implications on mutation frequencies was not undertaken. These restrictions apply not only to individual DSV lists but also the grouped analysis.

Akin to the second hit hypothesis implicated in the development of IPAH (Liu and Morrell, 2013), mutations in CTEPH may only carry functional effect following the occurence of a prior event (such

as an acute PE). As PE at young age is rare in population terms, CTEPH could conceivably be attributable to common genetic variation. This may compromise the use of exome sequencing as a strategy to identify underlying genetic predispostion as it inherently prioritises rare and undescribed variants. Potentially, CTEPH could be investigated by whole genome sequencing to interrogate both common and rare DSVs occuring in both coding and non-coding regions. Non-coding regions can harbour important regulatory function in protein transcription and their ommision using exomes may therefore overlook important pathogenic variants. However, presently both the cost and rarity of CTEPH samples preclude such work without considerable collaborative effort.

The significant advantage of parental-child trios is the opportunity to uncover *de novo* mutations. In sporadic diseases with no heritable trend, this mutation class is hypothesised to explain a larger majority of the genetic burden (Vissers et al., 2010). Significantly our trio analysis produced a relatively higher nmber of *de novo* DSVs, far greater than numbers found in previous studies (Sanders et al., 2012; Xu et al., 2011). *De novo* variation represent the most extreme form of genetic variation with their occurence varying considerably depending on genomic location, paternal age and local sequence content. The latter may be particularly dependant on DSV proximity to CpG islands (Shiraishi et al., 2002). Perhaps more importantly, proband and parental DNA was not sequenced simultaneously as samples were collected nearly one year apart. Although exome capture was similar between cohorts, it is unclear how this factor accounts for the increased number of *de novo* DSVs in this analysis.

De novo occurence of mutations, although more likely to be causative for sproadic disease, importantly do not represent sufficient evidence of disease causation by themselves; the frequency and distribution of mutations require further characterisation in matched unaffected controls. Currently, data analysis techniques in whole exome sequencing are in rapid evolution and are most challenging when applied to complex disease genetics. Importantly, exome studies do not completely bridge the gap between rare variant *association* and disease *causation* without further functional

characterisation of downstream effects. However, the emergence of candidate genes in unstudied complex diseases would represent an important step forward.

Pathway-based segregation of DSVs by predicted functional effect is not a new approach in exome analysis but is novel within CTEPH. In this analysis, an equal fraction of damaging DSVs was present within fibrinolytic pathways in probands and parents suggesting equally deleterious mutations existed in these cohorts. These results fail to support a putative role for defective fibrinolysis in CTEPH over and above genes lying within non-fibrinolytic pathways. This result may be considered surprising as probands were deliberately phenotyped with this mechanism of disease in mind. Of note, parental sequencing produced a similar proportion of non-synonymous DSVs within fibrinolytic genes. This finding perhaps supports a 'second hit' hypothesis in CTEPH suggesting the differentiating factor between probands and parents is not their genetic architecture but instead an environmental factor, such as the occurrence of PE. Isolated VTE has been investigated with a large GWAS that has suggested minor increases in risk of VTE for small numbers of SNPs (Heit et al., 2012). Large studies such as this are crucial if ultimately a candidate gene approach is to be adopted in CTEPH, assuming large enough numbers of patients can be sequenced.

Appendix 5.1

CPB2 SERPINE1 F12 HRG KLKB1 SERPINB8 SERPINB10 SERPINI2 SERPINF2 PLAT THBD SERPINC1 FGA PLG PPBP PF4 PLAU TAF1 F2 SULT1A3 F5 F11 SERPINB2 ELANE F3 TAT VWF F10 PROC F7 PWAR1 F8 TFPI ANXA2 APOH MMP10 APOA1 SERPINA5 CPA6 PROS1 C1S CPB1 HABP2 PLAUR LPA NF2 KLK1 CPA1 TTPA F2RL2 RIPK4 PPIC CLEC3B RARRES2 PDGFB FGB SERPING1 ANGPT2 SELP KNG1 ALOX12 CPN1 KRT1 SAA1 TMPRSS6 USF1 CPA3 ORM1 F2R F9 VTN CRP INS ITGB2 FN1 SDC1 FGG PTGIS EPO GP1BA CELSR2 SERPINI1 CHKA FAP IL6 ALB AGTR1 CTSB SELE F13A1 TIMP1 GPT IL1RN CD40 ITGAM IGFBP7 SERPINA3 SERPINE2 LEP APOB CTSD THBS1 IL1R1 DES SERPINA1 IL18 TRAF3 A2M MB EDN1 ADIPOQ TNF ACE MAP2K1 ENO1 HMGCR NRP1 IGF2R REN IL1A SST GH1

SOD1 IL1B MAPK8 MMP9 FGF2 MTHFR PRL ADAMTSL1 EGF IL2 IL8 IL10 IL1RAPL2 APP MAPK1 TGFB1 IFNG VEGFA

Candidate gene list obtained from ‘Genecards’ for ‘fibrinolysis’ keyword search

Chapter 6. Patient-reported outcomes assessed by CAMPHOR questionnaire predict clinical deterioration in Chronic Thromboembolic Pulmonary Hypertension and Idiopathic Pulmonary Arterial Hypertension

6.1 Introduction

CTEPH and IPAH are rare conditions which despite available treatments display overall poor survival but with heterogeneity in individual prognosis (Galie et al., 2009c). IPAH has traditionally been perceived as a progressive disease with uniformly poor outcome but improving trends in survival are emerging, suggesting that advances in medical therapy or greater diversity in patient phenotype may be responsible (Benza et al., 2012; Keogh et al., 2011). In CTEPH with a proximal distribution of thrombotic obstructions, PEA strongly impacts survival with surgery that restores haemodynamics to normal levels almost analogous to cure in the most expert hands (Mayer et al., 2011). However, in patients with a distal distribution of disease and in those experiencing functional limitation and persistently abnormal haemodynamics following PEA, outcomes are less well characterised.

Prognostic factors, both invasive and non-invasive, form a cornerstone of PAH management and are relevant both to medical therapy and transplantation referral (Gupta et al., 2011; Swiston et al., 2010). Individually however they behave inconsistently in estimating prognosis. As such their use has been supplanted by examining panels of clinical data, taking into account multiple disease factors (Galie et al., 2009b). None of these specifically include patient-reported outcome measures (PROMs) or measures of a patient's health-related quality of life (QoL). These are typically short, self-completed questionnaires and can be either generic or disease specific. In healthcare services they are increasingly perceived as a robust method of measuring treatment outcomes that are important from a patient perspective. Using PROMs for prognostic evaluation is a novel area in PH although there is a burgeoning interest in their use for other chronic lung diseases (Braido et al., 2011). Although generic PROMs may lack sensitivity in monitoring changes in single patients, there are advantages in

applying disease-specific versions including trying to better understand the complex relationship between treatment efficacy and patient outcomes particular to certain diseases.

The most widely studied PROM in PH is the Cambridge Pulmonary Hypertension Outcome Review (CAMPHOR) (McKenna et al., 2006), a PH-specific measure of health-related QoL. It is a questionnaire comprising three sections evaluating symptoms, activity levels and QoL and has undergone international validation in patients with PH of multiple aetiologies (Chua et al., 2006; Cima et al., 2012; Ganderton et al., 2011; Gomberg-Maitland et al., 2008). Furthermore it has shown good correlation with the Medical Outcomes Study 36-item short form (SF-36) and the six minute walk distance (6MWD) (Gomberg-Maitland et al., 2008).

This study aimed to broaden the current clinical application of CAMPHOR and hypothesised that scores would have prognostic value both in CTEPH and IPAH. Our primary aim was to determine whether baseline CAMPHOR scores predicted clinical deterioration (CD) in these diseases. Our secondary aims were to evaluate CAMPHOR's prognostic value when repeated over time and the additional value it provided at diagnosis after adjustment for the prognostic influence of NYHA Class and 6MWD.

6.2 Methods

This study was a retrospective analysis of data obtained from the Pulmonary Vascular Disease Unit database at Papworth Hospital between 2004 and 2012 corresponding to eight years of CAMPHOR use in our practice. All patients provided written informed consent in completing questionnaires. Data collection for this study was under the approval of the local research ethics committee (Huntingdon) who approved the use of CAMPHOR within a PH population from 2004 onwards (REC reference: H02/805).

6.2.1 Study Population: Inclusion and Exclusion criteria

The study population consisted of incident cases of CTEPH and IPAH between May 2004 and end March 2012. All patients must have undergone RHC satisfying the most contemporaneous World Symposium on PH criteria at diagnosis and be over 16 years. Patients with CTEPH consisted of two subgroups. The first subgroup comprised patients with a distal distribution unsuitable for PEA. The second comprised patients with continued functional limitation receiving targeted PH treatment when found to have persistently elevated mPAP (>=25 mmHg) at RHC at least 3 months post PEA. These are referred to as 'residual' within the CTEPH group.

Patients were excluded in the following circumstances: a proximal distribution of CTEPH treated by PEA, a change in diagnosis following initial assessment, prescription of targeted therapy predating the first CAMPHOR assessment, patients who died during their first admission, failure to complete CAMPHOR alongside assessment of 6MWD and NYHA, failure to meet the threshold for treatment under the national guidelines. The contribution of excluding factors is outlined in Figure 6.1.

6.2.2 Questionnaire

The CAMPHOR questionnaire contains 65 items in total, 25 relating to symptoms, 15 relating to patient's activity and 25 relating to QoL. It is negatively weighted; a higher score indicates worse QoL and greater functional limitation. Symptom and QoL items are both scored out of 25; "yes/true" scores 1 and "no/not true" scores 0. Activity items have three possible responses (score 0-2): giving a score out of 30. Each CAMPHOR assessment takes on average 10 minutes.

6.2.3 Outcome variables

The primary outcome was CD defined as hospital admission with symptoms of right heart failure, escalation of targeted therapy, transplantation, atrial septostomy, or death. CD was quantified from time zero taken as the first diagnosis of PH contemporaneous with initiation of targeted treatment for patients with distal CTEPH and IPAH. In the residual CTEPH group, time zero was taken from first assessment at least three months following PEA. In total there were 5 patients lost to follow up and these patients were censored at the last visit date. All patients were treated as per National UK standards of care for PH (National Pulmonary Hypertension Centres of the and Ireland, 2008) and follow up continued until all patients clinically deteriorated or until censoring at the end of data collection (23rd March 2012).

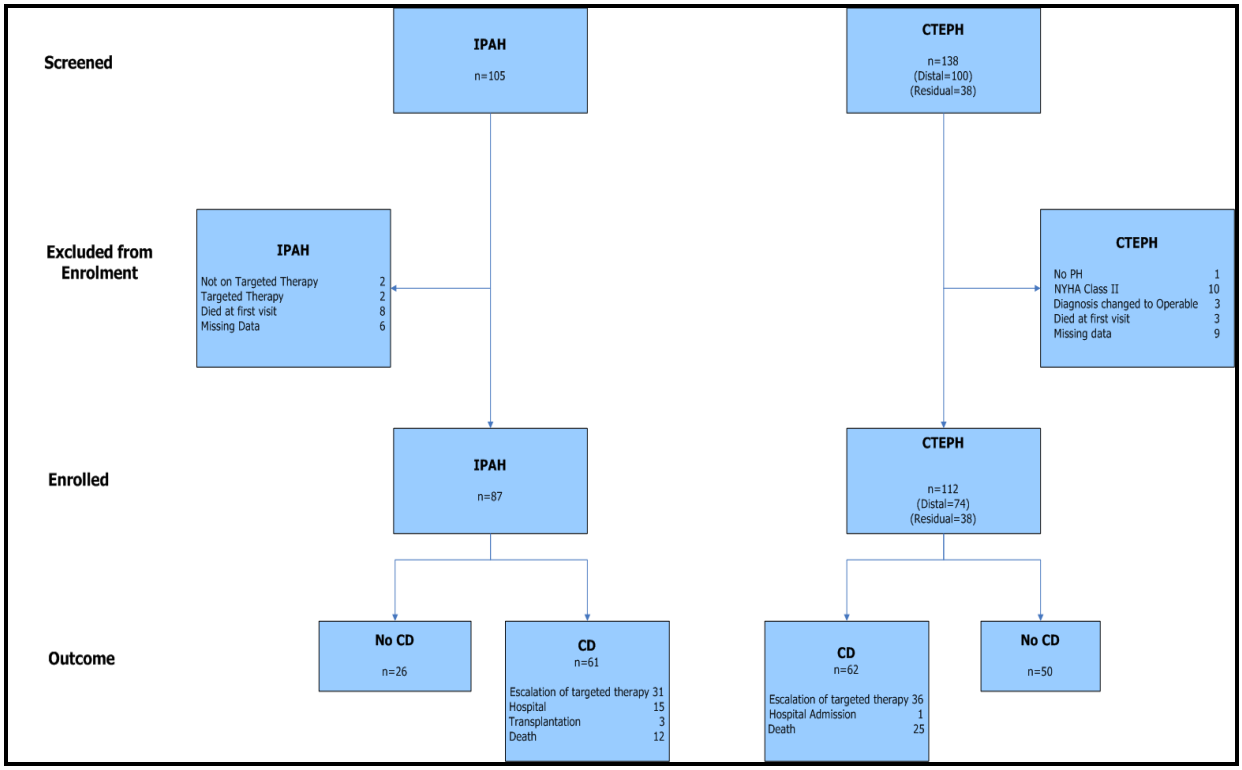

Figure 6.1

Patient pathway showing numbers screened, excluded, enrolled and those experiencing CD

6.2.4 Statistical Analysis

Patients diagnosed CTEPH and IPAH were analysed. Baseline information at time zero was summarised as mean and SD or frequency counts and proportions. CAMPHOR scales were analysed as total scores as well as each subcategory. There are no standard cut-offs for categorising total CAMPHOR score or CAMPHOR subscales. For Kaplan Meier plots total CAMPHOR score was split into 4 equal sized categories 0-19, 20-39, 40-59, 60-80 and subscales were split into 3 roughly equal sized categories; 0-8, 9-17 and 18+ for symptom and QoL and 0-9, 10-19 and 20+ for activity.

Time from treatment initiation to CD/censoring in the different categories was summarised on Kaplan-Meier plots with comparisons between categories by log-ranks tests. Univariable and multivariable Cox regression was used to assess independent risk predictors. Hazard Ratios and 95% confidence intervals were calculated to a 5% significance level. The association between CD and longitudinal information from CAMPHOR and clinical measures at 4 months and yearly intervals was analysed using univariable Cox regression with time-updated covariates, for missing covariate values the last measurement was carried forward. 20% and 24% of CTEPH and IPAH patients respectively had at least one prognostic factor missing at baseline. Missing baseline values were likely to be missing at random therefore missing values were imputed using multiple imputation to assess the robustness of the estimates from the complete case analysis. Since these analyses gave very similar results only the complete case analysis is included here.

6.3 Results

138 CTEPH patients and 105 IPAH and were screened with 112 and 87 respectively enrolled in the study. Patients were excluded for different reasons in CTEPH and IPAH groups (Figure 6.1). Baseline demographics, CAMPHOR scores and clinical data are shown in Table 6.1. Mean age in the IPAH group was lower and pulmonary haemodynamics were more severe. Total CAMPHOR scores and all

subscales were higher in the IPAH group consistent with worse self-assessment of symptoms. Notably 6MWD did not differ significantly at enrolment. Figure 6.1 shows the breakdown of CD for each group and demonstrates the majority of CD were a consequence of escalation of targeted therapies. In the CTEPH group, 49 of the total of 62 CD events occurred in the distal group and 13 in the residual group. 28/74 (38%) died in the distal group during the study compared to 7/38 (18%) in the residual group.

Variable	Units /Categories	CTEPH patients (n=112)	IPAH patients (n=87)
Mean Age		61.4 (14.8)	55.7 (16.3)
Age range		17 – 86	18 – 81
mPAP (mmHg)	Mean (S.D)	45.8 (11.8)	49.6 (10.5)
	Missing	2	9
PVR (Dyn)	Mean (S.D)	10.5 (5.6)	13.8 (5.0)
	Missing	14	22
Gender	Male	44 (39%)	35 (40%)
	Female	68 (61%)	52 (60%)
Total CAMPHOR score	Mean (S.D)	33.0 (16.8)	39.9 (17.2)
	Missing	17	13
Symptom score	Mean (S.D)	11.7 (6.2)	13.8 (6.2)
	Missing	15	12
Activity score	Mean (S.D)	11.5 (6.2)	13.9 (7.2)
	Missing	16	12
QoL score	Mean (S.D)	10.0 (6.5)	12.0 (6.3)
	Missing	17	13
6MWT (metres)	Mean (S.D)	277.7 (119.0)	271.9 (112.7)
	Missing	6	7
NYHA Class	2	22 (20%)	8 (9%)
	3	83 (74%)	61 (71%)
	4	7 (6%)	17 (20%)
	Missing	0	1
Type	Distal	74 (66%)	-
	Residual	38 (34%)	-

Table 6.1

Comparison of baseline characteristics

Neither gender nor age was associated with an altered risk of CD nor did age significantly affect the interval to CD during follow up. Freedom from CD was higher for patients with CTEPH up to 5 years after enrolment, after which it was similar to that for patients with IPAH (Figure 6.2). Survival was

consistent with recent international registries with no difference between the CTEPH and IPAH cohort (Figure 6.3) (Humbert et al., 2006; Thenappan et al., 2007).

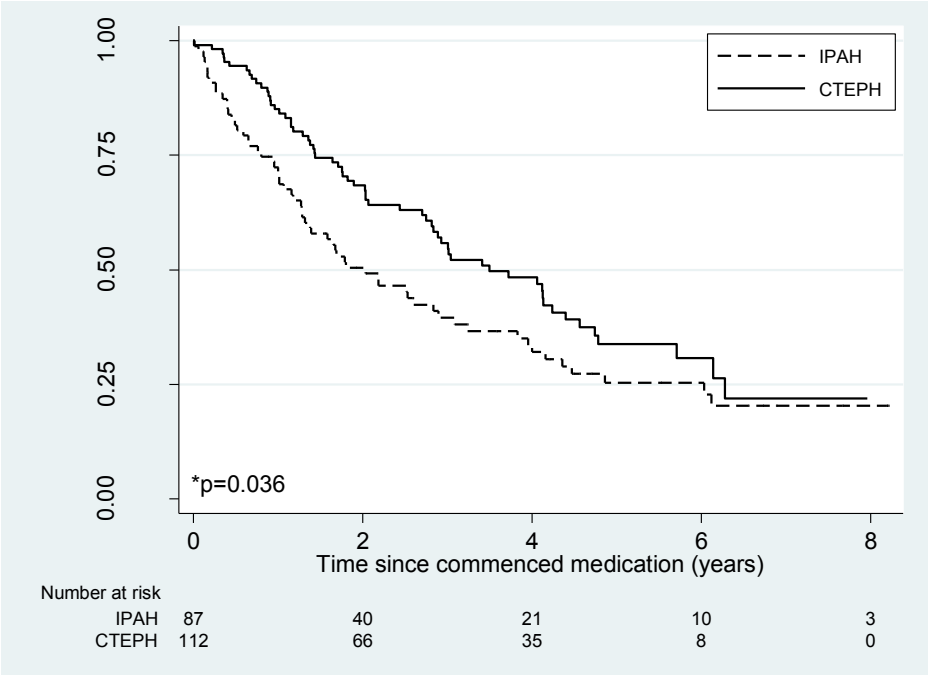

*Logrank Test P value

Figure 6.2

Kaplan- Meier plots displaying the cumulative proportion free from CD over the follow up period

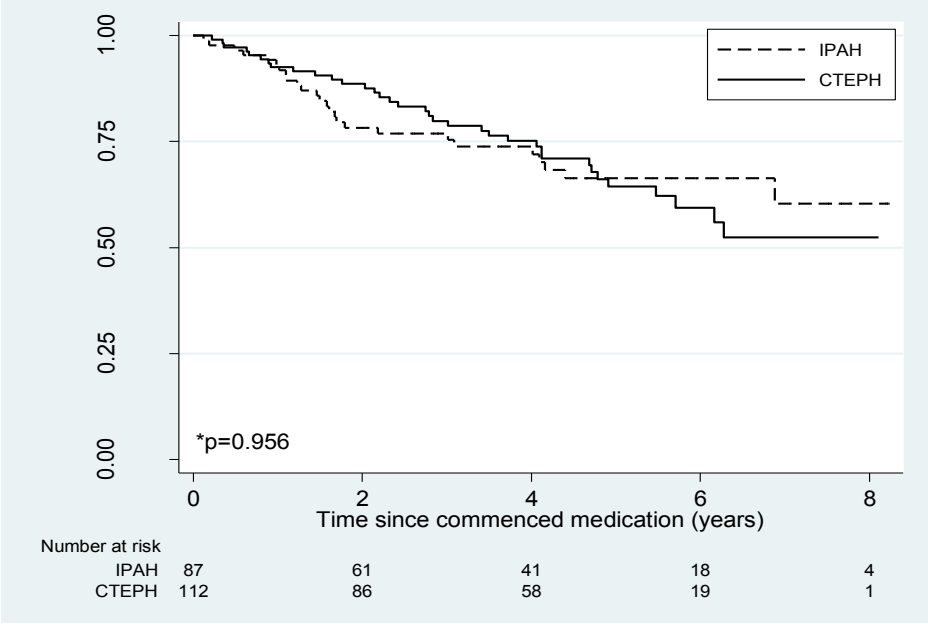

*Logrank test P value

Figure 6.3

Kaplan-Meier survival plots for both cohorts

6.3.1 Univariable analysis

In both CTEPH and IPAH groups baseline measurements of total CAMPHOR scores, all subscales and a higher NYHA Class were independent predictors of CD (Table 6.2). Haemodynamics mPAP and PVR also showed some predictive value. QoL scores between 0 – 8 and 9 – 17 showed similar rates of CD although a QoL score greater than 18 was associated with significantly higher rate of CD (Appendix 6.1 – page 121). In the CTEPH group, CD was significantly related to total CAMPHOR score and all CAMPHOR subscales (Figure 6.4a). In patients with IPAH, CD was significantly associated with higher categories of total CAMPHOR score and symptom and activity scores (Figure 6.4b). QoL scores between 0 – 8 and 9 – 17 showed similar rates of CD although a QoL score greater than 18 was associated with significantly higher rate of CD (Figure 6.5). A higher baseline 6MWD predicted a reduced likelihood of CD in both CTEPH and IPAH with a 50m increase associated with a significantly reduced hazard across the study population (Table 6.2). A total of 66 and 90 patients in the IPAH and CTEPH groups had total CAMPHOR, NYHA and 6MWD at baseline.

Variable	Units /Categories	CTEPH patients HR (95% CI)	P value*	IPAH patients HR (95% CI)	P value*
Total CAMPHOR	Unit score increase	1.04 (1.02 – 1.06)	<0.001	1.03 (1.01 – 1.05)	0.001
Symptom	Unit score increase	1.12 (1.07 – 1.18)	<0.001	1.09 (1.04 – 1.14)	0.001
Activity	Unit score increase	1.12 (1.07 – 1.17)	<0.001	1.06 (1.02 – 1.11)	0.002
QoL**	0 – 8			-	
	9 – 17	1.07 (1.03 – 1.12)	0.001	0.73 (0.38 – 1.40)	0.046
	18 – 25			1.79 (0.90 – 3.53)	
NYHA	2	-		-	
	3	2.67 (1.25 – 5.70)	0.013	1.59 (0.62 – 4.07)	0.007
	4	3.57 (1.06 – 12.06)		4.00 (1.42 – 11.27)	
6MWD	50m increase	0.79 (0.70 – 0.89)	<0.001	0.84 (0.75 – 0.95)	0.004
mPAP (mmHg)	5 mmHg increase	1.15 (1.03 – 1.29)	0.013	1.10 (0.96 – 1.25)	0.170
PVR (Dyn)	200 Dyn increase (2.5 Wood Units)	1.12 (0.99 – 1.27)	0.075	1.20 (1.04 – 1.38)	0.015
Type	Distal	-	<0.001	-	-
	Residual	0.37 (0.20 – 0.69)		-	-

Table 6.2

Univariable Cox proportional hazards models for clinical deterioration with baseline measurements as covariates. *Likelihood ratio test P value. **QoL unit score increase for CTEPH patients and categories for IPAH patients.

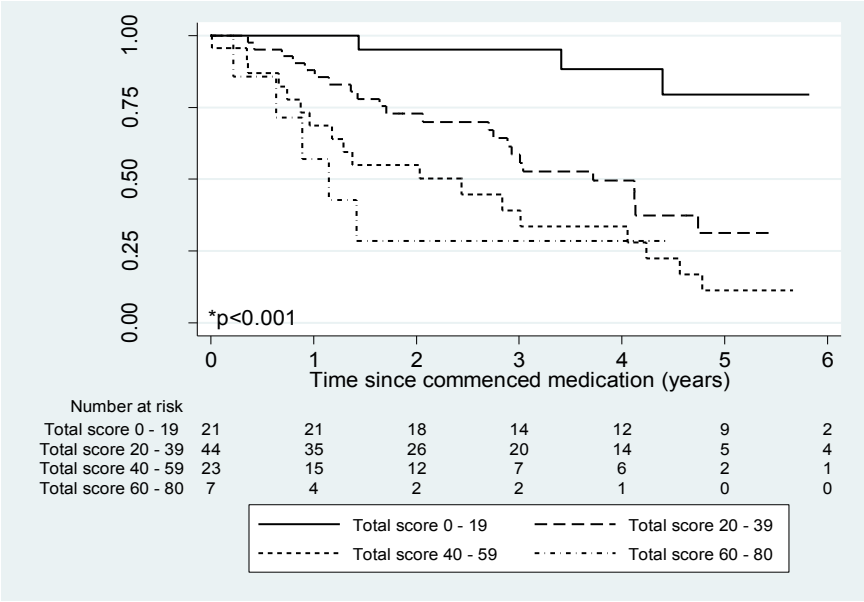

*Logrank test P value

Figure 6.4a

Kaplan- Meier plots displaying the cumulative proportion free from CD over the follow up period for different categories of total CAMPHOR at baseline for CTEPH patients

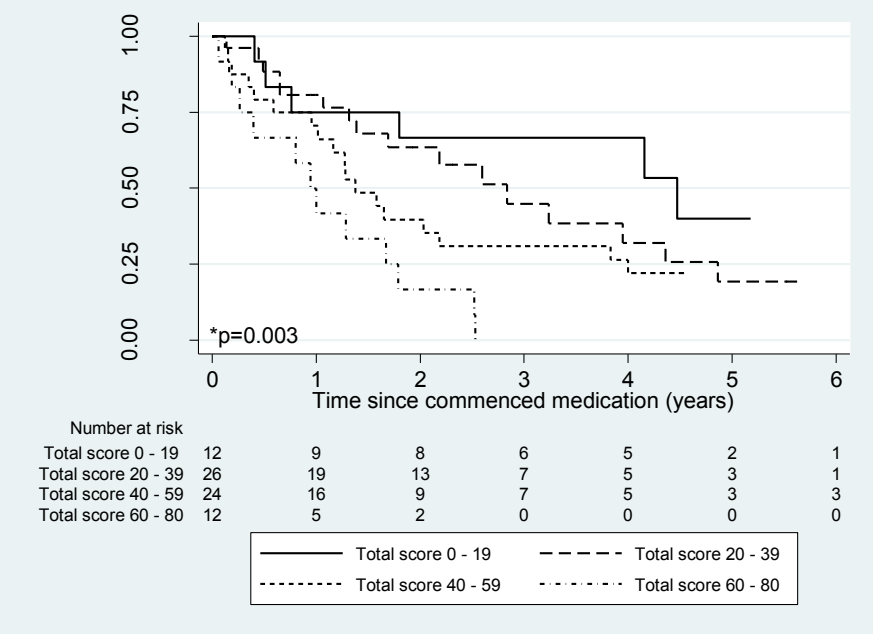

*Logrank test P value

Figure 6.4b

Kaplan- Meier plots displaying the cumulative proportion free from CD over the follow up period for different categories of total CAMPHOR at baseline for IPAH patients

6.3.2 Multivariable analysis

The multivariable modeling adjusted for the effect of NYHA class and 6MWD at baseline is shown in Table 6.3. In the CTEPH group, baseline symptom score and total CAMPHOR were of independent value with no significant effect seen from activity or QoL. Only a high QoL score provided an independent predictive effect of CD for patients with IPAH. Given CAMPHOR is correlated to 6MWD and NYHA, when both are adjusted for, the effect of each subscale is notably diluted. Further adjustment for mPAP and PVR increases the association of total CAMPHOR and it's subscales with CD (Appendix 6.2 – page 123) but these results should be interpreted with caution due to the low number of patients and CD events. 47 and 78 patients in the IPAH and CTEPH groups had total CAMPHOR, NYHA, 6MWD, mPAP and PVR at baseline.

		CTEPH patients		IPAH patients	
Variable	**Units /Categories**	**HR (95% CI)**	**P value***	**HR (95% CI)**	**P Value***
Total CAMPHOR	Unit score increase	1.03 (1.00 – 1.05)	0.027	1.02 (0.99 – 1.05)	0.158
Symptom	Unit score increase	1.08 (1.02 - 1.15)	0.006	1.05 (0.98 - 1.12)	0.143
Activity	Unit score increase	1.06 (1.00 - 1.13)	0.067	1.04 (0.98 - 1.10)	0.227
QoL**	0 – 8			-	
	9 -17	1.03 (0.98 – 1.09)	0.210	0.37 (0.16 - 0.84)	0.005
	18 -25			1.14 (0.47 - 2.78)	

*Likelihood ratio test P value. **QoL unit score increase for CTEPH patients and categories for IPAH patients

Table 6.3

Multivariable Cox proportional hazards models adjusted for NYHA and 6MWD for clinical deterioration with baseline measurements as covariates

6.3.3 Longitudinal analysis

Longitudinal analysis of total CAMPHOR scores, its subscales and 6MWD showed a direct association with CD (Table 6.4). NYHA Class was not analysed as a time-updated covariate as patients rarely changed class. The similar regression coefficients using Cox regression (Table 6.2) and time-updated covariates (Table 6.4) suggest that isolated CAMPHOR assessments over time add little to its predictive effect on CD determined at enrolment and that the effect of CAMPHOR does not change over time.

Variable	Units/Categories	CTEPH patients		IPAH patients	
		HR (95% CI)	P Value*	HR (95% CI)	P Value*
Total CAMPHOR score	Unit score increase	1.04 (1.02 – 1.05)	<0.001	1.04 (1.02 – 1.06)	<0.001
Symptom	Unit score increase	1.11 (1.06 – 1.15)	<0.001	1.11 (1.06 – 1.16)	<0.001
Activity	Unit score increase	1.12 (1.07 – 1.16)	<0.001	1.08 (1.04 – 1.12)	<0.001
QoL	Unit score increase	1.08 (1.04 – 1.12)	<0.001	1.08 (1.03 – 1.13)	<0.001
6MWD	50m increase	0.75 (0.67 – 0.84)	<0.001	0.81 (0.73 – 0.91)	<0.001

*Logrank Test P value

Table 6.4

Univariable Cox proportional hazards models with CAMPHOR scores as time updated covariates

6.4 Discussion

The current clinical application of CAMPHOR focuses on evaluation of patient perceptions in PH. We have shown for the first time a novel use for the CAMPHOR questionnaire obtained at diagnosis in its ability to predict CD in patients with CTEPH and IPAH. Similar to NYHA Class and 6MWD, both total CAMPHOR score and its subscales appear to act as risk predictors suggesting CAMPHOR may have prognostic importance. Following adjustment for 6MWD and NYHA Class, some predictive effect persists and further adjusting for haemodynamics, mPAP and PVR, increases the association of total CAMPHOR and it's subscales with CD. This may be explained by the loss of heterogeneity between CTEPH and IPAH after adjustment for NYHA, 6MWD, mPAP and PVR, leaving a clearer association between CAMPHOR and CD.

In keeping with existing knowledge, a lower 6MWD and higher NYHA Class at enrolment were associated with greater risk of CD. Gender had no significant effect. Contrasting with other studies, age did not predict rate of CD in either CTEPH or IPAH cohorts (Benza et al., 2012; Galie et al., 2008b; Hoeper et al., 2005b). This is most likely explained by our definition of CD being different

from that used in other interventional studies in that we did not incorporate a reduction in 6MWD or maintenance of NYHA Class within our CD criteria, both of which may act as more sensitive indicators of CD with advancing age (Howard, 2011). We intentionally chose our definition of CD in part because not all clinical measures were documented at each visit, the poor inter-observer correlation of NYHA Class assessment and because CD could have occurred without a 6MWD being undertaken if patients were too unwell. In spite of this the similar survival trends to large registries points to the observed rates of CD with advancing age being a genuine effect (Humbert et al., 2010; Lee et al., 2012).

Total baseline CAMPHOR is an 80 point scale so that a one unit increase is a small difference and unlikely to be clinically relevant. A more meaningful increase of 10 points on the total CAMPHOR scale has a univariable HR of 1.37 (1.14 – 1.64) for CTEPH and 1.51 (1.27 – 1.79) for IPAH, giving a 51% and 37% increase in the incidence of CD respectively. Whilst baseline total CAMPHOR scores demonstrate a significant predictive effect of CD in both CTEPH and IPAH, exceptions arise within subscales of CAMPHOR when analysed in isolation. For QoL within the IPAH cohort, the hazard ratio behaves non-linearly with an inferred protective effect against CD for QoL scores between 9-17 which reverts to a detrimental effect for scores of 18 or above. This is in contrast to trends demonstrated by symptom and activity scores.

Comparison between disease groups also suggests different CAMPHOR subscales harbour different predictive value. QoL of all three CAMPHOR subscales is the most likely to be subject to confounding. It is known that factors such as age, gender, education and income may impact on QoL, the contributions of which could not be encompassed within this study (Hopman et al., 2009). Similarly, feelings of depression, anxiety and hopelessness are well captured within QoL (McCollister et al., 2010). Although the small age and gender difference between groups, may account for some of the observed trends, we speculate that differing modes of presentation may affect risk of CD determined by CAMPHOR. Patients with IPAH generally experience more indolent onset of symptoms which may allow time for ‘protective’ lifestyle adaptations. The relatively abrupt onset of

CTEPH however, often predated by an acute embolic event, may precipitate different illness perceptions at first presentation.

Importantly, decisions to increase treatment would have been made following patient assessment using 6MWD and other assessment tools. CAMPHOR scores were collected and reviewed after any clinical decision was made meaning scores would not have affected treatment decisions and thus CD. Notably, the majority of CD events arose from escalation of targeted therapies in both CTEPH and IPAH cohorts. Differing trends in treatment of these diseases in the UK make cross-cohort comparison of rates of CD difficult to interpret as IPAH benefits from several licensed drug classes with more scope for escalation of treatment in the face of a poor response to an initial treatment agent. By contrast CTEPH has more limited licensed treatments and treatment with PAH licensed therapy is recommended generally only within clinical drug trials. Furthermore, UK treatment guidelines differ to European guidelines as treatment in the UK is driven more by overall clinical impression of PH physicians rather than targeted treatment towards fixed goals in functional capacity (Hoeper et al., 2005b). Obtaining an equivalent prescription of targeted therapies may therefore be impossible to achieve between IPAH and CTEPH in the face of clinically apparent patient deterioration although at baseline, data on targeted therapies prescribed within our cohorts (Appendix 6.3 – page 123) suggest similar treatment strategies between CTEPH and IPAH.

Survival did not differ significantly between CTEPH and IPAH cohorts. Deaths contributed more towards CD in the CTEPH group but a similar proportion of patients with IPAH died after an alternative CD event. Almost one third of our CTEPH cohort consisted of patients post-PEA presenting with persistent functional limitation. Clinical experience suggests that patients in this category exhibit more stable clinical courses compared to those with distal CTEPH and there are almost certainly differences in pulmonary circulatory responses that govern prognosis following major operative intervention (Freed et al., 2011). Although combining these two groups may therefore seem artificial, our primary intention in this study was to evaluate the prognostic power of patient perceptions using CAMPHOR and so for this reason their amalgamation is justifiable.

PAH therapies are generally licensed for symptomatic benefit based on studies using 6MWD as a surrogate for symptomatic change. The use of PROMs to monitor patients is appropriate as patients are primarily treated for symptoms as patients will often trade years of life for good quality life. The finding that CAMPHOR may also offer prognostic information should therefore be seen as an added benefit. Although lacking direct physiological links as a marker of cardiopulmonary function, CAMPHOR is patient-centred in contrast to more traditional assessment tools which as a group may be subject to observer variability and confounding factors. Given its highly disease-specific derivation, it may therefore have a novel use in selected populations with PH.

Despite a relatively large patient number, our study does have limitations. Cox regression used in our statistical analysis assumes constant risk ratios for predictive variables throughout the duration of a patient's follow up which may not clinically apply to our patients. In addition, clinical need determined the follow-up intervals. Therefore, longitudinal analysis was hampered by time-updated covariate measurements not being present.

6.5 Conclusions

Existing non-invasive parameters used in prognostic assessment in PAH have recognised limitations and this study has sought to broaden the application of a patient-centred assessment in PH. Recently published UK prognostic equations that derive risk scores in PAH may accurately predict survival but they still rely on invasive tests (Lee et al., 2012). Increasing attention is now turning towards the physical and emotional implications of living with incurable disease and CTEPH and IPAH populations should not be regarded as exceptional (Chen et al., 2008). The relatively limited response to PAH targeted treatments with persistent high mortality rate makes the clinical incorporation of patient perceptions into long term care an attractive step forward in an emerging era of goal-oriented therapy.

Appendix 6.1

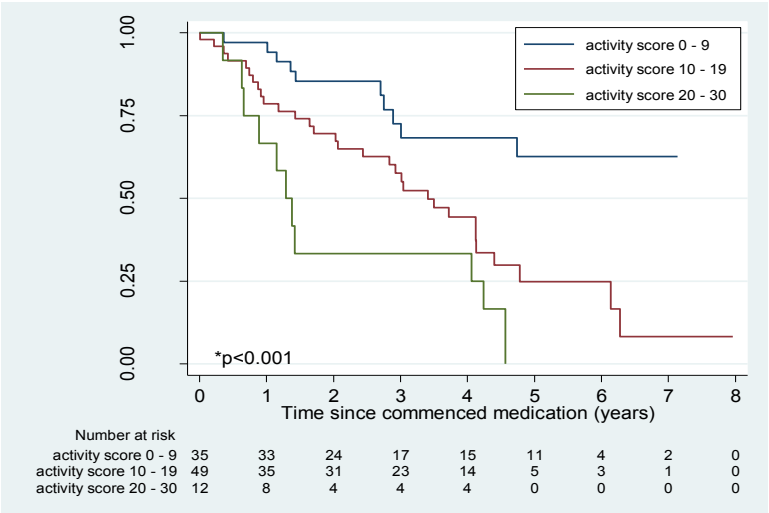

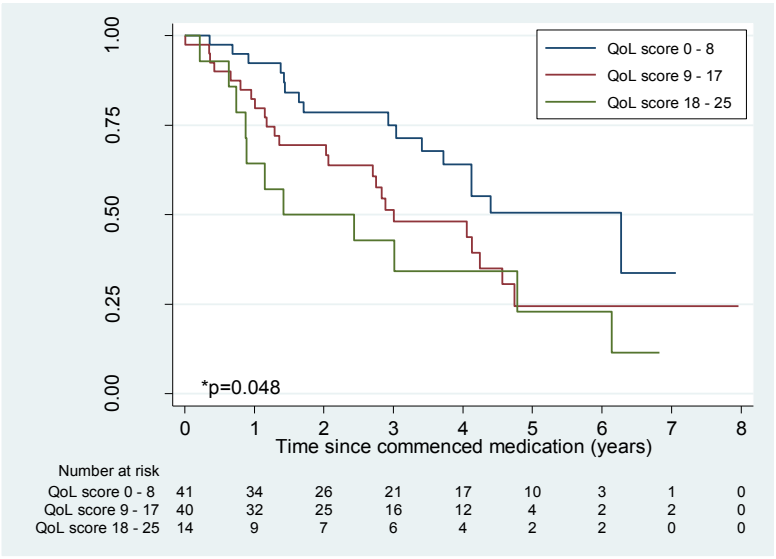

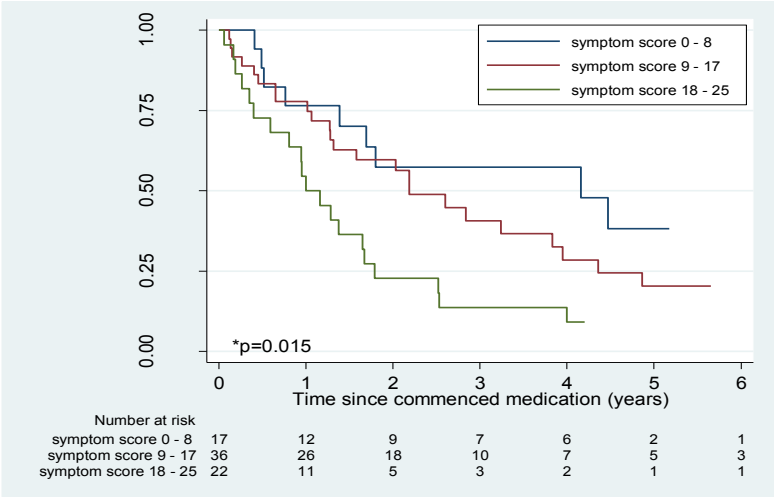

Kaplan- Meier plots displaying the cumulative proportion free from CD over the follow up period or different categories of the CAMPHOR subscales at baseline – CTEPH patients

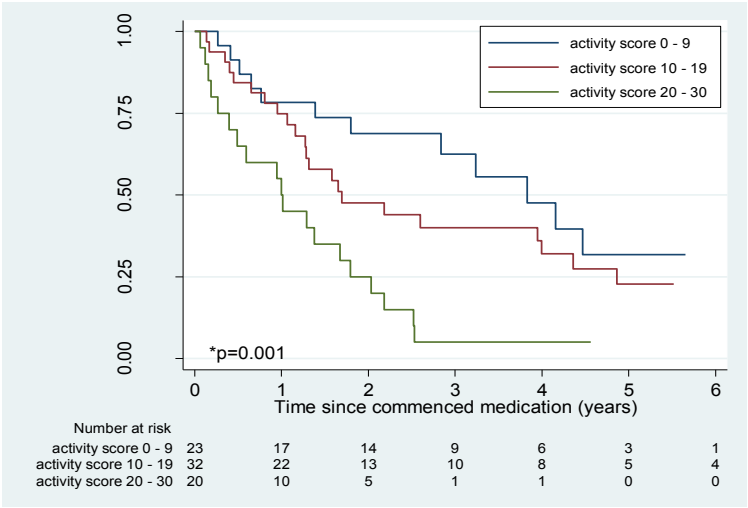

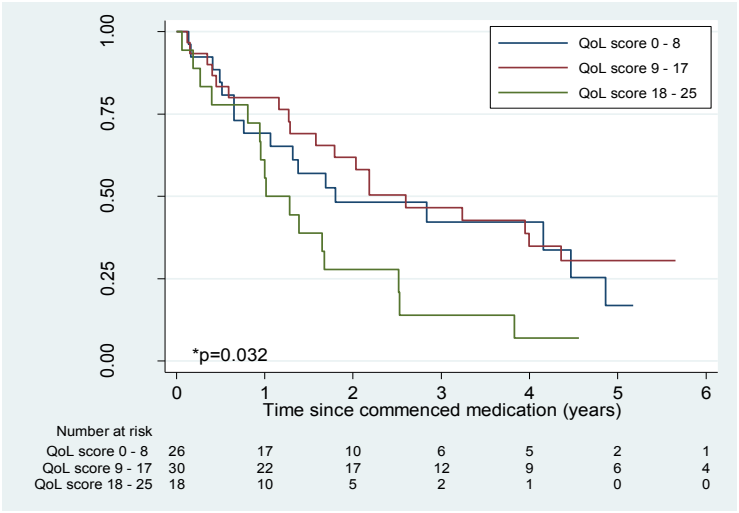

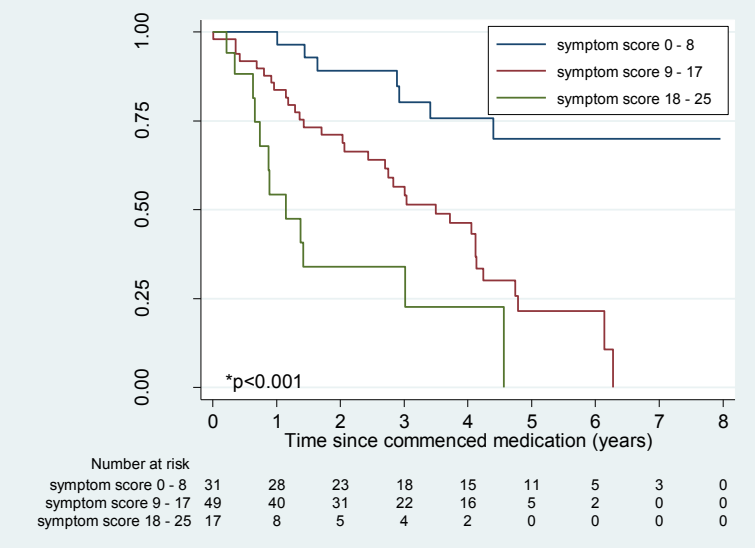

Kaplan- Meier plots displaying the cumulative proportion free from CD over the follow up period for different categories of the CAMPHOR subscales at baseline – IPAH patients

Appendix 6.2

Variable	Units /Categories	IPAH patients (N=47 (31 CD events)) HR (95% CI)	P value*	CTEPH patients*** HR (95% CI)	P value*
Total CAMPHOR	**Unit score increase**	1.05 (1.01 – 1.09)	0.005	1.04 (1.01 – 1.07)	0.004
Symptom	**Unit score increase**	1.11 (1.02 - 1.20)	0.013	1.11 (1.04 – 1.18)	0.001
Activity	**Unit score increase**	1.11 (1.02 - 1.20)	0.009	1.07 (1.00 1.15)	0.052
QoL**	**0 – 8**	-	0.012	1.06 (1.00 – 1.12)	0.049
	9 -17	0.36 (0.12 – 1.08)			
	18 -25	1.38 (0.45 – 4.24)			

Multivariable Cox proportional hazards models adjusted for NYHA, mPAP, PVR and 6MWD for clinical deterioration with baseline measurements as covariates. *Likelihood ratio test P value. **QoL unit score increase for CTEPH patients and categories for IPAH patients. ***CTEPH- symptom- N= 80 (44 got CD), activity- N= 79 (44 got CD), QoL and total- N= 78 (43 got CD)

Appendix 6.3

Targeted Therapy at Baseline	IPAH n=87 n(%)	CTEPH n=112 n(%)
Ambrisentan	0(0)	1(0.9)
Bosentan	38 (44)	42 (37.5)
Epoprostenol (IV)	9 (10.3)	2 (1.7)
Epoprostenol (IV) & Bosentan	1 (1.1)	0 (0)
Iloprost (nebulised)	6 (6.9)	4 (3.6)
Iloprost (nebulised) & Sildenafil	1 (1.1)	0 (0)
Sildenafil	26 (29.8)	51 (45.5)
Sitaxentan	4 (4.6)	1 (0.9)
Trial drug	2 (2.3)	11 (9.8)

Baseline targeted therapies for CTEPH and IPAH cohorts

Chapter 7: General Discussion

The work presented in this thesis encompasses several different approaches in attempt to further our understanding of chronic thromboembolic disease in humans. These include the application of invasive historical techniques used to study RV function, high throughput sequencing of patient DNA in the investigation of existing and novel disease mechanisms in CTEPH and the evaluation of patient-reported outcomes. CTEPH is positioned at the most extreme end of the thromboembolic spectrum where the RV is subjected to chronic pressure overload. From the outset, a primary hypothesis of the exome sequencing study suggested CTEPH develops from the co-ordinated interplay between genetic and environmental factors. However, emergent from the physiological studies is the striking heterogeneity in phenotype of patients with chronic thromboembolic obstruction. Proximal and distal CTEPH are established and separate clinical entities despite being indistinguishable pathologically. However, based on more detailed interrogation both at rest and on exercise, the RV demonstrates clear physiological variation in performance even within these phenotypes. In recent years, attention has refocused on the crosstalk between the RV and pulmonary circulation, intrinsically linked by properties of pulsatile flow in the pulmonary artery. Development of tools describing this interaction that ideally translate more easily into clinical use, will allow RV myocardial biology to be increasingly related to its downstream function.

Long term follow up studies have uniformly demonstrated that in one third to two thirds of patients suffering acute PE, perfusion recovery may be incomplete even years after the initial insult. However, thromboembolic obstruction in this setting fails to exclusively lead to symptomatic impairment raising questions over its functional importance. Chapter 3 describes a study of RV and pulmonary circulatory performance during this clinical period and using pressure volume catheterisation, the RV is shown to behave abnormally, most notably during diastole. Akin to the ischaemic cascade in the LV, diastolic impairment may signify early RV decompensation although this study does not provide firm evidence for this. Instead, RV *adaptation* is demonstrated that occurs within a normal

haemodynamic spectrum. Whilst this highlights important deficiencies in PVR as a descriptor of RV afterload, the clinical significance of RV adaptation remains unclear. Intrinsic myocardial dysfunction may be responsible for the observed RV changes. Alternatively, RV adaptation may signify early pathological embarkation towards RV hypertrophy. Such speculation requires serial follow-up and, as yet, it is not proven that patients with CTED deteriorate over time. Although pressure volume catheterisation has clear value in load-independent contractile assessment, its lower patient acceptability and expense mean any longer-term studies of RV adaptation are more likely to be pursued using non-invasive methods.

Early RV adaptation may be further investigated by molecular methods. Myocardial remodeling is regulated by hypertrophic and inflammatory gene expression and is known to be triggered by hypoxia and stress-activated pathways within the myocardium. Capacity for remodeling also demonstrates both inter and intra-species variation with no uniform threshold for its development identified to date. RV myocardial biopsies were beyond the ethical limits of this study but represent an attractive direction in which to further this work. Of particular interest would be the pattern of gene up-regulation in hypertrophic pathways in myocardial tissue exposed to varying degrees of pressure overload. This could potentially incorporate those patients found to have 'subclinical' RV adaptation on pressure volume assessment. Previous studies involving biopsies of RV myocardium have been hampered by the lack of standardised protocols for timing of biopsies within the disease course and by inconsistency in RV biopsy location in the myocardial wall. However, detailed patient phenotyping offered by pressure volume assessment may enable patients with early RV adaptation to be selectively targeted to improve our understanding of changes in the myocardial genetic profile.

In spite of an inferior patient acceptability, the merits of invasive cardiac catheterisation are notable during an era which has seen a paradigm shift toward non-invasive imaging modalities for RV functional assessment. This is in the main due to their improved image resolution and ability to perform serial assessments to track disease progression. RV ejection performance is determined by a number of factors: preload, afterload, RV wall thickness and contractility and in keeping with most

cardiac diseases, prognosis in all forms of PH is principally determined by myocardial dysfunction conferred by the property of contractility. In this regard, the conductance catheter demonstrates a clear advantage over non-invasive imaging; its capacity to measure dynamic ventricular volumes throughout the cardiac cycle. Assessment of RV volume is one of the most basic evaluations of RV function, currently best assessed by CMR although bedside 3D echocardiography may soon supplant this. Nevertheless, continued investment in invasive techniques that have a proven track record in RV contractile physiology, still appear warranted.

Chapter 4 used CPET to evaluate functional impairment in patients with thromboembolic obstruction. CPET has found a foothold in the PH clinic in the last ten years providing ancillary information on exercise limitation above and beyond the 6MWD. However, a lack of standardised CPET protocols within clinical trials has perhaps hampered its wider application in the PH clinic. This study suggests that in patients with persistent symptoms post PE, both an exercise gas exchange deficit and RV insufficiency contribute to exercise intolerance. Furthermore, CPET predicts abnormal resting haemodynamics with acceptable levels of stringency. Stratification of patients at risk of PH and earlier identification of a pulmonary vascular cause of exercise limitation are important objectives in patients being followed up for persistent symptoms post PE. Use of an exercise approach in this context may potentially avoid the need for ionising radiation which is advantageous in younger populations. Importantly, this study was limited by its highly selected population in whom radiological characteristics were predetermined prior to enrolment. The lack of simultaneous exercise haemodynamics also limit conclusions on the recruitable RV contractile reserve given RV pressure flow responses can vary on exercise. However, in the presence of chronic thromboembolic obstruction and apparent preservation of resting RV systolic function on echocardiogram, CPET represents a useful addition to the clinical assessment that could potentially indicate early deterioration in RV function.

High throughput sequencing in CTEPH represents a high risk strategy for isolating novel disease mechanisms and the sequencing of unrelated individuals to look for genetic disease origins is yet to

bear fruit in complex phenotypes. The premise of a novel genetic aetiology in CTEPH was based largely on its extremely low population prevalence and apparent evolution from defective fibrinolysis. However, a fibrinolytic origin is often contested in CTEPH pathogenesis as increasing evidence for the role of inflammation and angiogenesis has come to light. Exome sequencing requires an entirely unbiased approach to variant filtration especially when sequencing unrelated individuals in a disease with no predefined heritability. From the outset, patients were chosen on the basis of prior occurrence of PE, therefore inherently pre-selecting a major thrombembolic co-factor. A complimentary approach to control for the occurrence of prior PE may have involved sequencing individuals with CTEPH with no prior VTE episode or alternatively, a patient cohort with documented symptomatic and radiological resolution of abnormalities within three months of treatment for acute PE. However, neither of these groups was available for study within the ethical confines of this work.

CTEPH may be attributable to very rare mutations in a small number or variety of genes; however, our patient number appears to have been inadequate to identify causative mutations. Exome sequencing of unrelated individuals has to date only been applied successfully using small numbers of patients with Mendelian diseases. Furthermore, these patients have had much more clearly defined phenotypes with limited heterogeneity. Multiple interacting genes have the potential to dilute the genetic signal in complex diseases and results from the CTEPH probands produced lists of candidate genes that were too long for further investigation. However in future, this sequencing data could be combined with exome sequencing data from larger numbers of individuals with CTEPH and Biobanks to perform a stronger case-control analysis.

Comparison of fibrinolytic DSVs in probands and parental samples did not highlight a preponderance of damaging mutations as a likely contributor to CTEPH aetiology. Although damaging fibrinolytic mutations did exist in CTEPH probands, none were novel and therefore were unlikely to represent an *unknown* genetic predisposition. The trio approach was useful in that *de novo* mutations are purported to be more damaging that inherited variants. However, our study appeared to be numerically underpowered (ten parental child trios) given a recent study evaluating *de novo* mutations in non-

familial schizophrenia sequenced in excess of 50 affected trios and over 20 controls to identify 40 *de novo* mutations (Xu et al., 2011). Diseases attributable to *de novo* genetic variation exhibit relative stability in their global incidence. At present however, the epidemiology of CTEPH has been insufficiently characterised to either support of refute this hypothesis.

Finally, Chapter 6 described a retrospective analysis of the predictive value of the CAMPHOR on prognosis in two forms of PH. This study potentially has the furthest reaching consequences as prognostic markers provide invaluable guidance in treatment planning in PH. Of note, traditional markers of poor prognosis, including abnormal haemodynamics, functional class and 6MWD are shown to be no more valuable than those gleaned from simple patient questionnaires at diagnosis. This emphasises the value of patient perceptions in patients with PH and as a predictive model suggests that patient reported outcomes should form part of routine practice in all PH patients. In patients in whom invasive haemodynamic monitoring is not feasible, clinicians can feel increasingly confident that the CAMPHOR tracks disease progression more closely than is perhaps widely perceived.

In summary, this thesis tackles several aspects of pulmonary vascular function with attempt to uncover novel mechanisms in the aetiology and physiological monitoring of CTEPH. RV functional adaptation may be further understood through continued appreciation of historical RV assessment methods in combination with up to date non-invasive techniques. The underlying genetic architecture of CTEPH warrants continued investment with multiparalleled sequencing through collaborative approaches involving greater patient numbers.

Publications deriving from this work

C McCabe, S Preston, D Gopalan, J Dunning, J Pepke-Zaba. Cardiopulmonary exercise testing suggests beneficial response to pulmonary endarterectomy in a patient with normal pulmonary haemodynamics *Pulm Circ 2014; 4(1) ePub ahead of print*

C McCabe, B Rana, R Axell, P White, D Gopalan, J Pepke-Zaba, S Hoole. RV functional assessment: have new techniques supplanted the "old faithful" conductance catheter. *Cardiol Rev. 2014 Mar 11. [Epub ahead of print]*

C McCabe, P White, S Hoole, R Axell, B Agrawal, D Gopalan, N Screaton, L Shapiro, N Morrell, J Pepke-Zaba. Right ventricular dysfunction in chronic thromboembolic obstruction of the pulmonary artery: A Pressure Volume study using the conductance catheter *J Appl Physiol (1985)2014 Feb;116(4):355-63*.

C McCabe, G Deboeck, I Harvey, R Mackenzie-Ross, D Gopalan, N Screaton, J Pepke-Zaba. Inefficient exercise gas exchange identifies pulmonary hypertension in chronic thromboembolic obstruction of the pulmonary artery following acute pulmonary embolism *Thromb Res.* 2013 Dec;132(6):659-65

C McCabe, M Bennett, R MacKenzie-Ross, L Sharples, J Pepke-Zaba. Patient reported outcomes assessed by CAMPHOR questionnaire predict clinical deterioration in Idiopathic Pulmonary Arterial Hypertension and Chronic Thromboembolic Pulmonary Hypertension. *Chest*. 2013 Aug;144(2):522-30. doi: 10.1378/chest.12-2443

Abstracts derived from this work

C McCabe, S Hoole, P White, R Axell, L Shapiro, J Pepke-Zaba. Inefficient right ventriculo-arterial coupling contributes to reduced exercise capacity in pulmonary hypertension. Oral presentation: BTS Winter Meeting 2013

C McCabe, S Graf, K Sheares, J Pepke-Zaba, N Morrell. Whole exome sequencing identifies novel genetic variation in chronic thromboembolic pulmonary hypertension. Oral presentation: BTS Winter Meeting 2012

O Davies, **C McCabe**, J Pepke-Zaba, K Sheares. High dose oestrogens commenced for gender reassignment surgery may predispose to the development of chronic thromboembolic pulmonary vascular disease. Oral presentation: BTS Winter Meeting 2013

References

Adzhubei, I.A., Schmidt, S., Peshkin, L., Ramensky, V.E., Gerasimova, A., Bork, P., Kondrashov, A.S., and Sunyaev, S.R. (2010). A method and server for predicting damaging missense mutations. Nature methods *7*, 248-249.

Ali, T., Humphries, J., Burnand, K., Sawyer, B., Bursill, C., Channon, K., Greaves, D., Rollins, B., Charo, I.F., and Smith, A. (2006). Monocyte recruitment in venous thrombus resolution. Journal of vascular surgery *43*, 601-608.

Argiento, P., Vanderpool, R.R., Mule, M., Russo, M.G., D'Alto, M., Bossone, E., Chesler, N.C., and Naeije, R. (2012). Exercise stress echocardiography of the pulmonary circulation: limits of normal and sex differences. Chest *142*, 1158-1165.

Auger, W.R., Kerr, K.M., Kim, N.H., Ben-Yehuda, O., Knowlton, K.U., and Fedullo, P.F. (2004). Chronic thromboembolic pulmonary hypertension. Cardiology clinics *22*, 453-466, vii.

Auger, W.R., Permpikul, P., and Moser, K.M. (1995). Lupus anticoagulant, heparin use, and thrombocytopenia in patients with chronic thromboembolic pulmonary hypertension: a preliminary report. The American journal of medicine *99*, 392-396.

Baan, J., Jong, T.T., Kerkhof, P.L., Moene, R.J., van Dijk, A.D., van der Velde, E.T., and Koops, J. (1981). Continuous stroke volume and cardiac output from intra-ventricular dimensions obtained with impedance catheter. Cardiovascular research *15*, 328-334.

Baan, J., van der Velde, E.T., de Bruin, H.G., Smeenk, G.J., Koops, J., van Dijk, A.D., Temmerman, D., Senden, J., and Buis, B. (1984). Continuous measurement of left ventricular volume in animals and humans by conductance catheter. Circulation *70*, 812-823.

Badesch, D.B., Champion, H.C., Sanchez, M.A., Hoeper, M.M., Loyd, J.E., Manes, A., McGoon, M., Naeije, R., Olschewski, H., Oudiz, R.J.*, et al.* (2009). Diagnosis and assessment of pulmonary arterial hypertension. Journal of the American College of Cardiology *54*, S55-66.

Balady, G.J., Arena, R., Sietsema, K., Myers, J., Coke, L., Fletcher, G.F., Forman, D., Franklin, B., Guazzi, M., Gulati, M.*, et al.* (2010). Clinician's Guide to cardiopulmonary exercise testing in adults: a scientific statement from the American Heart Association. Circulation *122*, 191-225.

Bamshad, M.J., Ng, S.B., Bigham, A.W., Tabor, H.K., Emond, M.J., Nickerson, D.A., and Shendure, J. (2011). Exome sequencing as a tool for Mendelian disease gene discovery. Nature reviews Genetics *12*, 745-755.

Becattini, C., Agnelli, G., Pesavento, R., Silingardi, M., Poggio, R., Taliani, M.R., and Ageno, W. (2006). Incidence of chronic thromboembolic pulmonary hypertension after a first episode of pulmonary embolism. Chest *130*, 172-175.

Bellofiore, A., and Chesler, N.C. (2013). Methods for measuring right ventricular function and hemodynamic coupling with the pulmonary vasculature. Annals of biomedical engineering *41*, 1384-1398.

Benza, R.L., Miller, D.P., Barst, R.J., Badesch, D.B., Frost, A.E., and McGoon, M.D. (2012). An evaluation of long-term survival from time of diagnosis in pulmonary arterial hypertension from the REVEAL Registry. Chest *142*, 448-456.

Biesecker, L.G. (2010). Exome sequencing makes medical genomics a reality. Nature genetics *42*, 13-14.

Bishop, A., White, P., Chaturvedi, R., Brookes, C., Redington, A., and Oldershaw, P. (1997a). Resting right ventricular function in patients with coronary artery disease: pressure volume analysis using conductance catheters. International journal of cardiology *58*, 223-228.

Bishop, A., White, P., Groves, P., Chaturvedi, R., Brookes, C., Redington, A., and Oldershaw, P. (1997b). Right ventricular dysfunction during coronary artery occlusion: pressure-volume analysis using conductance catheters during coronary angioplasty. Heart *78*, 480-487.

Blyth, K.G., Groenning, B.A., Martin, T.N., Foster, J.E., Mark, P.B., Dargie, H.J., and Peacock, A.J. (2005). Contrast enhanced-cardiovascular magnetic resonance imaging in patients with pulmonary hypertension. European heart journal *26*, 1993-1999.

Bonderman, D., Jakowitsch, J., Redwan, B., Bergmeister, H., Renner, M.K., Panzenbock, H., Adlbrecht, C., Georgopoulos, A., Klepetko, W., Kneussl, M.*, et al.* (2008). Role for staphylococci in misguided thrombus resolution of chronic thromboembolic pulmonary hypertension. Arteriosclerosis, thrombosis, and vascular biology *28*, 678-684.

Bonderman, D., Martischnig, A.M., Vonbank, K., Nikfardjam, M., Meyer, B., Heinz, G., Klepetko, W., Naeije, R., and Lang, I.M. (2011). Right ventricular load at exercise is a cause of persistent exercise limitation in patients with normal resting pulmonary vascular resistance after pulmonary endarterectomy. Chest *139*, 122-127.

Bonderman, D., Turecek, P.L., Jakowitsch, J., Weltermann, A., Adlbrecht, C., Schneider, B., Kneussl, M., Rubin, L.J., Kyrle, P.A., Klepetko, W.*, et al.* (2003). High prevalence of elevated clotting factor VIII in chronic thromboembolic pulmonary hypertension. Thrombosis and haemostasis *90*, 372-376.

Bonderman, D., Wilkens, H., Wakounig, S., Schafers, H.J., Jansa, P., Lindner, J., Simkova, I., Martischnig, A.M., Dudczak, J., Sadushi, R.*, et al.* (2009). Risk factors for chronic thromboembolic pulmonary hypertension. The European respiratory journal *33*, 325-331.

Braido, F., Baiardini, I., Balestracci, S., Menoni, S., Balbi, F., Ferraioli, G., Bocchibianchi, S., and Canonica, G.W. (2011). Chronic obstructive pulmonary disease patient well-being and its relationship with clinical and patient-reported outcomes: a real-life observational study. Respiration; international review of thoracic diseases *82*, 335-340.

Brimioulle, S., Wauthy, P., Ewalenko, P., Rondelet, B., Vermeulen, F., Kerbaul, F., and Naeije, R. (2003). Single-beat estimation of right ventricular end-systolic pressure-volume

relationship. American journal of physiology Heart and circulatory physiology *284*, H1625-1630.

Brookes, C.I., White, P.A., Bishop, A.J., Oldershaw, P.J., Redington, A.N., and Moat, N.E. (1998). Validation of a new intraoperative technique to evaluate load-independent indices of right ventricular performance in patients undergoing cardiac operations. The Journal of thoracic and cardiovascular surgery *116*, 468-476.

Cabrol, S., Souza, R., Jais, X., Fadel, E., Ali, R.H., Humbert, M., Dartevelle, P., Simonneau, G., and Sitbon, O. (2007). Intravenous epoprostenol in inoperable chronic thromboembolic pulmonary hypertension. The Journal of heart and lung transplantation : the official publication of the International Society for Heart Transplantation *26*, 357-362.

Carr, I.M., Morgan, J., Watson, C., Melnik, S., Diggle, C.P., Logan, C.V., Harrison, S.M., Taylor, G.R., Pena, S.D., Markham, A.F.*, et al.* (2013). Simple and efficient identification of rare recessive pathologically important sequence variants from next generation exome sequence data. Human mutation *34*, 945-952.

Castelain, V., Herve, P., Lecarpentier, Y., Duroux, P., Simonneau, G., and Chemla, D. (2001). Pulmonary artery pulse pressure and wave reflection in chronic pulmonary thromboembolism and primary pulmonary hypertension. Journal of the American College of Cardiology *37*, 1085-1092.

Champion, H.C., Michelakis, E.D., and Hassoun, P.M. (2009). Comprehensive invasive and noninvasive approach to the right ventricle-pulmonary circulation unit: state of the art and clinical and research implications. Circulation *120*, 992-1007.

Channick, R.N., Simonneau, G., Sitbon, O., Robbins, I.M., Frost, A., Tapson, V.F., Badesch, D.B., Roux, S., Rainisio, M., Bodin, F.*, et al.* (2001). Effects of the dual endothelin-receptor antagonist bosentan in patients with pulmonary hypertension: a randomised placebo-controlled study. Lancet *358*, 1119-1123.

Chaturvedi, R.R., Kilner, P.J., White, P.A., Bishop, A., Szwarc, R., and Redington, A.N. (1997). Increased airway pressure and simulated branch pulmonary artery stenosis increase pulmonary regurgitation after repair of tetralogy of Fallot. Real-time analysis with a conductance catheter technique. Circulation *95*, 643-649.

Chen, H., Taichman, D.B., and Doyle, R.L. (2008). Health-related quality of life and patient-reported outcomes in pulmonary arterial hypertension. Proceedings of the American Thoracic Society *5*, 623-630.

Chesler, N.C., Roldan, A., Vanderpool, R.R., and Naeije, R. (2009). How to measure pulmonary vascular and right ventricular function. Conference proceedings : Annual International Conference of the IEEE Engineering in Medicine and Biology Society IEEE Engineering in Medicine and Biology Society Conference *2009*, 177-180.

Choi, M., Scholl, U.I., Ji, W., Liu, T., Tikhonova, I.R., Zumbo, P., Nayir, A., Bakkaloglu, A., Ozen, S., Sanjad, S.*, et al.* (2009). Genetic diagnosis by whole exome capture and massively parallel DNA sequencing. Proceedings of the National Academy of Sciences of the United States of America *106*, 19096-19101.

Chua, R., Keogh, A.M., Byth, K., and O'Loughlin, A. (2006). Comparison and validation of three measures of quality of life in patients with pulmonary hypertension. Internal medicine journal *36*, 705-710.

Cima, K., Twiss, J., Speich, R., McKenna, S.P., Grunig, E., Kahler, C.M., Ehlken, N., Treder, U., Crawford, S.R., Huber, L.C.*, et al.* (2012). The German adaptation of the Cambridge Pulmonary Hypertension Outcome Review (CAMPHOR). Health and quality of life outcomes *10*, 110.

Coche, E., Vlassenbroek, A., Roelants, V., D'Hoore, W., Verschuren, F., Goncette, L., and Maldague, B. (2005). Evaluation of biventricular ejection fraction with ECG-gated 16-slice CT: preliminary findings in acute pulmonary embolism in comparison with radionuclide ventriculography. European radiology *15*, 1432-1440.

Cole, J.W., Stine, O.C., Liu, X., Pratap, A., Cheng, Y., Tallon, L.J., Sadzewicz, L.K., Dueker, N., Wozniak, M.A., Stern, B.J.*, et al.* (2012). Rare variants in ischemic stroke: an exome pilot study. PLoS ONE *7*, e35591.

Danton, M.H., Greil, G.F., Byrne, J.G., Hsin, M., Cohn, L., and Maier, S.E. (2003). Right ventricular volume measurement by conductance catheter. American journal of physiology Heart and circulatory physiology *285*, H1774-1785.

Dantzker, D.R., and D'Alonzo, G.E. (1985). Pulmonary gas exchange and exercise performance in pulmonary hypertension. Chest *88*, 255S-257S.

Dartevelle, P., Fadel, E., Mussot, S., Chapelier, A., Herve, P., de Perrot, M., Cerrina, J., Ladurie, F.L., Lehouerou, D., Humbert, M.*, et al.* (2004). Chronic thromboembolic pulmonary hypertension. The European respiratory journal *23*, 637-648.

de Man, F.S., Handoko, M.L., van Ballegoij, J.J., Schalij, I., Bogaards, S.J., Postmus, P.E., van der Velden, J., Westerhof, N., Paulus, W.J., and Vonk-Noordegraaf, A. (2012). Bisoprolol delays progression towards right heart failure in experimental pulmonary hypertension. Circulation Heart failure *5*, 97-105.

Deboeck, G., Niset, G., Lamotte, M., Vachiery, J.L., and Naeije, R. (2004). Exercise testing in pulmonary arterial hypertension and in chronic heart failure. The European respiratory journal *23*, 747-751.

Dell'Italia, L.J. (1991). The right ventricle: anatomy, physiology, and clinical importance. Current problems in cardiology *16*, 653-720.

Dell'Italia, L.J. (2012). Anatomy and physiology of the right ventricle. Cardiology clinics *30*, 167-187.

Dell'Italia, L.J., and Santamore, W.P. (1998). Can indices of left ventricular function be applied to the right ventricle? Progress in cardiovascular diseases *40*, 309-324.

Dell'Italia, L.J., and Walsh, R.A. (1988a). Application of a time varying elastance model to right ventricular performance in man. Cardiovascular research *22*, 864-874.

Dell'Italia, L.J., and Walsh, R.A. (1988b). Right ventricular diastolic pressure-volume relations and regional dimensions during acute alterations in loading conditions. Circulation *77*, 1276-1282.

Deng, Z., Morse, J.H., Slager, S.L., Cuervo, N., Moore, K.J., Venetos, G., Kalachikov, S., Cayanis, E., Fischer, S.G., Barst, R.J., *et al.* (2000). Familial primary pulmonary hypertension (gene PPH1) is caused by mutations in the bone morphogenetic protein receptor-II gene. American journal of human genetics *67*, 737-744.

Dentali, F., Donadini, M., Gianni, M., Bertolini, A., Squizzato, A., Venco, A., and Ageno, W. (2009). Incidence of chronic pulmonary hypertension in patients with previous pulmonary embolism. Thrombosis research *124*, 256-258.

DePristo, M.A., Banks, E., Poplin, R., Garimella, K.V., Maguire, J.R., Hartl, C., Philippakis, A.A., del Angel, G., Rivas, M.A., Hanna, M., *et al.* (2011). A framework for variation discovery and genotyping using next-generation DNA sequencing data. Nature genetics *43*, 491-498.

Dogan, H., Kroft, L.J., Bax, J.J., Schuijf, J.D., van der Geest, R.J., Doornbos, J., and de Roos, A. (2006). MDCT assessment of right ventricular systolic function. AJR American journal of roentgenology *186*, S366-370.

Eichler, E.E., Flint, J., Gibson, G., Kong, A., Leal, S.M., Moore, J.H., and Nadeau, J.H. (2010). Missing heritability and strategies for finding the underlying causes of complex disease. Nature reviews Genetics *11*, 446-450.

Faludi, R., Komocsi, A., Bozo, J., Kumanovics, G., Czirjak, L., Papp, L., and Simor, T. (2008). Isolated diastolic dysfunction of right ventricle: stress-induced pulmonary hypertension. The European respiratory journal *31*, 475-476.

Fedullo, P.F., Auger, W.R., Channick, R.N., Moser, K.M., and Jamieson, S.W. (1995). Chronic thromboembolic pulmonary hypertension. Clinics in chest medicine *16*, 353-374.

Fedullo, P.F., Auger, W.R., Kerr, K.M., and Rubin, L.J. (2001). Chronic thromboembolic pulmonary hypertension. The New England journal of medicine *345*, 1465-1472.

Fedullo, P.F., Rubin, L.J., Kerr, K.M., Auger, W.R., and Channick, R.N. (2000). The natural history of acute and chronic thromboembolic disease: the search for the missing link. The European respiratory journal *15*, 435-437.

Feneley, M.P., Gavaghan, T.P., Baron, D.W., Branson, J.A., Roy, P.R., and Morgan, J.J. (1985). Contribution of left ventricular contraction to the generation of right ventricular systolic pressure in the human heart. Circulation *71*, 473-480.

Firth, A.L., Yau, J., White, A., Chiles, P.G., Marsh, J.J., Morris, T.A., and Yuan, J.X. (2009). Chronic exposure to fibrin and fibrinogen differentially regulates intracellular Ca2+ in human pulmonary arterial smooth muscle and endothelial cells. American journal of physiology Lung cellular and molecular physiology *296*, L979-986.

Freed, D.H., Thomson, B.M., Berman, M., Tsui, S.S., Dunning, J., Sheares, K.K., Pepke-Zaba, J., and Jenkins, D.P. (2011). Survival after pulmonary thromboendarterectomy: effect of residual pulmonary hypertension. The Journal of thoracic and cardiovascular surgery *141*, 383-387.

Freed, D.H., Thomson, B.M., Tsui, S.S., Dunning, J.J., Sheares, K.K., Pepke-Zaba, J., and Jenkins, D.P. (2008). Functional and haemodynamic outcome 1 year after pulmonary thromboendarterectomy. European journal of cardio-thoracic surgery : official journal of the European Association for Cardio-thoracic Surgery *34*, 525-529; discussion 529-530.

Galie, N., Brundage, B.H., Ghofrani, H.A., Oudiz, R.J., Simonneau, G., Safdar, Z., Shapiro, S., White, R.J., Chan, M., Beardsworth, A.*, et al.* (2009a). Tadalafil therapy for pulmonary arterial hypertension. Circulation *119*, 2894-2903.

Galie, N., Ghofrani, H.A., Torbicki, A., Barst, R.J., Rubin, L.J., Badesch, D., Fleming, T., Parpia, T., Burgess, G., Branzi, A.*, et al.* (2005). Sildenafil citrate therapy for pulmonary arterial hypertension. The New England journal of medicine *353*, 2148-2157.

Galie, N., Hoeper, M.M., Humbert, M., Torbicki, A., Vachiery, J.L., Barbera, J.A., Beghetti, M., Corris, P., Gaine, S., Gibbs, J.S.*, et al.* (2009b). Guidelines for the diagnosis and treatment of pulmonary hypertension: the Task Force for the Diagnosis and Treatment of Pulmonary Hypertension of the European Society of Cardiology (ESC) and the European Respiratory Society (ERS), endorsed by the International Society of Heart and Lung Transplantation (ISHLT). European heart journal *30*, 2493-2537.

Galie, N., Manes, A., Negro, L., Palazzini, M., Bacchi-Reggiani, M.L., and Branzi, A. (2009c). A meta-analysis of randomized controlled trials in pulmonary arterial hypertension. European heart journal *30*, 394-403.

Galie, N., Olschewski, H., Oudiz, R.J., Torres, F., Frost, A., Ghofrani, H.A., Badesch, D.B., McGoon, M.D., McLaughlin, V.V., Roecker, E.B.*, et al.* (2008a). Ambrisentan for the treatment of pulmonary arterial hypertension: results of the ambrisentan in pulmonary arterial hypertension, randomized, double-blind, placebo-controlled, multicenter, efficacy (ARIES) study 1 and 2. Circulation *117*, 3010-3019.

Galie, N., Rubin, L., Hoeper, M., Jansa, P., Al-Hiti, H., Meyer, G., Chiossi, E., Kusic-Pajic, A., and Simonneau, G. (2008b). Treatment of patients with mildly symptomatic pulmonary arterial hypertension with bosentan (EARLY study): a double-blind, randomised controlled trial. Lancet *371*, 2093-2100.

Gan, C.T., Holverda, S., Marcus, J.T., Paulus, W.J., Marques, K.M., Bronzwaer, J.G., Twisk, J.W., Boonstra, A., Postmus, P.E., and Vonk-Noordegraaf, A. (2007). Right ventricular diastolic dysfunction and the acute effects of sildenafil in pulmonary hypertension patients. Chest *132*, 11-17.

Ganderton, L., Jenkins, S., McKenna, S.P., Gain, K., Fowler, R., Twiss, J., and Gabbay, E. (2011). Validation of the Cambridge Pulmonary Hypertension Outcome Review (CAMPHOR) for the Australian and New Zealand population. Respirology *16*, 1235-1240.

Ghaye, B., Nchimi, A., Noukoua, C.T., and Dondelinger, R.F. (2006). Does multi-detector row CT pulmonary angiography reduce the incremental value of indirect CT venography compared with single-detector row CT pulmonary angiography? Radiology *240*, 256-262.

Ghofrani, H.A., D'Armini, A.M., Grimminger, F., Hoeper, M.M., Jansa, P., Kim, N.H., Mayer, E., Simonneau, G., Wilkins, M.R., Fritsch, A.*, et al.* (2013). Riociguat for the treatment of chronic thromboembolic pulmonary hypertension. The New England journal of medicine *369*, 319-329.

Gomberg-Maitland, M., Thenappan, T., Rizvi, K., Chandra, S., Meads, D.M., and McKenna, S.P. (2008). United States validation of the Cambridge Pulmonary Hypertension Outcome Review (CAMPHOR). The Journal of heart and lung transplantation : the official publication of the International Society for Heart Transplantation *27*, 124-130.

Gomez-Arroyo, J., Mizuno, S., Szczepanek, K., Van Tassell, B., Natarajan, R., dos Remedios, C.G., Drake, J.I., Farkas, L., Kraskauskas, D., Wijesinghe, D.S.*, et al.* (2013). Metabolic gene remodeling and mitochondrial dysfunction in failing right ventricular hypertrophy secondary to pulmonary arterial hypertension. Circulation Heart failure *6*, 136-144.

Gotthardt, M., Schipper, M., Franzius, C., Behe, M., Barth, A., Schurrat, T., Hoffken, H., Gratz, S., Joseph, K., and Behr, T.M. (2002). Follow-up of perfusion defects in pulmonary perfusion scanning after pulmonary embolism: are we too careless? Nuclear medicine communications *23*, 447-452.

Grothues, F., Moon, J.C., Bellenger, N.G., Smith, G.S., Klein, H.U., and Pennell, D.J. (2004). Interstudy reproducibility of right ventricular volumes, function, and mass with cardiovascular magnetic resonance. American heart journal *147*, 218-223.

Guey, L.T., Kravic, J., Melander, O., Burtt, N.P., Laramie, J.M., Lyssenko, V., Jonsson, A., Lindholm, E., Tuomi, T., Isomaa, B.*, et al.* (2011). Power in the phenotypic extremes: a simulation study of power in discovery and replication of rare variants. Genetic epidemiology.

Guo, Y.K., Gao, H.L., Zhang, X.C., Wang, Q.L., Yang, Z.G., and Ma, E.S. (2010). Accuracy and reproducibility of assessing right ventricular function with 64-section multi-detector row CT: comparison with magnetic resonance imaging. International journal of cardiology *139*, 254-262.

Gupta, H., Ghimire, G., and Naeije, R. (2011). The value of tools to assess pulmonary arterial hypertension. European respiratory review : an official journal of the European Respiratory Society *20*, 222-235.

Haddad, F., Doyle, R., Murphy, D.J., and Hunt, S.A. (2008). Right ventricular function in cardiovascular disease, part II: pathophysiology, clinical importance, and management of right ventricular failure. Circulation *117*, 1717-1731.

Hamdan, F.F., Daoud, H., Patry, L., Dionne-Laporte, A., Spiegelman, D., Dobrzeniecka, S., Rouleau, G.A., and Michaud, J.L. (2013). Parent-child exome sequencing identifies a de novo

truncating mutation in TCF4 in non-syndromic intellectual disability. Clinical genetics *83*, 198-200.

Hansen, J.E., Sun, X.G., Yasunobu, Y., Garafano, R.P., Gates, G., Barst, R.J., and Wasserman, K. (2004). Reproducibility of cardiopulmonary exercise measurements in patients with pulmonary arterial hypertension. Chest *126*, 816-824.

Hardziyenka, M., Surie, S., de Groot, J.R., de Bruin-Bon, H.A., Knops, R.E., Remmelink, M., Yong, Z.Y., Baan, J., Jr., Bouma, B.J., Bresser, P.*, et al.* (2011). Right ventricular pacing improves haemodynamics in right ventricular failure from pressure overload: an open observational proof-of-principle study in patients with chronic thromboembolic pulmonary hypertension. Europace : European pacing, arrhythmias, and cardiac electrophysiology : journal of the working groups on cardiac pacing, arrhythmias, and cardiac cellular electrophysiology of the European Society of Cardiology *13*, 1753-1759.

Heit, J.A., Armasu, S.M., Asmann, Y.W., Cunningham, J.M., Matsumoto, M.E., Petterson, T.M., and De Andrade, M. (2012). A genome-wide association study of venous thromboembolism identifies risk variants in chromosomes 1q24.2 and 9q. Journal of thrombosis and haemostasis : JTH *10*, 1521-1531.

Hoeper, M.M., Kramm, T., Wilkens, H., Schulze, C., Schafers, H.J., Welte, T., and Mayer, E. (2005a). Bosentan therapy for inoperable chronic thromboembolic pulmonary hypertension. Chest *128*, 2363-2367.

Hoeper, M.M., Markevych, I., Spiekerkoetter, E., Welte, T., and Niedermeyer, J. (2005b). Goal-oriented treatment and combination therapy for pulmonary arterial hypertension. The European respiratory journal *26*, 858-863.

Hoeper, M.M., Mayer, E., Simonneau, G., and Rubin, L.J. (2006). Chronic thromboembolic pulmonary hypertension. Circulation *113*, 2011-2020.

Hoey, E.T., Mirsadraee, S., Pepke-Zaba, J., Jenkins, D.P., Gopalan, D., and Screaton, N.J. (2011). Dual-energy CT angiography for assessment of regional pulmonary perfusion in patients with chronic thromboembolic pulmonary hypertension: initial experience. AJR American journal of roentgenology *196*, 524-532.

Hollenberg, M., and Tager, I.B. (2000). Oxygen uptake efficiency slope: an index of exercise performance and cardiopulmonary reserve requiring only submaximal exercise. Journal of the American College of Cardiology *36*, 194-201.

Hoole, S.P., Heck, P.M., White, P.A., Read, P.A., Khan, S.N., West, N.E., O'Sullivan, M., and Dutka, D.P. (2010). Stunning and cumulative left ventricular dysfunction occurs late after coronary balloon occlusion in humans insights from simultaneous coronary and left ventricular hemodynamic assessment. JACC Cardiovascular interventions *3*, 412-418.

Hopman, W.M., Harrison, M.B., Coo, H., Friedberg, E., Buchanan, M., and VanDenKerkhof, E.G. (2009). Associations between chronic disease, age and physical and mental health status. Chronic diseases in Canada *29*, 108-116.

Howard, L.S. (2011). Prognostic factors in pulmonary arterial hypertension: assessing the course of the disease. European respiratory review : an official journal of the European Respiratory Society *20*, 236-242.

Humbert, M., Monti, G., Brenot, F., Sitbon, O., Portier, A., Grangeot-Keros, L., Duroux, P., Galanaud, P., Simonneau, G., and Emilie, D. (1995). Increased interleukin-1 and interleukin-6 serum concentrations in severe primary pulmonary hypertension. American journal of respiratory and critical care medicine *151*, 1628-1631.

Humbert, M., Sitbon, O., Chaouat, A., Bertocchi, M., Habib, G., Gressin, V., Yaici, A., Weitzenblum, E., Cordier, J.F., Chabot, F.*, et al.* (2010). Survival in patients with idiopathic, familial, and anorexigen-associated pulmonary arterial hypertension in the modern management era. Circulation *122*, 156-163.

Humbert, M., Sitbon, O., Chaouat, A., Bertocchi, M., Habib, G., Gressin, V., Yaici, A., Weitzenblum, E., Cordier, J.F., Chabot, F.*, et al.* (2006). Pulmonary arterial hypertension in France: results from a national registry. American journal of respiratory and critical care medicine *173*, 1023-1030.

Humbert, M., Sitbon, O., and Simonneau, G. (2004). Treatment of pulmonary arterial hypertension. The New England journal of medicine *351*, 1425-1436.

International, P.P.H.C., Lane, K.B., Machado, R.D., Pauciulo, M.W., Thomson, J.R., Phillips, J.A., 3rd, Loyd, J.E., Nichols, W.C., and Trembath, R.C. (2000). Heterozygous germline mutations in BMPR2, encoding a TGF-beta receptor, cause familial primary pulmonary hypertension. Nature genetics *26*, 81-84.

Isakov, O., Perrone, M., and Shomron, N. (2013). Exome sequencing analysis: a guide to disease variant detection. Methods in molecular biology *1038*, 137-158.

Jardim, C., Rochitte, C.E., Humbert, M., Rubenfeld, G., Jasinowodolinski, D., Carvalho, C.R., and Souza, R. (2007). Pulmonary artery distensibility in pulmonary arterial hypertension: an MRI pilot study. The European respiratory journal *29*, 476-481.

Kang, D.K., Sun, J.S., Park, K.J., and Lim, H.S. (2011). Usefulness of combined assessment with computed tomographic signs of right ventricular dysfunction and cardiac troponin T for risk stratification of acute pulmonary embolism. The American journal of cardiology *108*, 133-140.

Kass, D.A., Yamazaki, T., Burkhoff, D., Maughan, W.L., and Sagawa, K. (1986). Determination of left ventricular end-systolic pressure-volume relationships by the conductance (volume) catheter technique. Circulation *73*, 586-595.

Keogh, A., Strange, G., McNeil, K., Williams, T.J., Gabbay, E., Proudman, S., Weintraub, R.G., Wlodarczyk, J., and Dalton, B. (2011). The Bosentan Patient Registry: long-term survival in pulmonary arterial hypertension. Internal medicine journal *41*, 227-234.

Keogh, A.M., Mayer, E., Benza, R.L., Corris, P., Dartevelle, P.G., Frost, A.E., Kim, N.H., Lang, I.M., Pepke-Zaba, J., and Sandoval, J. (2009). Interventional and surgical modalities of

treatment in pulmonary hypertension. Journal of the American College of Cardiology *54*, S67-77.

Khoury, D., McAlister, H., Wilkoff, B., Simmons, T., Rudy, Y., McCowan, R., Morant, V., Castle, L., and Maloney, J. (1989). Continuous right ventricular volume assessment by catheter measurement of impedance for antitachycardia system control. Pacing and clinical electrophysiology : PACE *12*, 1918-1926.

Kiezun, A., Garimella, K., Do, R., Stitziel, N.O., Neale, B.M., McLaren, P.J., Gupta, N., Sklar, P., Sullivan, P.F., Moran, J.L.*, et al.* (2012). Exome sequencing and the genetic basis of complex traits. Nature genetics *44*, 623-630.

Klok, F.A., van Kralingen, K.W., van Dijk, A.P., Heyning, F.H., Vliegen, H.W., and Huisman, M.V. (2010). Prospective cardiopulmonary screening program to detect chronic thromboembolic pulmonary hypertension in patients after acute pulmonary embolism. Haematologica *95*, 970-975.

Kominami, S., Tanabe, N., Ota, M., Naruse, T.K., Katsuyama, Y., Nakanishi, N., Tomoike, H., Sakuma, M., Shirato, K., Takahashi, M.*, et al.* (2009). HLA-DPB1 and NFKBIL1 may confer the susceptibility to chronic thromboembolic pulmonary hypertension in the absence of deep vein thrombosis. Journal of human genetics *54*, 108-114.

Kornet, L., Schreuder, J.J., van der Velde, E.T., Baan, J., and Jansen, J.R. (2000). A new approach to determine parallel conductance for left ventricular volume measurements. Cardiovascular research *48*, 455-463.

Ku, C.S., Polychronakos, C., Tan, E.K., Naidoo, N., Pawitan, Y., Roukos, D.H., Mort, M., and Cooper, D.N. (2013). A new paradigm emerges from the study of de novo mutations in the context of neurodevelopmental disease. Molecular psychiatry *18*, 141-153.

Kuehne, T., Yilmaz, S., Steendijk, P., Moore, P., Groenink, M., Saaed, M., Weber, O., Higgins, C.B., Ewert, P., Fleck, E.*, et al.* (2004). Magnetic resonance imaging analysis of right ventricular pressure-volume loops: in vivo validation and clinical application in patients with pulmonary hypertension. Circulation *110*, 2010-2016.

Lang, I.M., Marsh, J.J., Olman, M.A., Moser, K.M., Loskutoff, D.J., and Schleef, R.R. (1994). Expression of type 1 plasminogen activator inhibitor in chronic pulmonary thromboemboli. Circulation *89*, 2715-2721.

Lankeit, M., Dellas, C., Panzenbock, A., Skoro-Sajer, N., Bonderman, D., Olschewski, M., Schafer, K., Puls, M., Konstantinides, S., and Lang, I.M. (2008). Heart-type fatty acid-binding protein for risk assessment of chronic thromboembolic pulmonary hypertension. The European respiratory journal *31*, 1024-1029.

Larson, N.B., and Schaid, D.J. (2014). Regularized rare variant enrichment analysis for case-control exome sequencing data. Genetic epidemiology *38*, 104-113.

Latus, H., Binder, W., Kerst, G., Hofbeck, M., Sieverding, L., and Apitz, C. (2013). Right ventricular-pulmonary arterial coupling in patients after repair of tetralogy of Fallot. The Journal of thoracic and cardiovascular surgery *146*, 1366-1372.

Lee, W.T., Ling, Y., Sheares, K.K., Pepke-Zaba, J., Peacock, A.J., and Johnson, M.K. (2012). Predicting survival in pulmonary arterial hypertension in the UK. The European respiratory journal *40*, 604-611.

Leeuwenburgh, B.P., Steendijk, P., Helbing, W.A., and Baan, J. (2002). Indexes of diastolic RV function: load dependence and changes after chronic RV pressure overload in lambs. American journal of physiology Heart and circulatory physiology *282*, H1350-1358.

Leibundgut, G., Rohner, A., Grize, L., Bernheim, A., Kessel-Schaefer, A., Bremerich, J., Zellweger, M., Buser, P., and Handke, M. (2010). Dynamic assessment of right ventricular volumes and function by real-time three-dimensional echocardiography: a comparison study with magnetic resonance imaging in 100 adult patients. Journal of the American Society of Echocardiography : official publication of the American Society of Echocardiography *23*, 116-126.

Linenberger, M.L., Kindelan, J., Bennett, R.L., Reiner, A.P., and Cote, H.C. (2000). Fibrinogen bellingham: a gamma-chain R275C substitution and a beta-promoter polymorphism in a thrombotic member of an asymptomatic family. American journal of hematology *64*, 242-250.

Liu, D., and Morrell, N.W. (2013). Genetics and the molecular pathogenesis of pulmonary arterial hypertension. Current hypertension reports *15*, 632-637.

Majewski, J., and Rosenblatt, D.S. (2012). Exome and whole-genome sequencing for gene discovery: the future is now! Human mutation *33*, 591-592.

Maloney, J.D., Helguera, M.E., and Woscoboinik, J.R. (1992). Physiology of rate-responsive pacing. Cardiology clinics *10*, 619-633.

Manolio, T.A., Collins, F.S., Cox, N.J., Goldstein, D.B., Hindorff, L.A., Hunter, D.J., McCarthy, M.I., Ramos, E.M., Cardon, L.R., Chakravarti, A.*, et al.* (2009). Finding the missing heritability of complex diseases. Nature *461*, 747-753.

Marian, A.J. (2012a). Challenges in medical applications of whole exome/genome sequencing discoveries. Trends in cardiovascular medicine *22*, 219-223.

Marian, A.J. (2012b). Molecular genetic studies of complex phenotypes. Translational research : the journal of laboratory and clinical medicine *159*, 64-79.

Maughan, W.L., Shoukas, A.A., Sagawa, K., and Weisfeldt, M.L. (1979). Instantaneous pressure-volume relationship of the canine right ventricle. Circulation research *44*, 309-315.

Mauritz, G.J., Vonk-Noordegraaf, A., Kind, T., Surie, S., Kloek, J.J., Bresser, P., Saouti, N., Bosboom, J., Westerhof, N., and Marcus, J.T. (2012). Pulmonary endarterectomy normalizes interventricular dyssynchrony and right ventricular systolic wall stress. Journal of cardiovascular magnetic resonance : official journal of the Society for Cardiovascular Magnetic Resonance *14*, 5.

Mayer, E., Jenkins, D., Lindner, J., D'Armini, A., Kloek, J., Meyns, B., Ilkjaer, L.B., Klepetko, W., Delcroix, M., Lang, I.*, et al.* (2011). Surgical management and outcome of patients with chronic thromboembolic pulmonary hypertension: results from an international prospective registry. The Journal of thoracic and cardiovascular surgery *141*, 702-710.

McClellan, J., and King, M.C. (2010). Genetic heterogeneity in human disease. Cell *141*, 210-217.

McCollister, D.H., Beutz, M., McLaughlin, V., Rumsfeld, J., Masoudi, F.A., Tripputi, M., Yaeger, T., Weintraub, P., and Badesch, D.B. (2010). Depressive symptoms in pulmonary arterial hypertension: prevalence and association with functional status. Psychosomatics *51*, 339-339 e338.

McGuinness, C.L., Humphries, J., Waltham, M., Burnand, K.G., Collins, M., and Smith, A. (2001). Recruitment of labelled monocytes by experimental venous thrombi. Thrombosis and haemostasis *85*, 1018-1024.

McKay, R.G., Spears, J.R., Aroesty, J.M., Baim, D.S., Royal, H.D., Heller, G.V., Lincoln, W., Salo, R.W., Braunwald, E., and Grossman, W. (1984). Instantaneous measurement of left and right ventricular stroke volume and pressure-volume relationships with an impedance catheter. Circulation *69*, 703-710.

McKenna, S.P., Doughty, N., Meads, D.M., Doward, L.C., and Pepke-Zaba, J. (2006). The Cambridge Pulmonary Hypertension Outcome Review (CAMPHOR): a measure of health-related quality of life and quality of life for patients with pulmonary hypertension. Quality of life research : an international journal of quality of life aspects of treatment, care and rehabilitation *15*, 103-115.

McLaughlin, V.V., and Rich, S. (2004). Pulmonary hypertension. Current problems in cardiology *29*, 575-634.

Mechtcheriakova, D., Wlachos, A., Holzmuller, H., Binder, B.R., and Hofer, E. (1999). Vascular endothelial cell growth factor-induced tissue factor expression in endothelial cells is mediated by EGR-1. Blood *93*, 3811-3823.

Mereles, D., Ehlken, N., Kreuscher, S., Ghofrani, S., Hoeper, M.M., Halank, M., Meyer, F.J., Karger, G., Buss, J., Juenger, J.*, et al.* (2006). Exercise and respiratory training improve exercise capacity and quality of life in patients with severe chronic pulmonary hypertension. Circulation *114*, 1482-1489.

Metzker, M.L. (2010). Sequencing technologies - the next generation. Nature reviews Genetics *11*, 31-46.

Miniati, M., Fiorillo, C., Becatti, M., Monti, S., Bottai, M., Marini, C., Grifoni, E., Formichi, B., Bauleo, C., Arcangeli, C.*, et al.* (2010). Fibrin resistance to lysis in patients with pulmonary hypertension other than thromboembolic. American journal of respiratory and critical care medicine *181*, 992-996.

Miniati, M., Monti, S., Bottai, M., Scoscia, E., Bauleo, C., Tonelli, L., Dainelli, A., and Giuntini, C. (2006). Survival and restoration of pulmonary perfusion in a long-term follow-up of patients after acute pulmonary embolism. Medicine *85*, 253-262.

Morris, T.A. (2013). Why acute pulmonary embolism becomes chronic thromboembolic pulmonary hypertension: clinical and genetic insights. Current opinion in pulmonary medicine *19*, 422-429.

Morris, T.A., Marsh, J.J., Chiles, P.G., Auger, W.R., Fedullo, P.F., and Woods, V.L., Jr. (2006). Fibrin derived from patients with chronic thromboembolic pulmonary hypertension is resistant to lysis. American journal of respiratory and critical care medicine *173*, 1270-1275.

Morris, T.A., Marsh, J.J., Chiles, P.G., Magana, M.M., Liang, N.C., Soler, X., Desantis, D.J., Ngo, D., and Woods, V.L., Jr. (2009). High prevalence of dysfibrinogenemia among patients with chronic thromboembolic pulmonary hypertension. Blood *114*, 1929-1936.

Moser, K.M., Auger, W.R., and Fedullo, P.F. (1990). Chronic major-vessel thromboembolic pulmonary hypertension. Circulation *81*, 1735-1743.

Moser, K.M., Cantor, J.P., Olman, M., Villespin, I., Graif, J.L., Konopka, R., Marsh, J.J., and Pedersen, C. (1991). Chronic pulmonary thromboembolism in dogs treated with tranexamic acid. Circulation *83*, 1371-1379.

Naeije, R. (2013). Physiology of the pulmonary circulation and the right heart. Current hypertension reports *15*, 623-631.

Nagel, C., Prange, F., Guth, S., Herb, J., Ehlken, N., Fischer, C., Reichenberger, F., Rosenkranz, S., Seyfarth, H.J., Mayer, E.*, et al.* (2012). Exercise training improves exercise capacity and quality of life in patients with inoperable or residual chronic thromboembolic pulmonary hypertension. PLoS ONE *7*, e41603.

National Pulmonary Hypertension Centres of the, U.K., and Ireland (2008). Consensus statement on the management of pulmonary hypertension in clinical practice in the UK and Ireland. Thorax *63 Suppl 2*, ii1-ii41.

Ng, S.B., Buckingham, K.J., Lee, C., Bigham, A.W., Tabor, H.K., Dent, K.M., Huff, C.D., Shannon, P.T., Jabs, E.W., Nickerson, D.A.*, et al.* (2010). Exome sequencing identifies the cause of a mendelian disorder. Nature genetics *42*, 30-35.

Ng, S.B., Turner, E.H., Robertson, P.D., Flygare, S.D., Bigham, A.W., Lee, C., Shaffer, T., Wong, M., Bhattacharjee, A., Eichler, E.E.*, et al.* (2009). Targeted capture and massively parallel sequencing of 12 human exomes. Nature *461*, 272-276.

Niemann, P.S., Pinho, L., Balbach, T., Galuschky, C., Blankenhagen, M., Silberbach, M., Broberg, C., Jerosch-Herold, M., and Sahn, D.J. (2007). Anatomically oriented right ventricular volume measurements with dynamic three-dimensional echocardiography validated by 3-Tesla magnetic resonance imaging. Journal of the American College of Cardiology *50*, 1668-1676.

Olman, M.A., Marsh, J.J., Lang, I.M., Moser, K.M., Binder, B.R., and Schleef, R.R. (1992). Endogenous fibrinolytic system in chronic large-vessel thromboembolic pulmonary hypertension. Circulation *86*, 1241-1248.

Pagnamenta, A., Dewachter, C., McEntee, K., Fesler, P., Brimioulle, S., and Naeije, R. (2010). Early right ventriculo-arterial uncoupling in borderline pulmonary hypertension on experimental heart failure. J Appl Physiol (1985) *109*, 1080-1085.

Pengo, V., Lensing, A.W., Prins, M.H., Marchiori, A., Davidson, B.L., Tiozzo, F., Albanese, P., Biasiolo, A., Pegoraro, C., Iliceto, S.*, et al.* (2004). Incidence of chronic thromboembolic pulmonary hypertension after pulmonary embolism. The New England journal of medicine *350*, 2257-2264.

Pepke-Zaba, J., Delcroix, M., Lang, I., Mayer, E., Jansa, P., Ambroz, D., Treacy, C., D'Armini, A.M., Morsolini, M., Snijder, R.*, et al.* (2011). Chronic thromboembolic pulmonary hypertension (CTEPH): results from an international prospective registry. Circulation *124*, 1973-1981.

Pepke-Zaba, J., Jansa, P., Kim, N.H., Naeije, R., and Simonneau, G. (2013). Chronic thromboembolic pulmonary hypertension: role of medical therapy. The European respiratory journal *41*, 985-990.

Plumhans, C., Muhlenbruch, G., Rapaee, A., Sim, K.H., Seyfarth, T., Gunther, R.W., and Mahnken, A.H. (2008). Assessment of global right ventricular function on 64-MDCT compared with MRI. AJR American journal of roentgenology *190*, 1358-1361.

Poli, D., Grifoni, E., Antonucci, E., Arcangeli, C., Prisco, D., Abbate, R., and Miniati, M. (2010). Incidence of recurrent venous thromboembolism and of chronic thromboembolic pulmonary hypertension in patients after a first episode of pulmonary embolism. Journal of thrombosis and thrombolysis *30*, 294-299.

Pritchard, J.K. (2001). Are rare variants responsible for susceptibility to complex diseases? American journal of human genetics *69*, 124-137.

Pulido, T., Adzerikho, I., Channick, R.N., Delcroix, M., Galie, N., Ghofrani, H.A., Jansa, P., Jing, Z.C., Le Brun, F.O., Mehta, S.*, et al.* (2013). Macitentan and morbidity and mortality in pulmonary arterial hypertension. The New England journal of medicine *369*, 809-818.

Quarck, R., Nawrot, T., Meyns, B., and Delcroix, M. (2009). C-reactive protein: a new predictor of adverse outcome in pulmonary arterial hypertension. Journal of the American College of Cardiology *53*, 1211-1218.

Quiroz, R., Kucher, N., Schoepf, U.J., Kipfmueller, F., Solomon, S.D., Costello, P., and Goldhaber, S.Z. (2004). Right ventricular enlargement on chest computed tomography: prognostic role in acute pulmonary embolism. Circulation *109*, 2401-2404.

Rain, S., Handoko, M.L., Trip, P., Gan, C.T., Westerhof, N., Stienen, G.J., Paulus, W.J., Ottenheijm, C.A., Marcus, J.T., Dorfmuller, P.*, et al.* (2013). Right ventricular diastolic impairment in patients with pulmonary arterial hypertension. Circulation *128*, 2016-2025, 2011-2010.

Reesink, H.J., van der Plas, M.N., Verhey, N.E., van Steenwijk, R.P., Kloek, J.J., and Bresser, P. (2007). Six-minute walk distance as parameter of functional outcome after pulmonary endarterectomy for chronic thromboembolic pulmonary hypertension. The Journal of thoracic and cardiovascular surgery *133*, 510-516.

Reichenberger, F., Voswinckel, R., Enke, B., Rutsch, M., El Fechtali, E., Schmehl, T., Olschewski, H., Schermuly, R., Weissmann, N., Ghofrani, H.A.*, et al.* (2007). Long-term treatment with sildenafil in chronic thromboembolic pulmonary hypertension. The European respiratory journal *30*, 922-927.

Rensing, B.J., McDougall, J.C., Breen, J.F., Vigneswaran, W.T., McGregor, C.G., and Rumberger, J.A. (1997). Right and left ventricular remodeling after orthotopic single lung transplantation for end-stage emphysema. The Journal of heart and lung transplantation : the official publication of the International Society for Heart Transplantation *16*, 926-933.

Ribeiro, A., Lindmarker, P., Johnsson, H., Juhlin-Dannfelt, A., and Jorfeldt, L. (1999). Pulmonary embolism: one-year follow-up with echocardiography doppler and five-year survival analysis. Circulation *99*, 1325-1330.

Roeleveld, R.J., Marcus, J.T., Boonstra, A., Postmus, P.E., Marques, K.M., Bronzwaer, J.G., and Vonk-Noordegraaf, A. (2005). A comparison of noninvasive MRI-based methods of estimating pulmonary artery pressure in pulmonary hypertension. Journal of magnetic resonance imaging : JMRI *22*, 67-72.

Rosewich, H., Thiele, H., Ohlenbusch, A., Maschke, U., Altmuller, J., Frommolt, P., Zirn, B., Ebinger, F., Siemes, H., Nurnberg, P.*, et al.* (2012). Heterozygous de-novo mutations in ATP1A3 in patients with alternating hemiplegia of childhood: a whole-exome sequencing gene-identification study. Lancet neurology *11*, 764-773.

Ross, R.M. (2003). ATS/ACCP statement on cardiopulmonary exercise testing. American journal of respiratory and critical care medicine *167*, 1451; author reply 1451.

Rubin, L.J., Badesch, D.B., Barst, R.J., Galie, N., Black, C.M., Keogh, A., Pulido, T., Frost, A., Roux, S., Leconte, I.*, et al.* (2002). Bosentan therapy for pulmonary arterial hypertension. The New England journal of medicine *346*, 896-903.

Rudski, L.G., Lai, W.W., Afilalo, J., Hua, L., Handschumacher, M.D., Chandrasekaran, K., Solomon, S.D., Louie, E.K., and Schiller, N.B. (2010). Guidelines for the echocardiographic assessment of the right heart in adults: a report from the American Society of Echocardiography endorsed by the European Association of Echocardiography, a registered branch of the European Society of Cardiology, and the Canadian Society of Echocardiography. Journal of the American Society of Echocardiography : official publication of the American Society of Echocardiography *23*, 685-713; quiz 786-688.

Saba, T.S., Foster, J., Cockburn, M., Cowan, M., and Peacock, A.J. (2002). Ventricular mass index using magnetic resonance imaging accurately estimates pulmonary artery pressure. The European respiratory journal *20*, 1519-1524.

Sadler, D.B., Brown, J., Nurse, H., and Roberts, J. (1992). Impact of hemodialysis on left and right ventricular Doppler diastolic filling indices. The American journal of the medical sciences *304*, 83-90.

Sagawa, K. (1988). Cardiac contraction and the pressure-volume relationship (New York: Oxford University Press).

Sanders, S.J., Murtha, M.T., Gupta, A.R., Murdoch, J.D., Raubeson, M.J., Willsey, A.J., Ercan-Sencicek, A.G., DiLullo, N.M., Parikshak, N.N., Stein, J.L.*, et al.* (2012). De novo mutations revealed by whole-exome sequencing are strongly associated with autism. Nature *485*, 237-241.

Sanz, J., Garcia-Alvarez, A., Fernandez-Friera, L., Nair, A., Mirelis, J.G., Sawit, S.T., Pinney, S., and Fuster, V. (2012). Right ventriculo-arterial coupling in pulmonary hypertension: a magnetic resonance study. Heart *98*, 238-243.

Sanz, J., Kuschnir, P., Rius, T., Salguero, R., Sulica, R., Einstein, A.J., Dellegrottaglie, S., Fuster, V., Rajagopalan, S., and Poon, M. (2007). Pulmonary arterial hypertension: noninvasive detection with phase-contrast MR imaging. Radiology *243*, 70-79.

Schaldach, M. (1990). Automatic adjustment of pacing parameters based on intracardiac impedance measurements. Pacing and clinical electrophysiology : PACE *13*, 1702-1710.

Scheidl, S.J., Englisch, C., Kovacs, G., Reichenberger, F., Schulz, R., Breithecker, A., Ghofrani, H.A., Seeger, W., and Olschewski, H. (2012). Diagnosis of CTEPH versus IPAH using capillary to end-tidal carbon dioxide gradients. The European respiratory journal *39*, 119-124.

Schork, N.J., Murray, S.S., Frazer, K.A., and Topol, E.J. (2009). Common vs. rare allele hypotheses for complex diseases. Current opinion in genetics & development *19*, 212-219.

Sebat, J., Lakshmi, B., Malhotra, D., Troge, J., Lese-Martin, C., Walsh, T., Yamrom, B., Yoon, S., Krasnitz, A., Kendall, J.*, et al.* (2007). Strong association of de novo copy number mutations with autism. Science *316*, 445-449.

Shiraishi, M., Sekiguchi, A., Oates, A.J., Terry, M.J., and Miyamoto, Y. (2002). HOX gene clusters are hotspots of de novo methylation in CpG islands of human lung adenocarcinomas. Oncogene *21*, 3659-3662.

Simonneau, G., Robbins, I.M., Beghetti, M., Channick, R.N., Delcroix, M., Denton, C.P., Elliott, C.G., Gaine, S.P., Gladwin, M.T., Jing, Z.C.*, et al.* (2009). Updated clinical classification of pulmonary hypertension. Journal of the American College of Cardiology *54*, S43-54.

Sitbon, O., Humbert, M., Nunes, H., Parent, F., Garcia, G., Herve, P., Rainisio, M., and Simonneau, G. (2002). Long-term intravenous epoprostenol infusion in primary pulmonary hypertension: prognostic factors and survival. Journal of the American College of Cardiology *40*, 780-788.

Solda, P.L., Pantaleo, P., Perlini, S., Calciati, A., Finardi, G., Pinsky, M.R., and Bernardi, L. (1992). Continuous monitoring of right ventricular volume changes using a conductance catheter in the rabbit. J Appl Physiol (1985) *73*, 1770-1775.

Soon, E., Holmes, A.M., Treacy, C.M., Doughty, N.J., Southgate, L., Machado, R.D., Trembath, R.C., Jennings, S., Barker, L., Nicklin, P.*, et al.* (2010). Elevated levels of inflammatory cytokines predict survival in idiopathic and familial pulmonary arterial hypertension. Circulation *122*, 920-927.

Stitziel, N.O., Kiezun, A., and Sunyaev, S. (2011). Computational and statistical approaches to analyzing variants identified by exome sequencing. Genome biology *12*, 227.

Suga, H., and Sagawa, K. (1974). Instantaneous pressure-volume relationships and their ratio in the excised, supported canine left ventricle. Circulation research *35*, 117-126.

Suga, H., Sagawa, K., and Shoukas, A.A. (1973). Load independence of the instantaneous pressure-volume ratio of the canine left ventricle and effects of epinephrine and heart rate on the ratio. Circulation research *32*, 314-322.

Sugeng, L., Mor-Avi, V., Weinert, L., Niel, J., Ebner, C., Steringer-Mascherbauer, R., Bartolles, R., Baumann, R., Schummers, G., Lang, R.M.*, et al.* (2010). Multimodality comparison of quantitative volumetric analysis of the right ventricle. JACC Cardiovascular imaging *3*, 10-18.

Sun, X.G., Hansen, J.E., Oudiz, R.J., and Wasserman, K. (2001). Exercise pathophysiology in patients with primary pulmonary hypertension. Circulation *104*, 429-435.

Sun, X.G., Hansen, J.E., Oudiz, R.J., and Wasserman, K. (2002). Gas exchange detection of exercise-induced right-to-left shunt in patients with primary pulmonary hypertension. Circulation *105*, 54-60.

Sunagawa, K., Maughan, W.L., Burkhoff, D., and Sagawa, K. (1983). Left ventricular interaction with arterial load studied in isolated canine ventricle. The American journal of physiology *245*, H773-780.

Suntharalingam, J., Goldsmith, K., van Marion, V., Long, L., Treacy, C.M., Dudbridge, F., Toshner, M.R., Pepke-Zaba, J., Eikenboom, J.C., and Morrell, N.W. (2008). Fibrinogen Aalpha Thr312Ala polymorphism is associated with chronic thromboembolic pulmonary hypertension. The European respiratory journal *31*, 736-741.

Surie, S., Gibson, N.S., Gerdes, V.E., Bouma, B.J., van Eck-Smit, B.L., Buller, H.R., and Bresser, P. (2010). Active search for chronic thromboembolic pulmonary hypertension does not appear indicated after acute pulmonary embolism. Thrombosis research *125*, e202-205.

Swiston, J.R., Johnson, S.R., and Granton, J.T. (2010). Factors that prognosticate mortality in idiopathic pulmonary arterial hypertension: a systematic review of the literature. Respiratory medicine *104*, 1588-1607.

Tabima, D.M., Hacker, T.A., and Chesler, N.C. (2010). Measuring right ventricular function in the normal and hypertensive mouse hearts using admittance-derived pressure-volume loops. American journal of physiology Heart and circulatory physiology *299*, H2069-2075.

Tedford, R.J., Mudd, J.O., Girgis, R.E., Mathai, S.C., Zaiman, A.L., Housten-Harris, T., Boyce, D., Kelemen, B.W., Bacher, A.C., Shah, A.A.*, et al.* (2013). Right ventricular dysfunction in systemic sclerosis-associated pulmonary arterial hypertension. Circulation Heart failure *6*, 953-963.

Tennessen, J.A., Bigham, A.W., O'Connor, T.D., Fu, W., Kenny, E.E., Gravel, S., McGee, S., Do, R., Liu, X., Jun, G.*, et al.* (2012). Evolution and functional impact of rare coding variation from deep sequencing of human exomes. Science *337*, 64-69.

Thenappan, T., Shah, S.J., Rich, S., and Gomberg-Maitland, M. (2007). A USA-based registry for pulmonary arterial hypertension: 1982-2006. The European respiratory journal *30*, 1103-1110.

Thusberg, J., Olatubosun, A., and Vihinen, M. (2011). Performance of mutation pathogenicity prediction methods on missense variants. Human mutation *32*, 358-368.

Turhan, S., Tulunay, C., Ozduman Cin, M., Gursoy, A., Kilickap, M., Dincer, I., Candemir, B., Gullu, S., and Erol, C. (2006). Effects of thyroxine therapy on right ventricular systolic and diastolic function in patients with subclinical hypothyroidism: a study by pulsed wave tissue Doppler imaging. The Journal of clinical endocrinology and metabolism *91*, 3490-3493.

van der Plas, M.N., Reesink, H.J., Roos, C.M., van Steenwijk, R.P., Kloek, J.J., and Bresser, P. (2010). Pulmonary endarterectomy improves dyspnea by the relief of dead space ventilation. The Annals of thoracic surgery *89*, 347-352.

van der Zwaan, H.B., Helbing, W.A., McGhie, J.S., Geleijnse, M.L., Luijnenburg, S.E., Roos-Hesselink, J.W., and Meijboom, F.J. (2010). Clinical value of real-time three-dimensional echocardiography for right ventricular quantification in congenital heart disease: validation with cardiac magnetic resonance imaging. Journal of the American Society of Echocardiography : official publication of the American Society of Echocardiography *23*, 134-140.

van Wolferen, S.A., Marcus, J.T., Boonstra, A., Marques, K.M., Bronzwaer, J.G., Spreeuwenberg, M.D., Postmus, P.E., and Vonk-Noordegraaf, A. (2007). Prognostic value of right ventricular mass, volume, and function in idiopathic pulmonary arterial hypertension. European heart journal *28*, 1250-1257.

Veltman, J.A., and Brunner, H.G. (2012). De novo mutations in human genetic disease. Nature reviews Genetics *13*, 565-575.

Vissers, L.E., de Ligt, J., Gilissen, C., Janssen, I., Steehouwer, M., de Vries, P., van Lier, B., Arts, P., Wieskamp, N., del Rosario, M.*, et al.* (2010). A de novo paradigm for mental retardation. Nature genetics *42*, 1109-1112.

Walsh, T., McClellan, J.M., McCarthy, S.E., Addington, A.M., Pierce, S.B., Cooper, G.M., Nord, A.S., Kusenda, M., Malhotra, D., Bhandari, A.*, et al.* (2008). Rare structural variants disrupt multiple genes in neurodevelopmental pathways in schizophrenia. Science *320*, 539-543.

Waltham, M., Burnand, K.G., Collins, M., McGuinness, C.L., Singh, I., and Smith, A. (2003). Vascular endothelial growth factor enhances venous thrombus recanalisation and organisation. Thrombosis and haemostasis *89*, 169-176.

Wauthy, P., Naeije, R., and Brimioulle, S. (2005). Left and right ventriculo-arterial coupling in a patient with congenitally corrected transposition. Cardiology in the young *15*, 647-649.

Wauthy, P., Pagnamenta, A., Vassalli, F., Naeije, R., and Brimioulle, S. (2004). Right ventricular adaptation to pulmonary hypertension: an interspecies comparison. American journal of physiology Heart and circulatory physiology *286*, H1441-1447.

West, J.B. (1969). Ventilation-perfusion inequality and overall gas exchange in computer models of the lung. Respiration physiology *7*, 88-110.

Wolf, M., Boyer-Neumann, C., Parent, F., Eschwege, V., Jaillet, H., Meyer, D., and Simonneau, G. (2000). Thrombotic risk factors in pulmonary hypertension. The European respiratory journal *15*, 395-399.

Wong, C.L., Szydlo, R., Gibbs, S., and Laffan, M. (2010). Hereditary and acquired thrombotic risk factors for chronic thromboembolic pulmonary hypertension. Blood coagulation & fibrinolysis : an international journal in haemostasis and thrombosis *21*, 201-206.

Xie, Y., Burke, B.M., Kopelnik, A., Auger, W., Daniels, L.B., Madani, M.M., Poch, D.S., Kim, N.H., and Blanchard, D.G. (2014). Echocardiographic estimation of pulmonary vascular resistance in chronic thromboembolic pulmonary hypertension: utility of right heart Doppler measurements. Echocardiography *31*, 29-33.

Xu, B., Roos, J.L., Dexheimer, P., Boone, B., Plummer, B., Levy, S., Gogos, J.A., and Karayiorgou, M. (2011). Exome sequencing supports a de novo mutational paradigm for schizophrenia. Nature genetics *43*, 864-868.

Yang, Y., Muzny, D.M., Reid, J.G., Bainbridge, M.N., Willis, A., Ward, P.A., Braxton, A., Beuten, J., Xia, F., Niu, Z.*, et al.* (2013). Clinical whole-exome sequencing for the diagnosis of mendelian disorders. The New England journal of medicine *369*, 1502-1511.

Zhai, Z., Murphy, K., Tighe, H., Wang, C., Wilkins, M.R., Gibbs, J.S., and Howard, L.S. (2011). Differences in ventilatory inefficiency between pulmonary arterial hypertension and chronic thromboembolic pulmonary hypertension. Chest *140*, 1284-1291.